

University of Denver

Digital Commons @ DU

Electronic Theses and Dissertations

Graduate Studies

1-1-2013

Galvanic Corrosion of High-Temperature Low-Sag (HTLS) High Voltage Conductors: New Materials—New Challenges

Eva Håkansson
University of Denver

Follow this and additional works at: <https://digitalcommons.du.edu/etd>



Part of the [Mechanical Engineering Commons](#)

Recommended Citation

Håkansson, Eva, "Galvanic Corrosion of High-Temperature Low-Sag (HTLS) High Voltage Conductors: New Materials—New Challenges" (2013). *Electronic Theses and Dissertations*. 979.
<https://digitalcommons.du.edu/etd/979>

This Thesis is brought to you for free and open access by the Graduate Studies at Digital Commons @ DU. It has been accepted for inclusion in Electronic Theses and Dissertations by an authorized administrator of Digital Commons @ DU. For more information, please contact jennifer.cox@du.edu, dig-commons@du.edu.

GALVANIC CORROSION OF HIGH-TEMPERATURE LOW-SAG (HTLS) HIGH
VOLTAGE CONDUCTORS: NEW MATERIALS – NEW CHALLENGES

A Thesis

Presented to

the Faculty of Engineering and Computer Science

University of Denver

In Partial Fulfillment

of the Requirements for the Degree

Masters of Science

by

Eva Håkansson

June 2013

Advisor: Dr. Maciej Kumosa

© Copyright by Eva Håkansson 2013

All Rights Reserved

Author: Eva Håkansson

Title: Galvanic corrosion of High-Temperature Low-Sag (HTLS) high voltage conductors: New materials – new challenges

Advisor: Dr. Maciej Kumosa

Degree Date: June 2013

Abstract

High-Temperature Low-Sag (HTLS) high voltage overhead conductors offer higher operating temperatures, reduced resistance and less sag than conventional designs. With up to twice the current capacity for the same diameter conductor, they may help ease the power shortage in the constantly increasing electricity demand, but there might be some concerns about their corrosion resistance.

These new conductors use materials relatively new to the power industry, such as advanced carbon fiber polymer matrix composites and unique metal matrix composites/nano-composites predominantly used in aerospace industries. This study has made an initial assessment of potential galvanic corrosion problems in three very different HTLS designs: ACCC (Aluminum Conductor Composite Core), ACCR (Aluminum Conductor Composite Reinforced) and ACSS (Aluminum Conductor Steel Supported). In particular the ACCC design was evaluated for its resistance to corrosion and compared to the other designs.

The study concludes that all three designs can develop galvanic corrosion under certain circumstances. While the results are *not* sufficient to make service life predictions of any of the tested conductors, they point out the necessity of thorough corrosion testing of all new conductor designs.

Acknowledgements

A master's thesis is always a group effort. This study would never have been possible without help from other people. I would like to acknowledge the following:

Dr. Maciej Kumosa - my academic supervisor - for fighting tooth and nail to get me into the University of Denver, and then pushing me along in this new world of high voltage conductors and corrosion. • **Dr. Paul Predecki**, professor emeritus at DU, for having been equally important in the project. • **Bonneville Power Administration, Tri-State Generation and Transmission Association, Western Area Power Administration and the National Science Foundation (GOALI)** for financing this study. I want to give a particular thank you to **Ross Clark** (WAPA), **Art Mander** (Tri-State), **Allen Turner** (Tri-State) and **Michael Staats** (BPA). • **Dr. Dan Armentrout**, former chair of the MME Department at DU for supporting my first brave ideas for testing design. • **Dr. Richard E. Ricker** at NIST, Gaithersburg for providing knowledge and a very sound perspective on corrosion. • **Dr. Andy Slifka** with colleagues **Chris McCowan, Dave McColskey, Dr. Jeffrey Sowards** and **Liz Drexler** at NIST, Boulder and **Dr. John Drexler** at CU Boulder for invaluable help with microscopy. • **Dr. Euripides Solis-Ramos** for providing suggestions how to improve the thesis. • My parents **Lena and Sven Håkansson** for laying the foundation for my love of science. • **Bill Dubé** for being my husband and the love of my life, and convincing me to go to engineering school in the first place, and my dear friends **Prof. Dr. Wolfgang and Monika Schürer** for making it possible. • Last but not least, my office mates **Bruce Allen** and **Joe Hoffman** for cheering up the daily work. And everybody else that I have forgotten to mention....

Table of Contents

Chapter One: Introduction	1
1.1 High-Temperature Low-Sag (HTLS) conductors.....	4
1.1.1 Uprating by HTLS conductors.....	4
1.1.2 The studied conductors	10
1.2 Corrosion of high voltage conductors.....	15
1.2.1 Previous corrosion studies	15
1.2.2 Cost of corrosion.....	18
1.2.3 Corrosion protection	18
1.2.4 Monitoring for corrosion.....	19
1.3 Galvanic corrosion and other corrosion mechanisms in HV conductors.....	20
1.3.1 Corrosion – a natural phenomenon	20
1.3.2 Corrosion reactions in neutral electrolytes	22
1.3.3 Galvanic corrosion.....	27
1.3.4 Corrosion of aluminum	37
1.3.5 Corrosion of composites	41
1.3.6 Corrosion in the atmosphere	44
1.3.7 Prediction of corrosion mechanisms in the studied conductors.....	47
Chapter Two: Methodology.....	53
2.1 Corrosion testing in theory and practice	53
2.1.1 Laboratory vs. field testing	53
2.1.2 Corrosion testing standards.....	54
2.2 Design decisions for testing methods	55
2.2.1 Electrolyte and temperature	55
2.2.2 Oxygen and agitation	56
2.2.3 Mass loss vs. electrochemical tests.....	58
2.2.4 Duration of corrosion test	60
2.2.5 Reference electrodes	62
2.2.6 Sample design	63
2.2.7 The C ³ LARC instrument.....	65
2.3 Performed corrosion tests	68
2.3.1 Setup and procedure for mass loss tests (Test A-C)	69
2.3.2 Setup and procedure for electrochemical tests (Test D-F).....	77
Chapter Three: Results.....	86
3.1 Results from mass loss tests.....	86
3.1.1 Test A: Partially submerged.....	86
3.1.2 Test B: Fully submerged.....	94
3.1.3 Test C: Single strand.....	99
3.2 Results from electrochemical tests.....	101
3.2.1 Test D: Open circuit potential.....	101
3.2.2 Test E: Galvanic corrosion current	104
3.3 Error analysis	109

Chapter Four: Discussion.....	110
4.1 ACSR.....	110
4.2 ACSS.....	114
4.3 ACCC.....	118
4.4 ACCR.....	122
4.5 General discussion	129
Chapter Five: Conclusions.....	132
Suggestions for further research	135
Bibliography	136
Appendix A: Drawings for the C ³ LARC instrument.....	140
Appendix B: Acronyms, terminology and symbols.....	142

List of Figures

Figure 1: Thermal response of ACSR versus HTLS.	6
Figure 2: Cost of HTLS relative to ACSR.....	7
Figure 3: The four tested conductors.	10
Figure 4: Positions of some metals in order of energy required to convert their oxides to produce 1 kg of metal.	21
Figure 5: Splitting of water during corrosion of magnesium.....	23
Figure 6: Formation of $\text{Al}(\text{OH})_3$ on the ACCC sample.	26
Figure 7: Principle of galvanic corrosion between aluminum and graphite	28
Figure 8: Galvanic series.	30
Figure 9: Typical pitting corrosion of aluminum.....	38
Figure 10: Pitting corrosion.	39
Figure 11: The components of ACSR.....	48
Figure 12: The components of ACSS.	49
Figure 13: The components of ACCC.	50
Figure 14: The components of ACCR.	51
Figure 15: Dependency on agitation.	57
Figure 16: Salt bridge.....	62
Figure 17: Samples for galvanic corrosion testing.	64
Figure 18: The C ³ LARC testing cell as used for test A.	65
Figure 19: The C ³ LARC instrument.	66
Figure 20: Manufacturing of the C ³ LARC testing cell.....	67
Figure 21: C ³ LARC sample holders.	67

Figure 22: Electrical connections.....	67
Figure 23: The C ³ LARC testing cell used for Test A.....	70
Figure 24: Sample of ACCC mounted in the plastic sample holder.....	71
Figure 25: Test B – fully submerged.....	73
Figure 26: Samples for Test C.....	75
Figure 27: The aluminum strands after submersion for 7 days.....	75
Figure 28: Samples from Test B.....	76
Figure 29: Open circuit potential measurement.....	78
Figure 30: The ACCR sample at room temperature during Test E.....	81
Figure 31: Zero calibration of the galvanic current measurement circuit.....	82
Figure 32: Test F performed at 85°C.....	84
Figure 33: Test F performed at room temperature.....	85
Figure 34: Samples for Test F.....	85
Figure 35: Salt and corrosion products creeping up between the strands.....	86
Figure 36: Mass loss aluminum strands (Test A).....	87
Figure 37: Localized corrosion on ACSS, ACSR and ACCC.....	88
Figure 38: ACCR and ACCC after Test A.....	88
Figure 39: ACSS after Test A.....	89
Figure 40: Localized corrosion at the end of the ACSS sample.....	89
Figure 41: Mass loss core material (Test A).....	91
Figure 42: ACCC core after Test A.....	91
Figure 43: The core in the ACCC before removal.....	91
Figure 44: The loading bearing steel core in ACSR.....	92

Figure 45: Core strands of ACSS after Test A.	92
Figure 46: The metal-matrix composite core of ACCR after Test A,	93
Figure 47: Damage to the ACCR core.....	93
Figure 48: The metal matrix composite core of the ACCR after Test A.....	93
Figure 49: Mass loss aluminum strands (B)	94
Figure 50: More uniform corrosion of aluminum strands in Test B.....	95
Figure 51: Mass loss core material (Test B)	96
Figure 52: Typical sample before cleaning (Test B).	97
Figure 53: No signs of rust on the ACSR core (Test B).	97
Figure 54: Neither the ACSS core had any signs of rust (Test B).....	97
Figure 55: Three views of the same ACCC sample (Test B).	98
Figure 56: The ACCR sample before cleaning (Test B).....	98
Figure 57: End view of the ACCR core strands (Test B).	98
Figure 58: Mass loss aluminum strands (Test C).....	99
Figure 59: Samples after Test C.....	100
Figure 60: Open circuit potential (Test D).....	101
Figure 61: Open circuit potential vs. time (Test D)	102
Figure 62: Anodic galvanic corrosion current density (Test E).....	104
Figure 63: Galvanic corrosion current density (Test E).....	106
Figure 64: Galvanic corrosion current density for ACCR.	106
Figure 65: Theoretical open circuit potential in the conductor.....	108
Figure 66: Severe localized corrosion on the ACSS sample after Test A.	117
Figure 67: Three samples of ACCC core exposed to 85°C for approx. 100 days.	118

Figure 68: Build-up of corrosion products at the end of the ACCR core.	122
Figure 69: Initiation of corrosion pits along the fiber-matrix interface in the ACCR composite core.	128
Figure 70: The surface of un-corroded ACCR.	128
Figure 71: Drawing of lid for the C3LARC testing cell.	140
Figure 72: Drawing of sample holder for the C ³ LARC testing cell.	141

List of Tables

Table 1: Main features of the studied conductors.....	14
Table 2: Materials potentially active in the corrosion of ACSR.....	48
Table 3: Materials potentially active in the corrosion of ACSS.....	49
Table 4: Materials potentially active in the corrosion of ACCC.....	50
Table 5: Materials potentially active in the corrosion of ACCR.....	52
Table 6: Summary of the performed tests.....	68
Table 7: Test setup, partially submerged corrosion testing in saltwater (Test A).....	69
Table 8: Test setup, fully submerged corrosion testing in saltwater (Test B).....	72
Table 9: Test setup, fully submerged corrosion of single strands in saltwater.....	74
Table 10: Test setup, open circuit potential (Test D).....	77
Table 11: Test setup, galvanic corrosion current density (Test E).....	80
Table 12: Test setup, corrosion potential (Test F).....	83
Table 13: Results from Test A – partially submerged, 104 days, 85 ⁰ C.....	86
Table 14: Results from Test B – fully submerged, 62 days, 85 ⁰ C.....	94
Table 15: Results Test C – single strand, 62 days, 85 ⁰ C.....	99
Table 16: Results from Tests D open circuit corrosion potential.....	101
Table 17: Results from Test E galvanic corrosion current density.....	104
Table 18: Results from Tests F - open circuit corrosion potential (E_{corr}).....	107

CHAPTER ONE: INTRODUCTION

The constantly increasing use of electricity and the expansion of renewable energy sources are raising the demands on the electrical grid everywhere in the world. The grid in the U.S. is no exception. The increased demand will force the power industry to add new transmission lines and to upgrade, refurbish or replace existing transmission systems.

High-Temperature Low-Sag (HTLS) conductors may help ease the power shortage by delivering up to twice the current along the same rights of way and using the same towers (Jones, 2006). HTLS conductors offer less sag at high temperatures, higher annealing temperatures, and reduced resistance. They can replace conventional conductors with no or minimal modifications to structures and/or current right-of-ways. HTLS can thus significantly increase the rating of the transmission line with no or minimal licensing requirements or the public opposition to new right-of-ways. (Clairmont, 2008)

Most HTLS conductors use materials that are relatively new to the power industry, such as Polymer Matrix Composites (PMC) and Metal Matrix Composites (MMC). Even if these materials have a proven track record in other applications, there is a concern about the service life in the harsh service environment of transmission lines. (Jones, 2006)

Corrosion can be a problem both from a power transmission perspective and from a safety perspective. Localized elevated temperature can be caused by corroded aluminum wires or increased resistance in splices and joints. Corrosion can also promote fatigue cracking. Breakage of strands or lost cross-section will result in accelerated localized annealing and redistribution in mechanical loads. This may eventually lead to a catastrophic failure of the conductor, presenting a risk for people and property below the transmission line, as well as a risk for power blackouts. (Brennan, 2004)

This study has been requested by the sponsoring power utilities Western Area Power Administration (WAPA), Bonneville Power Administration (BPA) and Tri-State Generation and Transmission Association (Tri-State) because of the concern for the corrosion resistance of these new materials. Of particular concern is the possibility of galvanic corrosion between some of the new materials.

The original goal of the study was to compare the corrosion characteristics of three different HTLS conductors to a conventional ACSR conductor, but the very varying results from different tests show that much more work needs to be done before any conclusions can be made regarding the corrosion performance of HTLS conductors. The focus was therefore changed during the study to be an initial assessment of possible problems with galvanic corrosion in three HTLS conductors. The study does not aim to make any service life predictions. The conductors studied were selected and supplied to the project by the sponsoring utilities.

The study has also been partly financed by the National Science Foundation (NSF) through the *Grant Opportunities for Academic Liaison with Industry* (GOALI) project.

The study was performed at the University of Denver over the period 2011-2013.

1.1 High-Temperature Low-Sag (HTLS) conductors

1.1.1 Uprating by HTLS conductors

Sagging conductors touching overgrown trees has been a contributing factor in major power outages. This was the case in the large North American Blackout in 2003. A transmission line sagged and touched the top of a tree, causing a short circuit. The short circuit triggered a cascading chain of events that darkened eastern parts of the United States and Canada. (Jones, 2006) (Wald, 2004) The problem of sagging power lines has increased in recent years due to increased electricity demand and long-distance power transfer. The capacity has not kept pace with the increasing demand due to the difficulty of obtaining public approval for new rights-of-way. (Jones, 2006)

The overwhelming majority of the existing overhead transmission lines are 1950s vintage steel-reinforced aluminum conductors (ACSR). These conductors will only maintain sufficient strength and stiffness up to about 100°C. If the temperature goes higher, the steel will lose its yield strength and the power line sags. (Jones, 2006) For a very limited time, ACSR can be operated up to 125°C. (EPRI, 2002) If it sags too much, it might touch a tree or other object and trigger a blackout. (Jones, 2006)

Developed countries with major electrical infrastructures are confronted with three coinciding critical issues related to these existing conductors. The first is the age of the infrastructure. Most of the electrical grid was constructed after 1945, which results in the age of the assets being well over 50 years. This leads us to the second issue, which is that the design life of much of the infrastructure is about 50 years. In many cases it has matured beyond serviceability and/or economic life. It will need some form of life

extension. A life extension would have been much easier if it wasn't for the third issue – the need to increase the capacity of the grid. This situation places extraordinary demands on utilities to uprate the existing electrical infrastructure. (Brennan, 2004)

Line rating is the amount of power in terms of amps that a transmission line can transmit (or is allowed to transmit). The criterion for rating of transmission lines is the limitation of conductor temperature to a certain temperature. The reasons for the temperature limit are twofold: 1) Fear of losing strength (thermally limited), 2) Fear of exceeding clearance limits (clearance limited). (Clairmont, 2008)

The thermal rating of a transmission line can be increased (uprated) by replacing the original (typically) ACSR conductors with a high-temperature low-sag (HTLS) conductor of the same diameter. The advantages of HTLS conductors are: 1) they are capable of high-temperature continuous operating above 100°C without loss of tensile strength or permanent increase in the sag, 2) they have lower sag at high temperature, meaning that the ground and underbuild clearances can still be met despite a higher operating temperature. (EPRI, 2002) Figure 1 illustrates how HTLS conductors can be operated at higher temperature – and thus higher currents – with the same or less sag.

The *thermal* rating can be increased by 20 to 80 % of the existing transmission line when reconductored with an HTLS conductor. The degree of uprating depends on whether the replacement HTLS conductor is able to reach its maximum allowed operating temperature within the clearance limits. (EPRI, 2002) This means that up to twice the current can be transmitted using the same diameter conductor, the same towers and the same right-of-ways. (Jones, 2006)

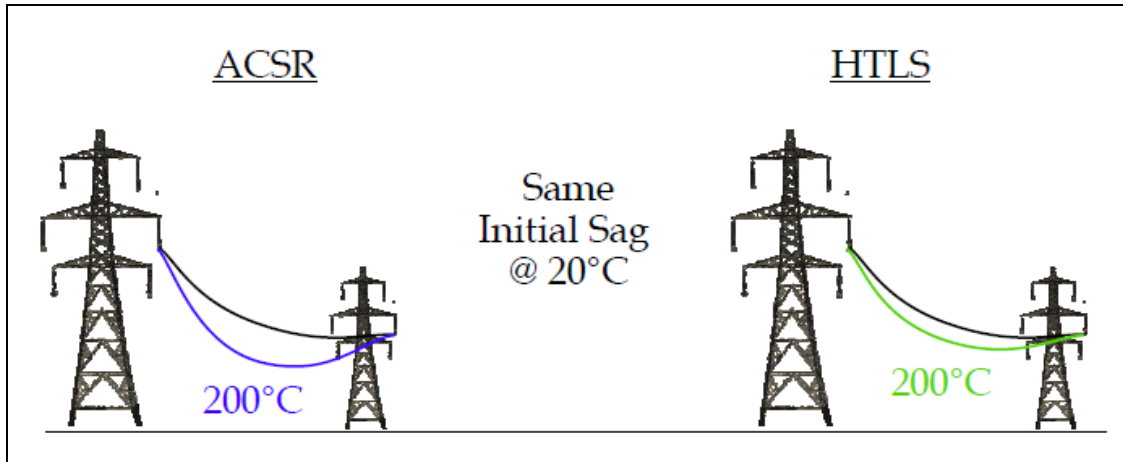


Figure 1: Thermal response of ACSR versus HTLS.
Source: (Lancaster, 2011)

Cost of HTLS

The cost of a HTLS conductor is 2 to 12 times higher than for a conventional ACSR conductor (see Figure 2). On the other hand, HTLS conductors can carry twice the current for a conductor of the same diameter and use the existing towers. (Clairmont, 2008) (Lancaster, 2011)

The greater current-carrying capacity will, in many cases, compensate for the considerably higher price. Despite its three times higher price, Utah Power found the HTLS conductors cost-effective because no new towers had to be erected. (Jones, 2006) The higher strength and lower weight also means that the towers can be further apart. According to CTC Global, manufacturer of ACCC HTLS conductors, a Chinese customer choose ACCC since they could use 16 % fewer towers. (Jones, 2006)

With a conventional design, the conductor itself represents 20 to 40 % of the total cost of a transmission line (Ergon Energy, 2013). This relation can change significantly with HTLS since the conductor is more expensive but fewer towers might be needed, as

the examples above demonstrate. With the higher price tag come higher expectations. The utilities want to know that these new novel materials will perform at least as well as the conventional conductor designs. If they don't, the utilities will want to know how to predict the service life to adjust the economic calculations.

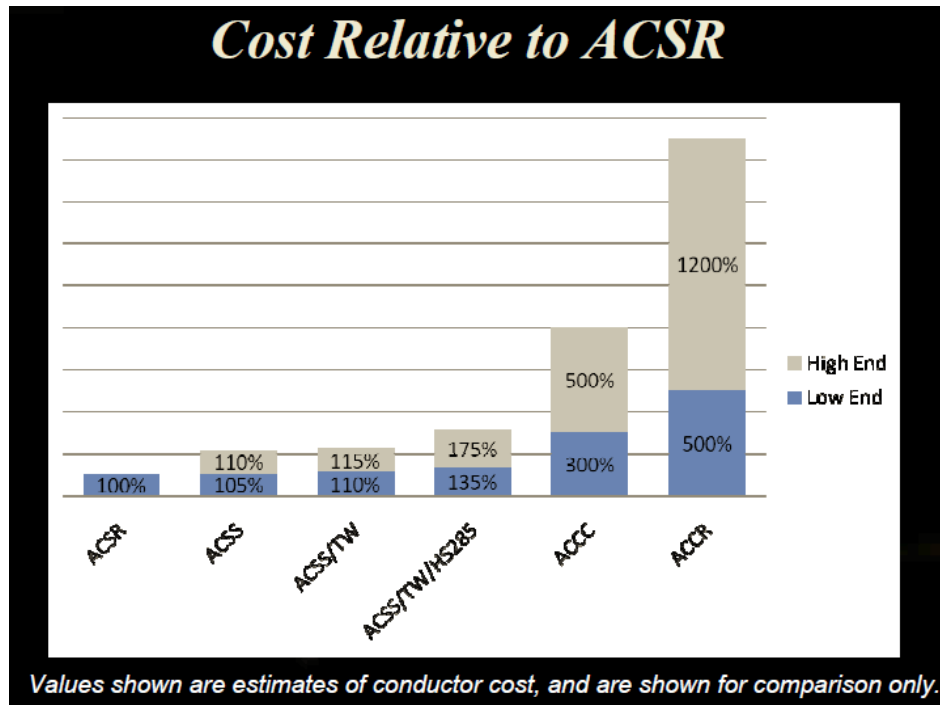


Figure 2: Cost of HTLS relative to ACSR.
Source: (Lancaster, 2011) (See Appendix B for acronyms)

HTLS Designs

HTLS conductors are characterized by their high-temperature capability without excessive sag. A combination of new materials and new designs are used to achieve this. The most prominent materials are strong and light advanced composite materials used so far principally by aerospace. The composites give stronger and lighter cores, enabling increased conductor aluminum cross-sections without increasing weight or diameter of

the conductor. That combined with the higher operating temperature – up to 200°C or higher – means up to twice the ampacity with less sag than before. (Jones, 2006)

There are a few manufacturers of HTLS conductors: Southwire (ACSS), 3M (ACCR), J-Power (Gap), LS Cable (Invar), and CTC (ACCC). (Clairmont, 2008) In this study, ACSS, ACCR and ACCC have been studied. Gap and Invar conductors have not been studied. The four studied conductors are described in detail in section 1.1.2.

New materials – new concerns

Aluminum replaced copper as the main material for overhead transmission lines at the turn of the 20th century. (Wolf, 2007) Since then, the steel-reinforced aluminum conductors, known as ACSR, have dominated and represent the overwhelming majority of the existing overhead transmission lines. (EPRI, 2002) With the introduction of the HTLS conductors, it is essentially the first time in 100 years that completely new materials are being used in high voltage conductors. Some HTLS conductors use novel materials that are relatively new to the power industry, such as PMCs or MMCs. Others utilize improved more classical materials such as high-strength steel. Even if these materials have a proven track record in other applications, there is a concern about the service life in the harsh environment of many transmission lines.

The most difficult obstacle for the new conductor technologies might be the attitudes of utility officials themselves. John K. Chan, project manager for overhead transmission cable at EPRI has shown skepticism regarding polymer core conductors from a splicing point of view, asking “Tell me how you connect plastics”. (Wald, 2004)

The asset value of the North American electricity infrastructure is more than \$1 trillion. The infrastructure serves over 100 million customers. There are more than 3,200 electric distribution utilities, more than 10,000 electric generating units with a combined annual production of 1 million MWh, and more than 300,000 miles of transmission lines with voltages of 139 to 765 kV. (Riggs Larsen, 2011) The enormous value of the grid and of the transmitted electricity makes the utilities hesitant to introduce new technology. “Typically, power utilities are very conservative”, John K. Chan said. “They don’t want anything without a proven record. You can imagine what happens if you have a blackout”. (Wald, 2004) For this reason, most utilities are taking a wait-and-see stance, particularly when it comes to the composite core conductors. The medium-term results of the early installations will help determine whether they want to make the switch. (Jones, 2006). It has historically taken at least 20 years for a new conductor design to go from inception to acceptance. Aluminum conductors with high-strength steel cores (ACSS) have recently been widely accepted among the utilities, despite the fact that the design was patented in 1969. (EPRI, 2002)

HTLS conductors will only be a viable alternative for large-scale installations if they can gain the power utilities’ confidence from a corrosion point of view. It has historically taken at least 20 years for a new conductor to go from inception to acceptance (EPRI, 2002). With the rapid increase in electricity demand, we cannot afford to wait 20 years for HTLS conductors.

1.1.2 The studied conductors

Four different conductors were tested and evaluated in this study:

- *ACCC - Aluminum Conductor Composite Core*
- *ACCR - Aluminum Conductor Composite Reinforced*
- *ACSS - Aluminum Conductor Steel Supported*
- *ACSR - Aluminum Conductor Steel Reinforced*

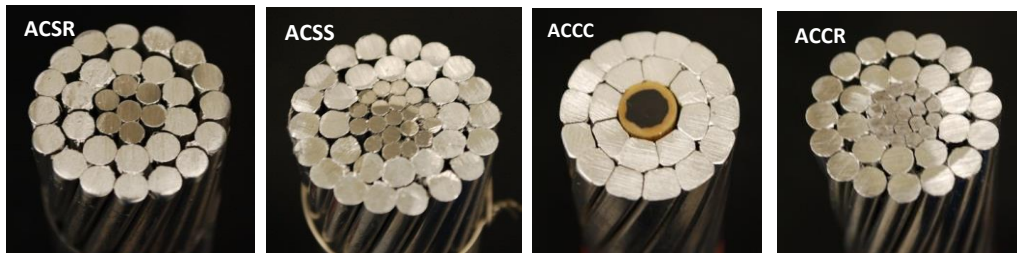


Figure 3: The four tested conductors.

The tested conductors consist of current carrying aluminum strands wrapped around cores of coated steel, MMCs, or PMCs (these components will hereafter be referred to as the “aluminum strands” and the “core”).

ACSR has a galvanized steel core surrounded by hard-drawn current carrying strands of 1350-H19 aluminum alloy. It was introduced in 1907 and is still the most widely used conductor type. (Thrash, 2013) The conductor can have multiple layers of strands, depending of the size of the conductor. (Taihan Electric Wire Co Ltd, 2013) The tested specimen has 7 steel strands and 26 aluminum strands and was not treated with corrosion-resistant grease.

ACSR is a conventional conductor (not HTLS) and was used as the baseline comparison in this study.

ACSS has a very similar design to the traditional ACSR conductor, but the core is of Galfan-coated high strength steel instead of galvanized steel. It can be operated at 250°C continuously without losing strength. (Lancaster, 2011) “Galfan” is a zinc-5 % aluminum-mischmetal-alloy (Matweb 3. , 2013). The current carrying aluminum strands are made of 1350-O fully annealed aluminum. The chemical composition is identical to the 1350-H19 alloy in ACSR, but the heat treatment is different. Just like ACSR, ACSS is available in different sizes with different numbers of strands and layers. The tested specimen had 19 steel strands and 30 aluminum strands, and it was not treated with grease.

ACCC is based on a PMC core with a diameter of approximately 9.5 mm (3/8”). The hybrid material with a unidirectional carbon fiber/epoxy composite in the middle and a fiberglass/epoxy composite on the outside is manufactured through simultaneous pultrusion. The final core is a straight solid and stiff but bendable rod, very similar to a fishing rod or golf club shaft. ACCC is the only one of the four studied conductors where the core does not contribute to the conductivity.

The fiberglass composite layer serves as a galvanic corrosion barrier between the carbon fiber composite and the surrounding aluminum strands. The composite matrix is a high temperature epoxy and the conductor can be operated at up to 180°C, according to the manufacturer.

The ACCC conductor is always stranded with trapezoidal strands (CTC-Global, 2012) (the other tested conductors are also available with trapezoidal strands). The tested specimen has 22 aluminum strands.

ACCR has a MMC core surrounded by current-carrying strands of Aluminum-Zirconium (Al-Zr) alloy. The mechanical properties of the Al-Zr alloy are similar to hard-drawn 1350-H19, but the annealing temperature of the Al-Zr alloy is over 230°C compared to about 90°C for 1350-H19. ACCR can be operated continuously at 210°C. The emergency operation temperature is 240°C, and is allowed during 1000 hours cumulative over the life of the conductor. (3M, 2012)

The composite core consists of unidirectional, continuous aluminum oxide fibers (α -Al₂O₃) in a high-purity aluminum matrix. The fiber diameter is approximately 12 μ m and the volume fraction of fibers is 50-55 % (Deve, 2013). Both the composite core and the aluminum alloy outer strands contribute to the strength and conductivity. (3M, 2012) The tested specimen has 19 composite strands in the core and 26 aluminum-zirconium strands, and was not treated with grease.

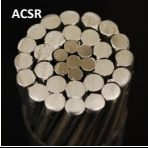
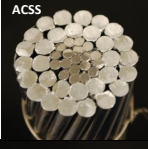

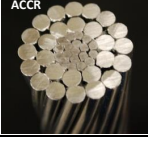
According to the manufacturer, the ACCR conductor has very good corrosion resistance, similar to an all-aluminum conductor. (3M 2. , 2005) Since both current carrying strands and the core are aluminum based, the manufacturer states that "... there is no galvanic coupling between the core and the stranded aluminum wires, which would also be subject to corrosion." (3M Composite Conductor Program, publication date unknown) ACCR is currently being tested in the salt air in Hawaii (Wald, 2004), where

the constant trade winds from the ocean create a very corrosive environment (McCullough, 2005). The manufacturer concludes that static dynamic and environmental resistance of ACCR meets or exceeds the performance of ACSR (Johnson, 2010).

All these three types of HTLS conductors are installed in longer or shorter sections in the U.S. and in other parts of the world. 34,000 miles of ACSS is installed in the U.S. (data from 2008) (Clairmont, 2008), while the total installed length of ACCR is currently about 1600 miles (Deve, 2013).

The tested specimen of ACSS was of Redwing 795 kcmil size, while the other three were Drake 795 kcmil conductors. All tested samples came from new and unused conductors, but the ACCC and ACSS specimens had been stored outdoors for several years.

Manufacturer information regarding the tested specimens can be requested from the Western Area Power Administration for the ACCC, ACCR and ACSR specimens and from the Bonneville Power Administration for the ACSS specimen.

Table 1: Main features of the studied conductors.					
Type	Abbreviation	Full name	Material for current carrying strands	Material for load bearing core	Cross-section view
Conv. conductor	ACSR	Aluminum Conductor Steel Reinforced	Aluminum alloy 1350-H19	Galvanized steel strands.	
HTLS conductor	ACSS	Aluminum Conductor Steel Supported	Aluminum alloy 1350-O	High-strength steel strands coated with 5 % aluminum-mischmetal-alloy (also known as “Galfan” (Matweb 3. , 2013)).	
	ACCC	Aluminum Conductor Composite Core	Aluminum alloy 1350-O	Hybrid polymer matrix composite with carbon fibers in the middle and fiberglass on the outside. Approx. 65 % fiber fraction.	
	ACCR	Aluminum Conductor Composite Reinforced	Aluminum-Zirconium alloy	Metal-matrix composite strands – α -Al ₂ O ₃ fibers in a high-purity aluminum matrix. Approx. 50-55 % fiber volume fraction.	

1.2 Corrosion of high voltage conductors

1.2.1 Previous corrosion studies

It has been difficult to obtain a clear picture of the corrosion problems of high voltage conductors, even for the conventional designs such as ACSR, which has been in use for over 100 years. While some investigators claim that they last “forever” and that degradation of towers and insulators is a bigger concern (Wald, 2004), others say that corrosion is the major factor in the degradation of transmission lines (Moreira, 2008) (Mayer, 1998). The difference in opinion is likely caused by the large variations in the corrosive nature of different environments.

A selection of studies of conventional conductors is presented below. With the exception of the manufacturer’s own testing of ACCR (Colbert, 2005), no corrosion study of HTLS conductors has been found.

The service environment is critical

All parts of the transmission line such as conductors, towers, insulators etc. can corrode or degrade, but the conductor itself is often the most vulnerable component. The service life of the entire transmission line is often limited by deterioration of the conductor. Both the aluminum strands and the steel core in ACSR are prone to corrosion. (Mayer, 1998) The design life for a conventional ACSR conductor is about 50 years. Many installed conductors have exceeded their forecasted mean useful life. The consequences are decreased reliability of the system and public safety. Studies have

shown that outages increase 3-5 times in conductors that are 70-80 years old compared to conductors that are 10-30 years of age. (Harvard, 1991) However, the key factor in conductor corrosion is moisture and pollution. As long as the conductors are kept clean they can last up to 100 years. In these cases, the insulators and towers might fail before the conductors, particularly if they are hung from wooden towers. Wooden towers often start to rot after about 40 years. (Sutton, 2010)

Industrial and marine environments are significantly more corrosive to transmission line conductors than rural environments. The two principal atmospheric pollutants that increase the corrosion rate are chloride ions and sulfur compounds. (Moreira, 2008) (Rhaiem, 2012) In coastal areas the aluminum suffers from accelerated corrosion, while in inland industrial areas the corrosion of the galvanized steel core is more prevalent. (Mayer, 1998) The content of NaCl in the atmosphere can be one to two orders of magnitude larger in coastal and marine environment than in rural, urban and industrial environments. (Moreira, 2008) NaCl and other salts can also be present on transmission lines close to highways treated with de-icing salt. (EPRI 2. , 2000) The corrosion rate can vary along the conductor with higher rates in areas of higher pollution and in areas with sudden temperature and/or humidity changes. (Moreira, 2008)

A study performed by Ontario Hydro, Canada of aluminum strands for ACSR conductors that have been in service for 61-69 years showed pitting corrosion damage. The urban-industrial environment caused the largest corrosion depth, while rural and semi-rural environments caused less corrosion damage (Harvard, 1991).

In a study from Venezuela of a 400 kV transmission line located in a coastal environment, 20 samples of aluminum-based conductors were placed next to the transmission line in two different locations. The samples were evaluated after 10, 12 and 14 months. During these time periods, the amount of chloride (Cl^-) and sulfates (SO_2) in the atmosphere as well as the humidity were measured. At 14 of the 17 test stations, a humectation time of over 5000 h/year and high concentration of chlorides and sulfates were measured. These parameters indicate that 80 % of the stations were in an atmosphere categorized as corrosiveness grade C4 – “high”. (Linares, 2006) The conductor samples showed large corrosion pits in the aluminum. The pits were deeper in the 14 month samples than in the 10 months samples. (Linares, 2006)

As the Venezuelan study above indicates, the so called “time of wetness” or humectation time (TDH) is highly affecting the corrosion rate. TDH is evaluated based on relative humidity and temperature. TDH is defined as the number of hours per year that the relative humidity is over 80 % and the temperature is $\geq 0^\circ\text{C}$. Electrolytic corrosion, which completely dominates in conductor corrosion, can only occur when there is water present on the conductor. (Moreira, 2008) The large differences in humidity between different areas of the U.S. are likely the reason for the different opinions about corrosion problems of transmission lines. A power company operating in Phoenix, Arizona will have a completely different experience of corrosion than a utility in Portland, Oregon or Oahu, Hawaii.

1.2.2 Cost of corrosion

The annual cost of corrosion in the world is estimated to \$2.2 trillion (Goch, 2013). In the U.S. alone, the cost is estimated to be \$276 billion annually, of which \$6.9 billion is in electrical utilities (NACE, 2002). Although no exact number could be found for the cost of corrosion of transmission line conductors, the cost is definitely significant for the power utilities – a cost that is passed on to the customers.

1.2.3 Corrosion protection

The strands in the conductors can be protected by a sacrificial coating made from a less noble metal. If the strands are made of an aluminum alloy, a pure aluminum clad coating may protect the aluminum alloy due to the sacrificial anode effect. Such a coating works well even if it is imperfect (Isozaki, 2008) (Davis, 1999). The entire conductor can also be protected by anti-corrosive grease in corrosive environments (Isozaki, 2008), (Taihan Electric Wire Co Ltd, 2013), (Karabay, 2004), (EPRI 2. , 2000).

The load bearing steel core wires in ACSR are protected by galvanization. The average life for the galvanization is 40-50 years, depending on the environment. (Riggs Larsen, 2011) The coatings are available in different weights. The standard is weight class A, but weight class B and C as well as aluminum clad steel are also available for high corrosivity areas such as industrial zones or coastal areas (Thrash, 2013).

For highly corrosive areas, more expensive all-aluminum conductors are sometimes used. All-aluminum conductors have better corrosion resistance since they are

mono-metallic and do not suffer from galvanic corrosion (Rhaiem, 2012), (Ergon Energy, 2013), (Thrash, 2013), (Karabay, 2004).

Every kind of corrosion protection makes the conductor more expensive. The fact that there is a market for the more expensive corrosion-protected conductors shows that there are clearly problems with corrosion in certain environments.

1.2.4 Monitoring for corrosion

The most common method of inspection of overhead transmission lines is visual assessment. It can be performed from the ground or from the air. (Mayer, 1998) The main problem with visual inspection is that corrosion of conductors remains hidden from view until a very advanced stage (Karabay, 2004).

Thermal imaging, often deployed from helicopters, is used to inspect for aluminum corrosion. This method can only detect severe corrosion with many strands distorted and bulging. Early stages of corrosion damage cannot be detected with this method. (Mayer, 1998)

There are some methods available to detect corrosion in ACSR conductors through measurement of the magnetic properties of steel and zinc with remote controlled devices. However, experience has shown that the corrosion has to be quite severe to be detected by this method. The internal corrosion is practically undetectable for the first 30 years of a conductor's lifetime. The method does only work on ACSR conductors. (EPRI 2. , 2000) For all other conductor types, only visual and thermal camera inspection appears to be currently available.

1.3 Galvanic corrosion and other corrosion mechanisms in HV conductors

The term “corrosion” is often used in relation to metals, but today’s corrosion specialists also talk about “corrosion” of non-metallic materials such as polymers, ceramics glasses and composites. “Corrosion” comes from the Latin’s “corrodere”, which means “to eat away” (Groysman, 2010).

This study concentrates on corrosion of metals, and the term “degradation” or “aging” is going to be used for the breakdown of other materials such as polymers or PMCs .

Some of the corrosion literature makes a clear difference between a “metal” and an “alloy”. A metal is a pure element such as iron, nickel, aluminum etc., while an alloy is a material having metallic properties and composed of two or more elements of which at least one is a metal. (Groysman, 2010) However, this thesis is using the term “metal” both for pure metal and for alloys.

1.3.1 Corrosion – a natural phenomenon

The metal in high voltage conductors and other aluminum and steel structures *wants* to corrode. Most metals occur in nature as minerals and ores. The mineral or ore is a more favorable form, from an energy perspective, and large amounts of energy are needed to covert, for example, aluminum ore to aluminum. This high energy state in the metallic form is the driving force of corrosion. The energy used in the production of the metal is returned when the metal corrodes and reverts back to its original state in which it was found. The energy stored in the metal is relatively large for metals such as aluminum

and iron, and relatively low for metals such as gold, silver, and copper (see Figure 4: Positions of some metals in order of energy required to convert their oxides to produce 1 kg of metal.) The higher the energy, the higher is the metals tendency to release this energy by corrosion. (Roberge, 2008)

	Metal	Oxide	Energy (MJ kg ⁻¹)
Highest Energy	Li	Li ₂ O	40.94
	Al	Al ₂ O ₃	29.44
	Mg	MgO	23.52
	Ti	TiO ₂	18.66
	Cr	Cr ₂ O ₃	10.24
	Na	Na ₂ O	8.32
	Fe	Fe ₂ O ₃	6.71
	Zn	ZnO	4.93
	K	K ₂ O	4.17
	Ni	NiO	3.65
	Cu	Cu ₂ O	1.18
	Pb	PbO	0.92
	Pt	PtO ₂	0.44
	Ag	Ag ₂ O	0.06
Lowest Energy	Au	Au ₂ O ₃	-0.18

Figure 4: Positions of some metals in order of energy required to convert their oxides to produce 1 kg of metal.
Source: (Roberge, 2008)

Gibbs Free Energy

A better way to look at the corrosion process is from the perspective of Gibbs free energy. The change in Gibbs free energy in going from reactants to reaction products can be used to predict the possibility for a corrosion reaction. Only when the change in Gibbs free energy is negative ($\Delta G^\circ T < 0$), *can* the corrosion reaction happen spontaneously. However, the negative value of the Gibbs energy change only points out the *possibility* of the reaction, not its *probability* or rate. Kinetic restrictions always prevail over thermodynamic possibilities. (Groisman, 2010)

1.3.2 Corrosion reactions in neutral electrolytes

Most corrosion of metals occurs in the presence of aqueous solutions such as rain, seawater or process water. This is called *corrosion in the presence of aqueous electrolytes*. Corrosion of metals can also occur in the presence of *non-electrolytes* such as O₂, Cl₂, or acetone. (Groysman, 2010) This study is focusing only on corrosion in the presence of aqueous electrolytes.

Corrosion mechanisms in electrolytes are often dependent on pH. The tests performed in this study used electrolytes that had a pH close to neutral. The following sections will cover corrosion mechanisms of mainly aluminum in a neutral electrolyte containing NaCl.

Electrochemical corrosion

Corrosion of metals is almost always an electrochemical process, which means that it is a chemical reaction involving transfer of electrons. Corrosion is also a process that involves simultaneous oxidation and reduction. (Roberge, 2008)

The oxidation and reduction can occur on different metals that are in electrical contact. This is the case in galvanic corrosion (more about galvanic corrosion in section 1.3.3). The oxidation and reduction can also occur on the *same* metal, as illustrated in Figure 5. (Roberge, 2008)

Oxidation occurs at the anodic site where ions form and electrons are released, which causes deterioration of the metal. The simultaneous reaction at the cathodic site consumes the electrons generated at the anode. The two sites have to be in direct

(metallic) electrical contact for the transfer of electrons, and in contact through the electrolyte for transfer of ions. The oxidation and reduction processes will have equivalent rates. (Roberge, 2008) It is a common misconception that the flow of electricity through the electrolyte also is a flow of electrons. This is not correct. The conduction of electricity through the electrolyte – which balances the flow of electrons through the metal – is a flow of *ions*. If there is no water and/or no ions, no corrosion will take place. (Groisman, 2010)

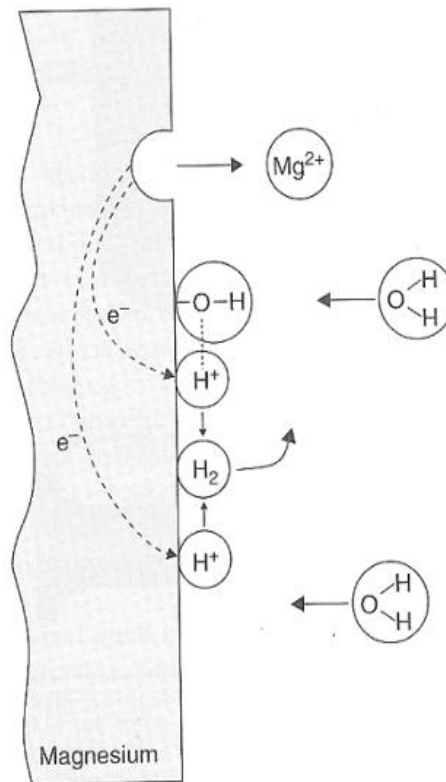
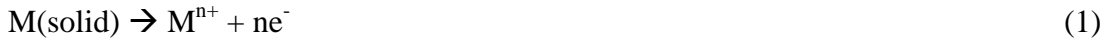


Figure 5: Splitting of water during corrosion of magnesium.
Source: (Roberge, 2008)

Aluminum will be used as an example to demonstrate the nature of corrosion with simultaneous oxidation and reduction reactions.

Anodic reactions

The general anodic reaction during corrosion is:



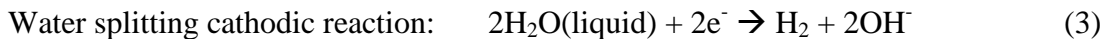
where the value of n depends on the nature of the metal (it is always 3 for aluminum, while it can vary for iron). (Roberge, 2008)

For aluminum, the anodic reaction is:



Cathodic reactions

There are a number of different possible cathodic reactions. The reaction depends both on the metals involved and environmental factors such as pH and dissolved oxygen. The anodic corrosion of aluminum in neutral electrolytes sometimes develops enough energy to split water directly on the cathodic site. Figure 5 illustrates this process using the corrosion of magnesium as an example.



Another very common cathodic reaction in neutral or basic solutions exposed to the atmosphere is oxygen reduction:

The oxygen reduction cathodic reaction is: $O_2 + 2H_2O + 4e^- \rightarrow 4OH^-$ (4)

(Roberge, 2008)

All the cathodic reactions have one thing in common – they consume the electrons released in the anodic reaction(s). There can be multiple cathodic reactions, as well as multiple anodic reactions occurring simultaneously. (Roberge, 2008)

Combined reaction for aluminum

On a global level, the corrosion reaction is the sum of the anodic and cathodic reactions. (Vargel, 2004) The two most likely combined reactions for corrosion of aluminum components of the high voltage conductors tested in this study are the following:

Splitting of water:

Anodic reaction: $Al(\text{solid}) \rightarrow Al^{3+} + 3e^-$

Cathodic reaction: $2H_2O(\text{liquid}) + 2e^- \rightarrow H_2 + 2OH^-$

Overall corrosion reaction (balanced): $2Al + 6H_2O(\text{liquid}) \rightarrow 2Al(OH)_3 + 3H_2$

Reduction of oxygen:

Anodic reaction: $Al(\text{solid}) \rightarrow Al^{3+} + 3e^-$

Cathodic reaction: $O_2 + 2H_2O + 4e^- \rightarrow 4OH^-$

Overall corrosion reaction (balanced): $4Al + 3O_2 + 6H_2O(\text{liquid}) \rightarrow 4Al(OH)_3$

Both reactions result in the formation of aluminum hydroxide $\text{Al}(\text{OH})_3$ ¹.

Aluminum hydroxide is insoluble and precipitates as a white gel. Either or both cathode reaction can occur at the same time. (Vargel, 2004)



Figure 6: Formation of $\text{Al}(\text{OH})_3$ on the ACCC sample.

¹ Powder X-ray Diffraction (XRD) of the dried corrosion products supports the suggested reactions. The pattern displayed matches for gibbsite, boehmite and bayerite, which are all forms of aluminum hydroxide. However, the XRD pattern was somewhat inconclusive since there was also a large amorphous phase present. There could therefore have been other corrosion products present that could not be identified with XRD.

1.3.3 Galvanic corrosion

When two different metals are in contact with each other and an electrolyte such as rain or moisture is present, galvanic corrosion may occur. This may also be the case for a metal and a nonmetallic conductor such as a carbon fiber composite. Galvanic corrosion is named after Luigi Galvani, who discovered the effect. Galvanic corrosion is caused by the difference in the susceptibility of two metals to corrode. (Roberge, 2008)

Galvanic corrosion is often listed as its own form of corrosion, but should really be considered a corrosion *mechanism* rather than a corrosion *reaction*. Galvanic corrosion is a mechanism that accelerates corrosion, including pitting and crevice corrosion, but does not otherwise change the type of corrosion. (The galvanic action simply accelerates the corrosion rate, making an existing corrosion problem even worse). (Davis, 1999)

When a metal is in electric contact with a more noble material, the less noble material corrodes more rapidly than it would have done in the absence of the more noble material. Galvanic corrosion can be severe in highly conductive aqueous media such as seawater and salt spray from de-iced highways. When salt is not present, the galvanic corrosion is rarely significant. (Davis, 1999)

Galvanic corrosion can be compared to the function of a battery with its two electrodes and the electrolyte. Three conditions must be met simultaneously for galvanic corrosion to take place (Vargel, 2004):

- two metals of different nature,
- presence of an electrolyte,
- electrical continuity.

If one of these three conditions is not met, galvanic corrosion will not occur. For example, if the two metals are not in direct electrical contact with each other, no electrons can flow and no anodic or cathodic reaction will take place. If there is no water present, no ions can flow and no reaction will take place.

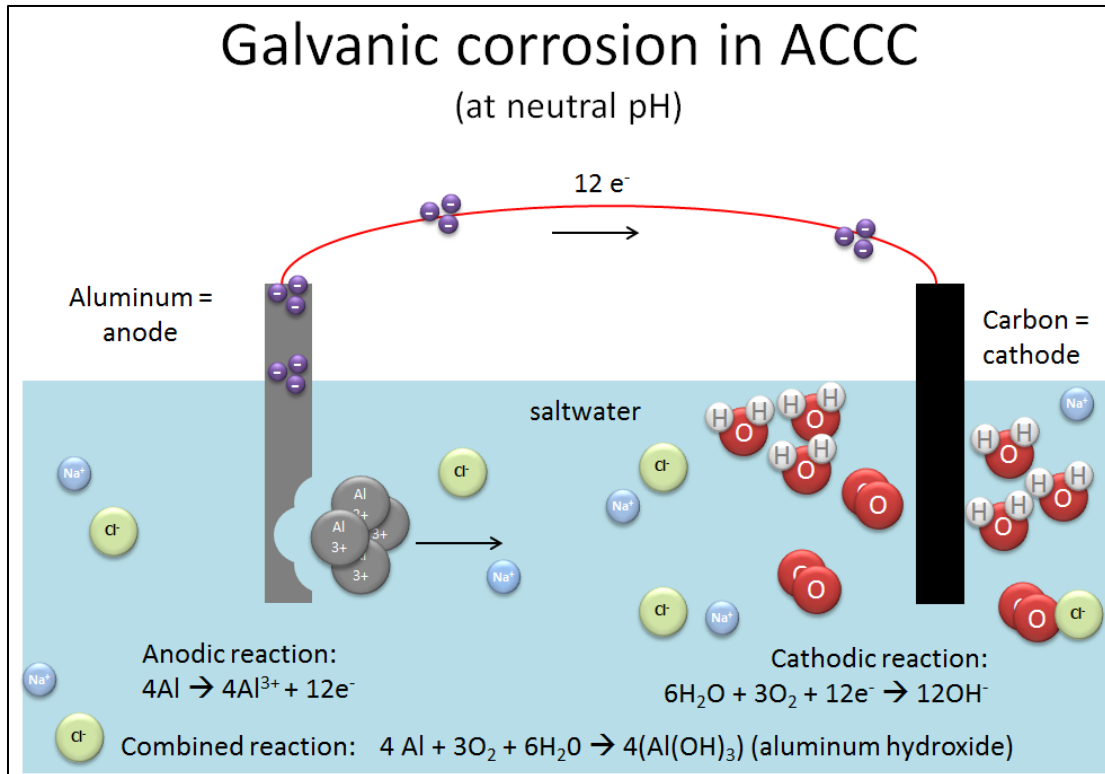


Figure 7: Principle of galvanic corrosion between aluminum and graphite in saltwater.

Galvanic series

The galvanic series (Figure 8) can be used to predict the *possibility* of galvanic corrosion. Experience shows that galvanic corrosion may be a problem if two metals in direct contact have a difference in corrosion potential (ΔU) of more than 100-250 mV. (Groysman, 2010), (Vargel, 2004) It should be noted that the open circuit potential only

predicts the *possible direction* of galvanic corrosion. The potential difference is grossly inadequate for predicting the magnitude of galvanic corrosion since it does not take into account factors such as polarization and area ratio effects (Roberge, 2008).

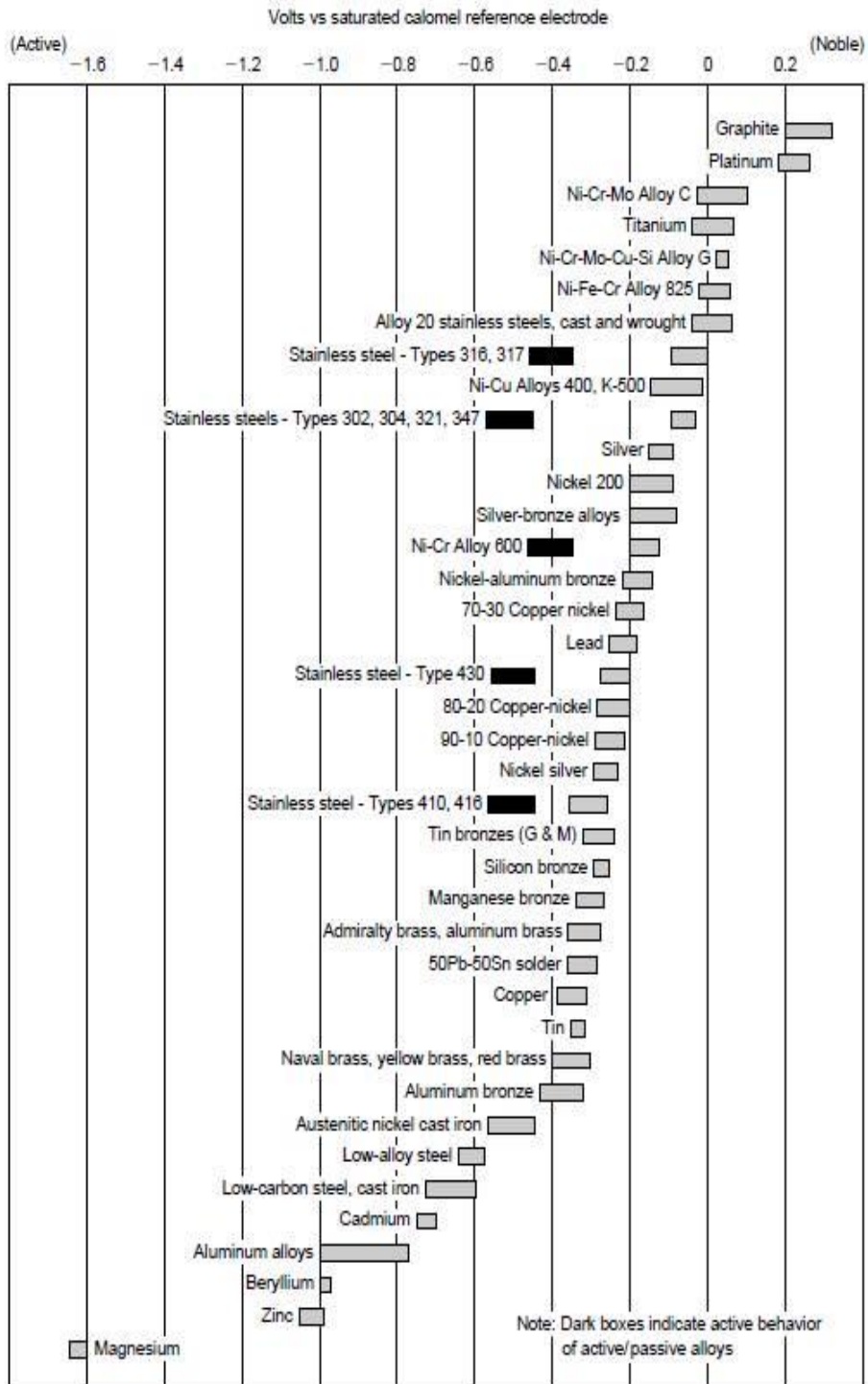


Figure 8: Galvanic series.

Electromotive force series for metals and alloys in sea water at 5-30°C (dark boxes indicate active behavior of active-passive alloys). Source: ASTM Note that other temperatures and other electrolytes may give different values.

Electromotive force ΔU or E

The electromotive force E (or sometimes called ΔU (Mandel, 2012)) is the difference between the electric potentials of the cathodic reaction and the anodic reaction. It is this potential difference that drives the galvanic corrosion. (Groysman, 2010)

The electromotive force E is related to Gibbs free energy by the following equation (known as the Nernst equation):

$$\Delta G = - n F E \quad (5)$$

where ΔG is the change of Gibbs free energy, n is the number of moles electrons taking part in the reaction and F is Faraday's constant ($9.6483399 \times 10^4 \text{ C mol}^{-1}$). (Groysman, 2010)

Differential concentration cells

Galvanic corrosion is typically associated with dissimilar metals, but galvanic corrosion can under certain conditions also occur on the *same* metal. Acceleration of corrosion can also be caused by phenomena known as differential aeration cells and concentration cells. The difference in concentration of some component in the electrolyte leads to discrete cathodic and anodic regions on the same metal, which accelerates the corrosion. (Goch, 2013) (NACE/ASTM, 2012) Pitting and crevice corrosion (covered in section 1.3.4) can be seen as galvanic corrosion on a micro scale.

Galvanic corrosion kinetics

While the thermodynamics determine if a corrosion process can occur, the *kinetics* controls the rate of the corrosion process. Measurement of the galvanic current will give information about corrosion rate, but the interpretation is difficult since the rate of the corrosion, and thus the flow of the current, can be controlled by one or more of the following: (Gamry Instruments, 2011)

1. **Concentration polarization**, also known as “**diffusion controlled**”, where the rate of the reaction is controlled by the rate at which reactants arrive at the metal or graphite surface. The diffusion of oxygen at the cathode (the carbon fibers in the case of ACCC) is often not fast enough to sustain the highest possible rate of corrosion. In that case, the corrosion rate is diffusion limited.
2. **Oxide formation**, which may or may not lead to passivation, can alter the surface of the material(s) and therefore change the rate or nature of the corrosion.
3. **Other effects** such as preferential dissolution of one alloy component can also change the rate or the nature of the corrosion.
4. A **mixed process** where more than one cathodic or anodic reaction occurs at the same time might complicate the model and the interpretation. One example is the simultaneous reduction of oxygen and hydrogen ions. (Gamry Instruments, 2011)

Surface area effect

The anodic and cathodic processes happen simultaneously, and the electrons released at the anodic site are immediately consumed at the cathodic site. There is no net accumulation of charges anywhere. The anodic current is always equal to the cathodic current. However, this does not mean that the current densities are equal. If the anodic and cathodic surfaces have different areas, they will have different current densities (Roberge, 2008).

The implications of the surface area ratio can be severe in certain corrosion situations. The effect of a certain amount of anodic current will be much greater when concentrated on a small area than spread over a much larger area. Another possible implication of a much smaller anodic area is less cathodic polarization, which will help maintaining the voltage of the galvanic couple at a value close to the open circuit potential. The much smaller anodic area gives rise to a particularly vicious form of galvanic corrosion. A very large cathode area connected to a very small anode area is the most unfavorable ratio in most practical corrosion situations. (Roberge, 2008)

Influence of conductivity

The conductivity of the electrolyte is an important parameter in galvanic corrosion. The electrical resistance of the electrolyte affects the corrosion rate. Ohm's law is applicable for aqueous solutions. The lower the resistance (R), the higher the corrosion current (I_{corr}):

$$I_{\text{corr}} = V/R = (E_k - E_a)/R \quad (6) \text{ (Groisman, 2010)}$$

where I_{corr} is the corrosion current, V is the electromotive force of the reactions (the difference between the cathodic potential E_k and the anodic potential E_a), and R is the resistance of the electrolyte.

As mentioned above, the corrosion current through the electrolyte is a flow of ions, not electrons. Therefore, the electrical conductance (the inverse of the resistance) in aqueous solutions is determined by the mobility of ions, not electrons. The higher the mobility of ions, the higher the ability to carry the electric corrosion current between the anodic and cathodic sites and the greater the galvanic corrosion and the more aggressive the solution is towards the metals. (Groysman, 2010), (Vargel, 2004)

Influence of temperature

In general, all metals become more electronegative in saltwater with increased temperature. (Schumacher, 1979) An increase in temperature is often expected to increase the galvanic corrosion rate. However, an increase in temperature decreases the solubility of oxygen, which will decrease the corrosion of steel. Increased temperature can also promote the formation of the natural oxide layer. Extended periods of high temperature can also change the microstructure and thereby also the corrosion behavior. The influence of temperature on the corrosion rate is clearly complex. (Vargel, 2004)

Dissolved oxygen

As can be seen in the reactions presented in previous sections, oxygen often plays a big role in corrosion. Corrosion of metals such iron occurs only if dissolved oxygen is present. (Vargel, 2004), (Roberge, 2008)

For aluminum, the situation is more complex. The corrosion of aluminum is governed by the oxide layer. While dissolved oxygen may increase the corrosion rate due to an increase in the cathodic reaction, dissolved oxygen will also promote the formation of the oxide layer that reduces the corrosion rate. (Vargel, 2004) Just as with temperature, the influence of dissolved oxygen may be complex.

Effect of pH

The pH is a very important factor in corrosion. Steel has poor corrosion resistance in acidic aqueous solutions, while aluminum has poor corrosion resistance both in highly acidic and highly alkaline media. (Vargel, 2004)

Passivation

By means of the phenomenon known as passivation, the galvanic current can change by six orders of magnitude during a corrosion experiment. Passivation is the formation of a stable oxide layer on the surface of the metal, which prevents further corrosion. In some cases, the oxide layer can break in local areas allowing significant corrosion to occur in a small area. This is called pitting corrosion. (Gamry Instruments, 2011)

Faraday's Law – mass loss calculations from galvanic current

The mass loss due to galvanic corrosion can be calculated using Faraday's law (7) (Vargel, 2004):

$$m = \frac{1}{F} \cdot \frac{A}{n} \cdot I \cdot t \quad (7)$$

where

m is the mass lost [g]

A is the atomic mass of the metal (27 g/mole for aluminum)

n is the valency (3 for aluminum)

I is the current [A]

t is the time [s]

F is the Faraday constant (96 485 C/mol)

To use Faraday's law to calculate loss of thickness due to corrosion, the corrosion has to be uniform. This is typically not the case for aluminum in neutral saltwater.

Faraday's law can still be used to calculate the loss of mass, but the results have to be interpreted with caution and one must keep in mind that the law may dramatically underestimate the problem when localized corrosion occurs. (Vargel, 2004) (Gamry Instruments, 2011)

1.3.4 Corrosion of aluminum

Aluminum, which is a major component in all the tested conductors, is a thermodynamically reactive metal with such a complex corrosion behavior that it deserves its own section. Despite its reactive nature, aluminum has generally excellent corrosion resistance due to the naturally formed passive oxide film on its surface. (Davis, 1999) The passive film is, however, susceptible to localized breakdown resulting in accelerated corrosion of the underlying material. This is typically called pitting corrosion if the attack initiates on an open surface and crevice corrosion at an occluded site. (Frankel G.S., 2003)

Pitting corrosion

Pitting corrosion occurs both during permanent and intermittent contact with aqueous media containing Cl^- ions such as seawater, rain water and humidity (Vargel, 2004). Aluminum is prone to pitting and crevice corrosion in aqueous electrolytes with neutral or close to neutral pH (4.0 to 8.5) (Davis, 1999), which basically includes all natural environments such as seawater, surface water and moist air (Vargel, 2004). The severity of the pitting corrosion depends more on the quantity of chlorides or other anions than on pH variations. (Vargel, 2004) At pH below 4.0 and above 8.5, the corrosion of aluminum is more uniform and can be very rapid since the oxide layer is not stable at these pH levels. (Davis, 1999)

Pitting and crevice corrosion are autocatalytic in their nature. Once the passive film is broken and the pit starts to grow, the local environment is altered in such a way

that further pit growth is promoted. The pit growth rate is often limited by the mass-transport of metal ions from the pit. (Frankel G.S., 2003)

Pitting corrosion is an example of an active-passive cell, in which the anode is the metal in the active state and the cathode is the same metal in the passive state (NACE/ASTM, 2012). A similar phenomenon can also occur on a more global level between two similar or identical aluminum alloys. If one of the materials has a problem maintaining its passivity for some reason, the difference in corrosion potential (E_{corr}) between the two metals can result in an electromotive force that accelerates the corrosion. The result will be more severe corrosion of the active material, which will work as a sacrificial anode and protect the more passive material. The corrosion may in its turn cause a change of the environment (such as decreased pH at the corroding site) that even further accelerates the corrosion. (Davis, 1999)

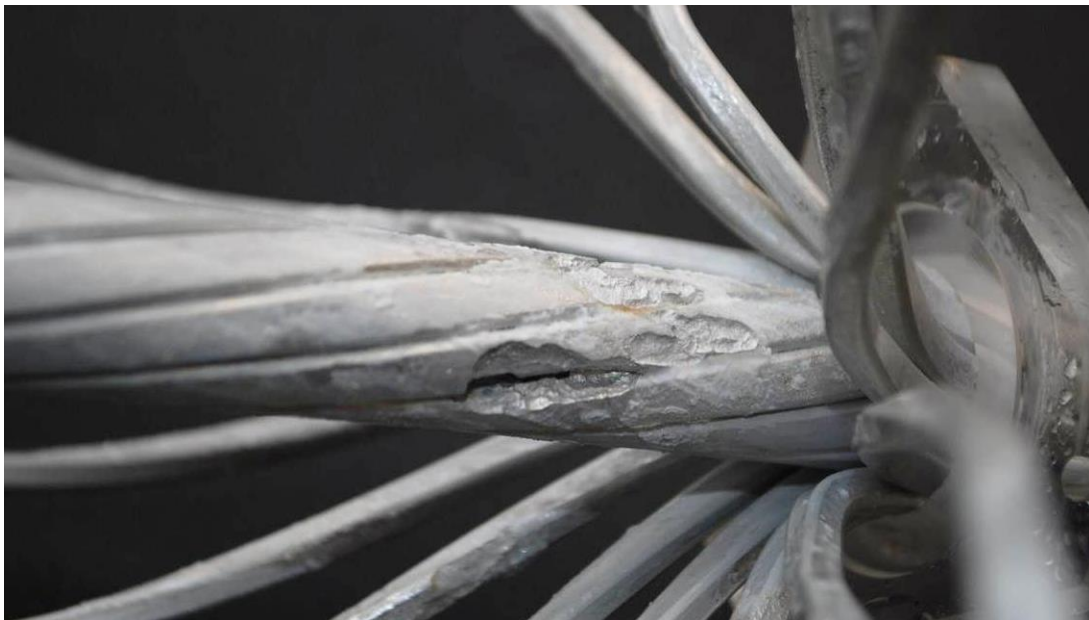


Figure 9: Typical pitting corrosion of aluminum.
The strands of an ACCC conductor after 3 months submersion in 85°C, 3 wt. % seasalt aqueous solution.

Effect of microstructure

The breakdown of the passive film on aluminum can be strongly affected by alloying and microstructure. Corrosion pits initiate at physical or chemical inhomogeneities on the surface. Scratches, inclusion, dislocations, second-phase particles, intermetallic particles and grain boundaries can all initiate pitting corrosion. Rough surfaces are also more susceptible to pitting corrosion than smooth surfaces. (Vargel, 2004), (Frankel G.S., 2003) Aluminum-matrix composites for the above reason are often very susceptible to corrosion (more about corrosion of aluminum matrix composites in section 1.3.5). (Davis, 1999)

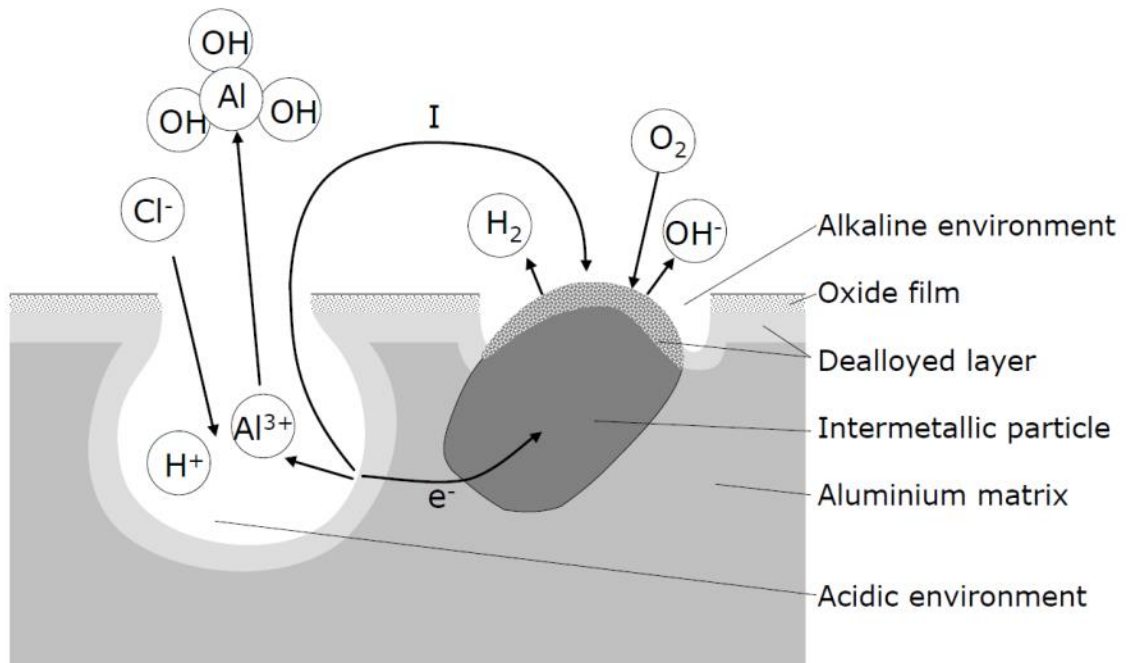


Figure 10: Pitting corrosion.

Generalized illustration of pitting corrosion of aluminum due to microscale galvanic corrosion caused by an intermetallic particle. Source: (Svenningsen, 2003)

Galvanic corrosion between aluminum alloys

While galvanic corrosion between aluminum and galvanized steel in ACSR is well-known (Ergon Energy, 2013) (Brennan, 2004), it appears to be less known that galvanic corrosion also can occur between different aluminum alloys in an all-aluminum structure (Davis, 1999).

The corrosion potentials of some aluminum alloys are different enough to cause galvanic corrosion problems. Galvanic corrosion may occur between the 1000-series and 2000-series, as well as the 3000-series and 7072. While this can cause problems, it can also be used for cathodic protection by cladding the less noble alloy onto the more noble alloy. (Vargel, 2004)

1.3.5 Corrosion of composites

Aluminum-based Metal Matrix Composites (MMC)

The incorporation of fibers or another reinforcing phase into an aluminum-based matrix can significantly alter the corrosion behavior. Galvanic corrosion can occur between the reinforcement and the matrix, which has been particularly a problem for graphite fiber reinforced aluminum. Crevices and pores caused by the reinforcement may act as preferential sites for localized corrosion, even if there is no galvanic coupling between the reinforcement and the matrix. The reports of corrosion rates range from no increase in corrosion rate to a significant increase compared to the neat matrix material. (Davis, 1999)

Continuous fiber graphite/aluminum MMCs were introduced in the 1960s. While the manufacturing processes of these composites have been improved, the problem with galvanic corrosion caused by the potential difference between the graphite fibers and the aluminum matrix remains. Corrosion rates of up to 80 times higher than the neat matrix material has been shown in saltwater at room temperature. Severe exfoliation corrosion has been observed in seawater, leading to catastrophic failure within 30 days. The highly accelerated corrosion is believed to result from the aluminum carbides that form at the fiber/matrix interface during the fabrication. The aluminum carbide alters the properties of the normally passive aluminum film along the interface and make the composite more susceptible to corrosion. (Davis, 1999)

Aluminum oxide (Al_2O_3) fibers in aluminum matrix do not suffer from galvanic corrosion between the two phases. Aluminum oxide is not conductive and cannot create a

galvanic coupling to aluminum. A study of aluminum oxide fibers in 6061 aluminum alloy referenced in (Davis, 1999) reported preferential corrosion at the fiber/matrix interface. This study suggests that the corrosion resistance of this kind of composite is highly dependent on the compounds formed at the fiber/matrix interface.

Another study of mica particles in an aluminum alloy matrix also reports increased corrosion rates in saltwater. The increased corrosion rate was attributed to two simultaneous processes, 1) the mica particles prevented the formation of a continuous passive layer, and 2) the mica particles provided sites for pitting and crevice corrosion. MMC with aluminum matrix and boron fibers has showed similar increased corrosion rated with concentration of the corrosion at the fiber/matrix interface. (Davis, 1999)

J.R. Davis (Davis, 1999) concludes that effective coating protection must be employed for long-term use of MMCs in service environments where water may be present.

Graphite reinforced Polymer Matrix Composites (PMC)

PMCs reinforced with carbon fibers or other conductive fibers may be active in the corrosion of metal. Carbon fibers are often not completely embedded in the matrix, and can therefore participate in galvanic corrosion if an electrolyte is present. Carbon is more noble than most metals (see the galvanic series in Figure 8), and can cause a strong corrosive attack of metallic components. (Vargel, 2004) (Mandel, 2012) In the case of ACCC, the carbon fibers can act as a noble electrode if the galvanic barrier is damaged.

The galvanic corrosion can indirectly also cause degradation of the polymer matrix. The release of OH^- ions by the cathode reaction may damage certain polymers. (Vargel, 2004)

1.3.6 Corrosion in the atmosphere

As described in previous sections, most forms of metal corrosion occur via electrochemical reactions at the interface between the metal and an electrolyte. In atmospheric corrosion, the electrolyte is a thin film of moisture on the metal surface. (Gamry Instruments, 2011) The nature and composition of the electrolyte plays an important role (Linares, 2006).

The corrosivity of the atmosphere ranges from benign to severely corrosive (Mayer, 1998). The main cause of corrosion of overhead transmission lines is the presence of aggressive species in the atmosphere such as Cl^- and SO_2 in combination with humidity. (Rhaiem, 2012) (Syed, 2006) Salt depositions on transmission lines are carried by the wind in the form minute sea water particles. The wind can carry the particles far inside the continental land. The particles finally fall on the transmission line surface. (Builes, 2008) Acid smoke from waste disposal facilities can cause rapid corrosion of ACSR conductors. The acid corrosion proceeds at much higher speed than sea salt corrosion. (Isozaki, 2008) Acid corrosion will not be covered in this study.

The interaction between pollution and humidity is also complex. Pollution such as dust and salt may lower the critical degree of relative humidity at which corrosion occurs. Rain, on the other hand, can either increase the corrosion by supplying water, or reduce the corrosion rate by washing away accumulated pollution such as salt. (Vargel, 2004)

Fog, unlike rain, does not clean the surface of the conductor. Fog is therefore often a much more aggressive environment than rain. (Vargel, 2004)

Effect of humidity and temperature

The effect of humidity and time of wetness was mentioned earlier. Atmospheric corrosion is often intermittent since it can only occur when water is present (Vargel, 2004). The presence of water and the corrosion rate are also a function of the conductor temperature, which may be related to the amount of power being transmitted.

The effect of temperature on atmospheric corrosion is complex. Increased temperatures typically stimulate corrosive attacks by increasing the rate of diffusion and of electrochemical reactions. If the humidity stays constant, increased temperature leads to increased corrosion rate. However, increased temperature generally leads to increased evaporation of the electrolyte. This reduces the time of wetness, which results in an overall reduced corrosion rate. (Syed, 2006)

At temperatures below the freezing point of the electrolyte the electrochemical corrosion rate is negligible. (Syed, 2006)

Dissolved oxygen

The thin film of moisture, whose thickness typically does not exceed a few hundred micrometers, can be assumed to always be saturated with oxygen. (Vargel, 2004)

Corrosion mechanisms in the atmosphere

The most frequent forms of atmospheric corrosion of bare aluminum structures are pitting corrosion and galvanic corrosion. Pitting corrosion does typically occur in aluminum, but the rate of pit deepening decreases with time. There is always a risk of galvanic corrosion where aluminum is connected to other metals, particularly containing

copper, lead or steel, as well as structures of graphite such as carbon fiber composite or graphite filled polymers. The risk of galvanic corrosion is greatest in marine atmospheres due to the presence of chlorides and humidity. However, experience shows that the connection between aluminum and galvanized steel rarely leads to problems provided that the design is such that retention of moisture is avoided. (Vargel, 2004) This literature study showed that galvanic corrosion is indeed a problem between aluminum and galvanized steel, perhaps because the conductors with multiple strands do retain moisture. Splices and connectors are often also susceptible to corrosion, probably for the same reason.

1.3.7 Prediction of corrosion mechanisms in the studied conductors

ACSR

Galvanic corrosion is one of the major factors in the deterioration of ACSR. As can be predicted from the galvanic series in Figure 8, the corrosion due to the presence of saltwater begins with loss of galvanization on the steel strands in the core since zinc is less noble than aluminum. When the galvanization has been lost on the steel strands, ACSR will corrode rapidly due to galvanic corrosion between aluminum and steel. Aluminum acts as the anode and consequently corrodes rapidly. (Karabay, 2004)

Studies have shown that the corrosion is linear with time. The corrosion causes loss of current-carrying capacity and loss of mechanical strength. The loss of strength in the real service environment can be up to 1 % per year. Using a failure criterion that the conductor should be replaced when it has reached 85 % of the nominal breaking strength, the transmission line needs to be recondored about 20 years after the loss of galvanization has started. (Karabay, 2004)

Based on corrosion theory and the literature study, it is expected that ACSR will show galvanic corrosion in the tests performed in this study. Due to the high concentration of Cl^- ions in the electrolyte of 3 wt. % seasalt, pitting corrosion of the aluminum is also expected. It is also expected that the corrosion rate will be higher at 85°C than at room temperature.

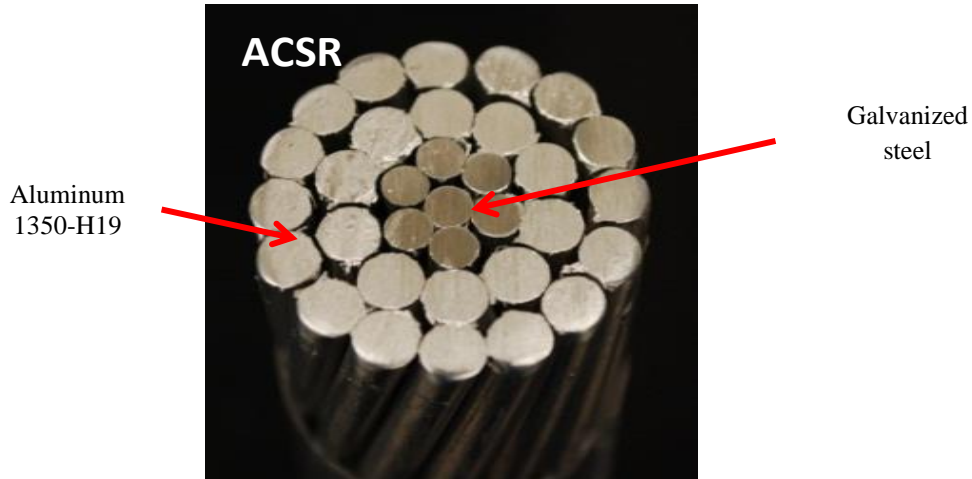


Figure 11: The components of ACSR.

Table 2: Materials potentially active in the corrosion of ACSR			
Component:	Material:	Chemical composition:	Comment:
Aluminum strands	Al 1350-H19	Aluminum ($\geq 99.5\%$) Iron ($\leq 0.40\%$) Silicon ($\leq 0.10\%$) (Matweb 2. , 2013)	Only components $\geq 0.10\%$ listed here.
Steel strands	Galvanization	Zinc	
	Steel	Iron Carbon	

ACSS

Because of the similar designs, the corrosion performance of ACSS is expected to be similar to ACSR. The Galfan coating is claimed to give a better passive barrier protection than regular galvanization, and to last a minimum of two times longer in an outdoor environment (GalvInfo Center, 2011). The aluminum strands in ACSS have the identical chemical composition as the aluminum strands in ACSR, but a different heat treatment. The different heat treatment may or may not affect the corrosion performance.

Since Galfan consists of 93-96 % zinc, a similar galvanic coupling to aluminum would be expected.

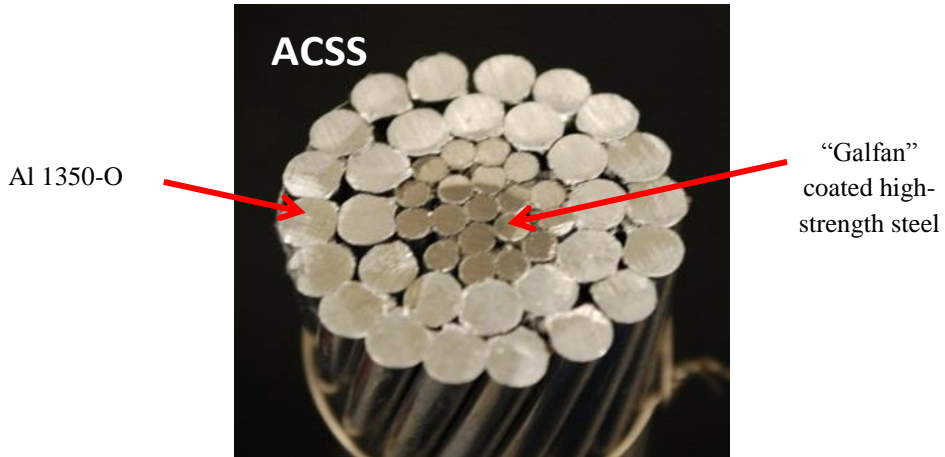


Figure 12: The components of ACSS.

Table 3: Materials potentially active in the corrosion of ACSS			
Component:	Material:	Chemical composition:	Comment:
Aluminum strands	Al 1350-O	Aluminum ($\geq 99.5\%$) Iron ($\leq 0.40\%$) Silicon ($\leq 0.10\%$) (Matweb, 2013)	Only components $\geq 0.10\%$ listed here.
Steel strands	“Galfan” coating	Zinc (93.56-95.77 %) Aluminum (4.2-6.2 %) Rare earth metals (Ce + La) (0.03-0.10 %), Iron ($\leq 0.075\%$), Silicon ($\leq 0.015\%$), Cadmium ($\leq 0.005\%$) Lead (0.005 %), Tin (0.002 %) (Matweb 3. , 2013)	
	Steel	Iron Carbon	

ACCC

In the un-damaged conductor, the exposed surface materials are aluminum (in the form of 1350-O in the current carrying aluminum strands) and the fiberglass composite galvanic barrier.

The carbon fiber composite will only be exposed if the conductor is damaged, aged or has manufacturing flaws. If the carbon fiber composite is exposed, galvanic corrosion may occur between the carbon fibers and aluminum.

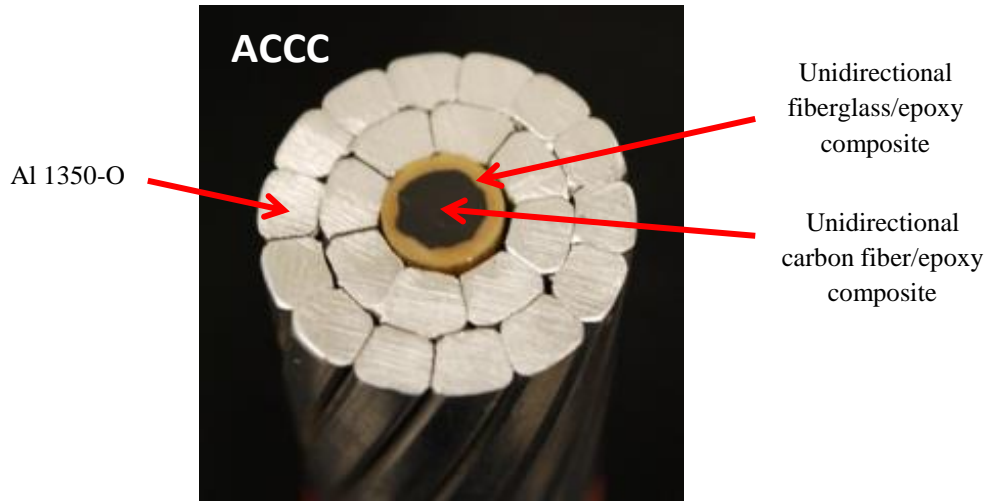


Figure 13: The components of ACCC.

Table 4: Materials potentially active in the corrosion of ACCC			
Component:	Material:	Chemical composition:	Comment:
Aluminum strands	Al 1350-O	Aluminum ($\geq 99.5\%$) Iron ($\leq 0.40\%$) Silicon ($\leq 0.10\%$) (Matweb, 2013)	Only components $\geq 0.10\%$ listed here.
Carbon fiber core	Carbon fibers	Carbon (approx. 65 % volume fraction of the composite)	

ACCR

Table 5 lists the materials that can potentially be active in the corrosion of ACCR. In the un-corroded and un-damaged conductor, the exposed surfaces materials are the aluminum matrix of the metal composite and the Al-Zr alloy in the current carrying aluminum strands. The Al_2O_3 fibers will be exposed if the matrix material corrodes (or melts, wears off, etc). The fibers are assumed to not be directly active in the corrosion process since they are not conductive.

No data regarding corrosion potential has been found for the Al-Zr alloy, and the exact chemical composition is not known since the alloy is defined by its mechanical properties and not by its chemical composition. However, the aluminum alloys in ACCR are not among the ones listed in (Vargel, 2004) as having potential galvanic corrosion problems. The manufacturer has made the same conclusion as demonstrated by this quote: “... *there is no galvanic coupling between the core and the stranded aluminum wires, which would also be subject to corrosion.*” (3M Composite Conductor Program, publication date unknown). According to the manufacturer, the ACCR conductor has very good corrosion resistance, similar to an all-aluminum conductor. (3M 2. , 2005)

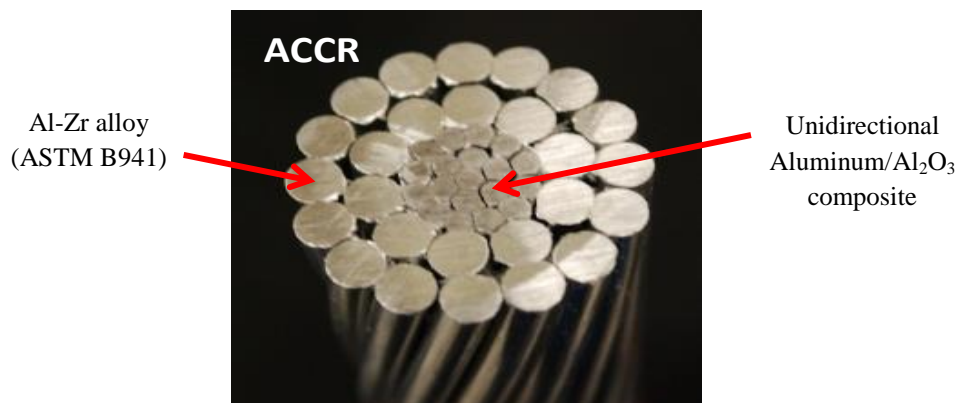


Figure 14: The components of ACCR.

Table 5: Materials potentially active in the corrosion of ACCR			
Component:	Material:	Chemical composition:	Comment:
Aluminum strands	Al-Zr alloy	Aluminum Zirconium	The Al-Zr alloy for electrical purposes is defined by its mechanical properties in ASTM B941-10, not by its chemical composition. The chemical composition can therefore vary. (ASTM 2. , 2010)
Metal matrix composite	Matrix	Aluminum	Data from manufacturer
	Fibers	Al ₂ O ₃	Approx. 50-55 % volume fraction of fibers. (Deve, 2013)

CHAPTER TWO: METHODOLOGY

In order to assess the corrosion resistance of new materials and designs, accelerated corrosion testing is necessary. This chapter describes the theory and the design decisions behind the six different accelerated tests performed in this study, as well as the detailed procedures of all six tests.

2.1 Corrosion testing in theory and practice

2.1.1 Laboratory vs. field testing

Predicting galvanic corrosion is always problematic. There is no way to reliably predict galvanic corrosion other than direct measurements in the exact environment of interest (Roberge, 2008). Even if laboratory tests can be used to obtain an indication of corrosion performance, for some materials such as ordinary steel and stainless steel, laboratory tests always show more severe results than are actually observed under the real outdoor service conditions. Laboratory tests can, nevertheless, *predict a possible risk of galvanic corrosion*. (Vargel, 2004)

It is often an open question if and how laboratory results correlate with field testing or the real service environment. The main problem with accelerated laboratory testing for prediction of corrosion behavior is that different tests often give different results. Field testing is necessary to make reliable service life predictions. The atmospheric corrosion of aluminum has mainly been investigated through field studies

(Syed, 2006). The literature study performed within this study also showed that most of the data for corrosion of high voltage conductors comes from evaluation of removed conductors and from field testing.

2.1.2 Corrosion testing standards

There are a large number of standard corrosion tests. ASTM and NACE are the largest corrosion standardization bodies in the U.S., but ISO and other organizations have similar tests. Standards are necessary to obtain comparable testing results from different laboratories. Standard tests are used for many routine tests, such as salt spray testing of coatings. (Vargel, 2004)

To characterize new products, corrosion tests are often performed on both the new product and the one that is to be replaced. (Vargel, 2004) This is the exact approach taken in this study.

Due to the pioneer nature of this study, a mix of standard and non-standard tests was used. The main reason for the deviation from ASTM standard tests was that more accelerated tests were desired. Since the HTLS conductors are designed to operate at high temperatures, it was of interest to also test them at a temperature higher than typical for standard corrosion tests. The tests performed and their relation to ASTM standards is described in section 2.3.

2.2 Design decisions for testing methods

2.2.1 Electrolyte and temperature

Accelerated laboratory corrosion testing is often performed in brine solutions containing 3-5 % NaCl. These solutions are selected to be as aggressive as possible while still being selective. (Vargel, 2004) Synthetic seawater is sometimes used for structures that will be used in marine environments. (ASTM, 2008)

In this study, a 3 wt. % aqueous seasalt solution was chosen. (Vargel, 2004) Since the conductors typically are not used in a marine environment but in an environment where salt can come from many different sources, an aerated solution of Morton™ Brand Natural Seasalt in distilled water was used instead of the standardized ASTM D1141 Substitute Ocean Water (ASTM, 2008) that is expensive and requires tedious preparation.

The pH on a conductor can vary drastically from very acidic to very alkaline, but slightly acidic rain is probably more common than alkaline due to SO₂ and NO_x pollution from power plants. The initial pH of the electrolyte used in this study was around 5.0. At the end of the long-term tests, the pH of the electrolyte had increased to approximately 8.0. The pH was not adjusted during any of the tests.

The temperature of 85°C was selected after extensive discussion. The high altitude of Denver makes the boiling point of water to be about 95°C. We wanted to stay well below the boiling point to avoid excessive loss of electrolyte. At the same time we wanted a higher temperature since the HTLS conductors are designed to operate at higher temperature than conventional conductors. 85°C was the temperature where we expected some moisture to still be present on the conductor during fog and rain, and it was within

the operating range for the testing equipment. The electrochemical tests D, E and F were also performed at room temperature.

2.2.2 Oxygen and agitation

As mentioned in section 1.3, the influence of dissolved oxygen may be complex particularly for aluminum. The electrolyte in the real service environment can be assumed to be saturated with oxygen (see section 1.3.6), therefore aerated electrolyte was used for all tests in this study. The air was finely dispersed using an air stone either below or next to the tested sample.

The aeration also provided agitation. Initial experiments performed at the beginning of this study showed that the galvanic corrosion between small samples of carbon fiber composite and aluminum in aerated 3 wt. % seasalt aqueous solution sometimes is highly polarization (diffusion) limited. In those experiments (for which procedures and results are not reported in this thesis), the corrosion current could increase up to an order of magnitude with agitation. Agitation was completely dominating in 3 wt. % seasalt solution, making other effects such as spacing and temperature negligible.

Experiments were performed to find the relation between mixing/agitation and reaction rate, and to find out if there was a level of agitation where the reaction was not diffusion limited anymore. These experiments showed that agitation with an air flow of about 0.5 liter/minute in a 4000 ml electrolyte volume, finely dispersed with an air stone directly under or next to the reacting samples was required to make the reaction not limited by diffusion.

To determine if this was the case also with the whole conductor samples, the aeration was turned on and off in 30 minute intervals during the entire test.

The cycling on and off gives additional information about the corrosion process since it shows if it is diffusion limited or not. If the reaction rate is diffusion limited, the resulting plot of the galvanic corrosion current as a function of time will have the characteristic square wave form as in Figure 15.

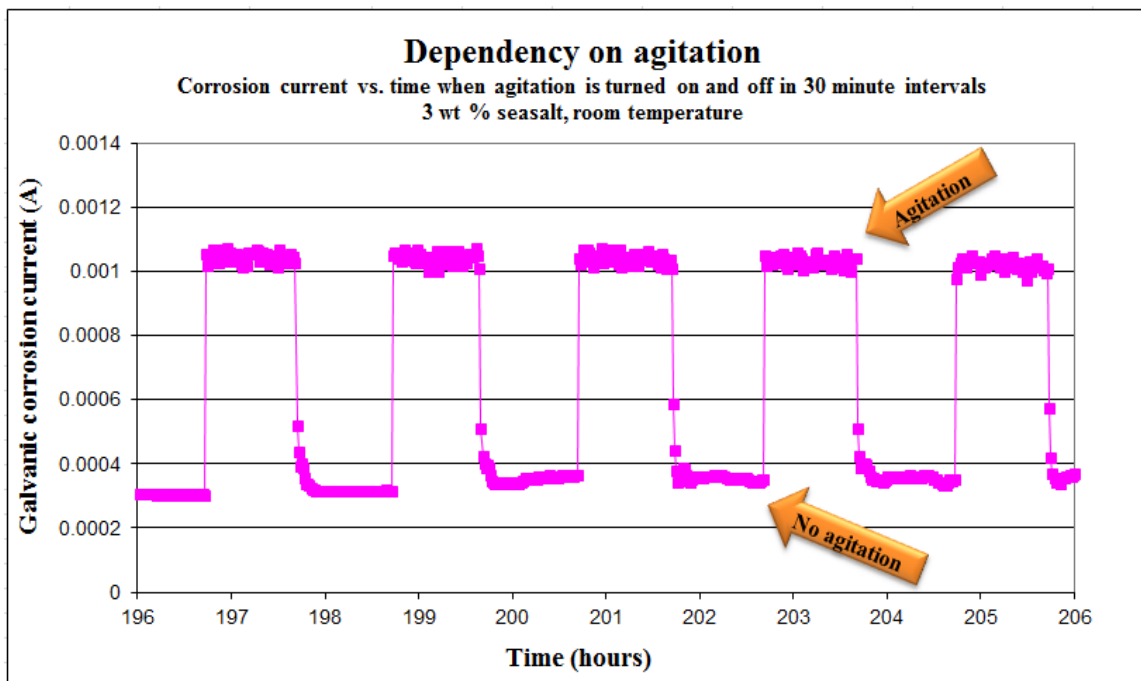


Figure 15: Dependency on agitation.
Initial galvanic corrosion tests showed a strong dependency on agitation of the electrolyte.
The electrodes in the experiment were aluminum and carbon fiber composite.

2.2.3 Mass loss vs. electrochemical tests

Mass loss measurement is the oldest evaluation method for corrosion tests (Vargel, 2004). The simple “weight loss method” means that the corroding sample is weighed during and/or after the test and the mass loss is calculated. The mass loss is often recalculated to “thickness loss” or “corrosion penetration per unit time”. This is considered a very reliable and precise test, but can take a long time to perform (days, months or even years). (Groisman, 2010) Three different mass loss tests have been performed in this study.

Electrochemical testing methods are popular both in industry and academia because they often can be carried out in hours instead of months or years. Electrochemical methods are very fast, but more complicated, less reliable, and less precise. For metals in aqueous solution of electrolytes, the corrosion rate can often be defined within 10 to 20 minutes of testing. (Groisman, 2010)

Electrochemical methods have been extensively used since the 1950s, but the peculiar corrosion mechanisms of aluminum considerably limit the usefulness of these methods for aluminum-based materials. The electrochemical behavior of aluminum is strongly influenced by the presence of a natural aluminum oxide film on the surface. The layer is formed instantly (within 1 ms) and the measured potential always represents a mixed potential between the oxide layer and the metal. Due to the formation of the oxide layer, it is often necessary to wait for several hours, or even several days, before the potential of aluminum is stable enough for an accurate measurement. Because of aluminum’s complex corrosion behavior, electrochemical testing methods can only be

used in very special cases of corrosion and under very well-controlled conditions, or for fundamental studies. (Vargel, 2004)

Since this study is indeed a fundamental study of HTLS conductors, we determined that electrochemical tests would add important information regarding the possible corrosion mechanisms in HTLS conductors subjected to saltwater. Three different electrochemical tests were performed in addition to the three mass loss tests.

2.2.4 Duration of corrosion test

The length of a corrosion test is a very important factor. If the test is too short, it might not give us any information. If the test is too long, there might be no sample left to analyze. (Groysman, 2010)

The corrosion rate and time to full dissolution of a sample depends on several parameters such as initial mass and surface area, type and concentration of the electrolyte (acid, saltwater etc.), temperature, and agitation. In some electrolytes, a sample will virtually never be dissolved. This is for example the case with aluminum in fresh water. While other samples, such as iron in hydrochloric acid, might fully dissolve within minutes or hours. A too short, too mild test might make two samples with widely different corrosion performance appear to have the same corrosion resistance. (Groysman, 2010)

104 days (approximately 3 months) was chosen for the first mass loss test in this study to ensure there would be sufficient corrosion damage to evaluate. That length of time caused severe corrosion and revealed several interesting corrosion mechanisms. The duration for the second mass loss test was cut down to 62 days (2 months) in order to have results in time for the bi-annual sponsor meeting.

The first electrochemical tests of open circuit potential in the whole conductor samples were run for 30 days to study potential changes over time. The galvanic corrosion current was tested for 20 hours, which is much longer than typical. However, for the ACCR sample this was still not enough to reveal the corrosion mechanism at 85°C, so the test for that particular sample was eventually extended to 10 days. The

duration for the last electrochemical test with a reference electrode was 60 minutes as specified in the applied standard. (Detailed procedures are found in section 2.3.

2.2.5 Reference electrodes

A silver-silver chloride (Ag-AgCl) reference electrode was chosen due to its ease of use and absence of toxic metals. The open circuit potential at 25°C is +0.222 V compared to the standard hydrogen electrode (SHE) that is traditionally used for electrochemical measurements. (Bates, 1978)

To protect the reference electrode during high temperature tests, the reference electrode was used in a 4M KCl electrolyte saturated with silver. This decreases the risk of foreign ions diffusing into the reference electrode. A salt bridge connected the half-cell, with the reference electrode, to the other half-cell, with the tested sample in 3 wt. % seasalt aqueous solution (see Figure 16).

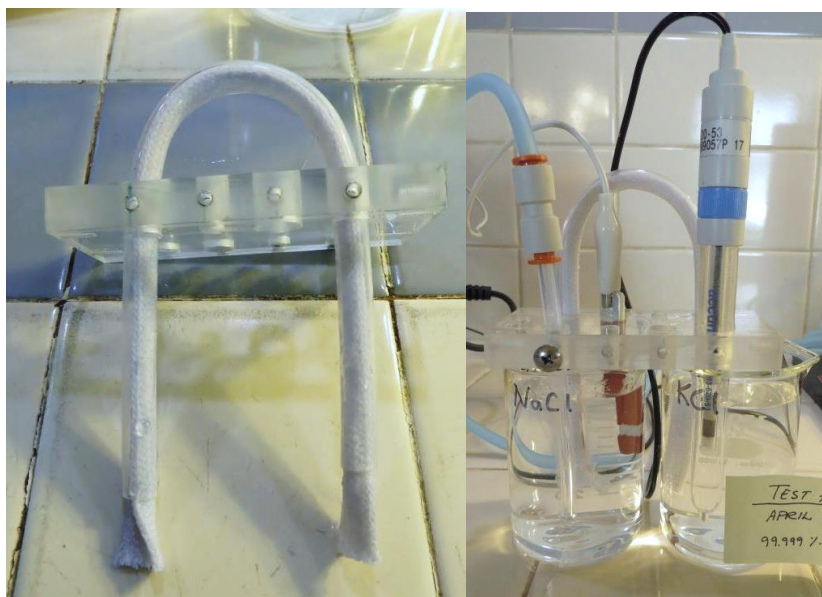


Figure 16: Salt bridge.

The salt bridge made of a cotton string in a Teflon tube (left), the reference electrode in silver-saturated 4M KCl connected to the actual testing environment through a salt bridge (right).

2.2.6 Sample design

The sample design is also an important parameter that may affect the outcome of a test. (Groysman, 2010) In this study, the decision was made to test a combination of samples of the whole conductor and samples of the individual components (aluminum strands and core strands). Information regarding sample sizes and designs can be found in the procedures (section 2.3).

Galvanic corrosion testing in actual geometry

The sample design used to measure the corrosion potential and the galvanic corrosion current in the actual geometry deserves particular attention. This is a sample design that we have never seen used before.

In the unaltered conductor, the core material and the current carrying aluminum strands are in direct electrical contact. This is why there may be galvanic corrosion. To measure the galvanic current or difference in potential, the two materials must be separated. If the two materials are tested individually, synergistic effects existing only in the actual geometry might be missed. A new sample design was developed to allow measurement of both open circuit potential and galvanic corrosion current in the actual conductor geometry:

5. The core was pushed out of the conductor sample. For the samples with coated steel cores, the exposed ends were coated with RTV (silicone rubber) to avoid direct contact between the steel and the electrolyte. The cores of all designs except ACCC were then wrapped in polyester fabric (see Figure 17A). Due to the unique design of ACCC, an alternative method was used where the fiberglass

galvanic barrier was removed on a 200 mm long section of the core (see Figure 17C).

The sample was then re-assembled (see Figure 17B). A digital multimeter was used to make sure there was no electrical connection between the two materials.

6. When the sample was partially submerged in the electrolyte, the fabric allowed for conduction of ions but not electrons. The open circuit potential was measured between the core and the aluminum strands in Test D. In Test E, the two materials were electrically connected through an external circuit and the galvanic corrosion current could easily be measured.



Figure 17: Samples for galvanic corrosion testing.

Manufacturing of the samples for galvanic corrosion current measurements. A: The core is wrapped in fabric to avoid electrical connection but still allow ion flow. B: The conductor is re-assembled. C: For ACCC, the carbon fiber composite was exposed for a similar effect.

2.2.7 The C³LARC instrument

The budget did not allow for purchase of commercial equipment, particularly not since the non-standard tests would have required extensive custom modifications.

Instead, a new testing apparatus was designed and built for this study. The test equipment was dubbed C³LARC - *Composite Conductor Corrosion Lifetime Accelerated Testing Cell*. The testing cell is based on ASTM standards where they were applicable.

The fundamental idea with C³LARC was that it should be inexpensive to build and easy to adapt to different tests.

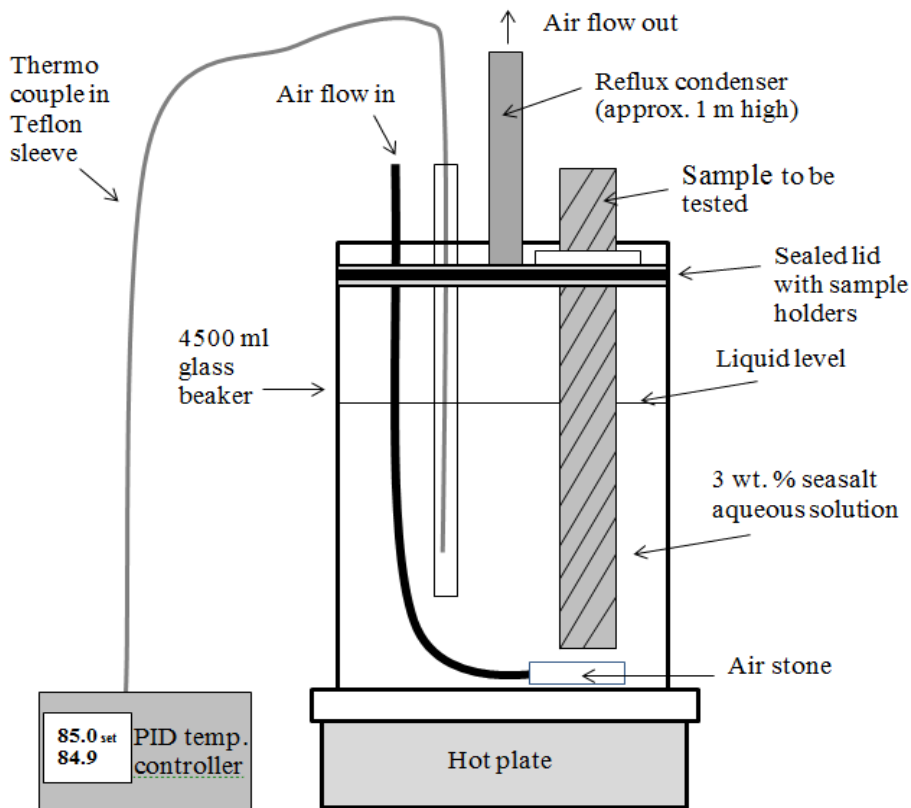
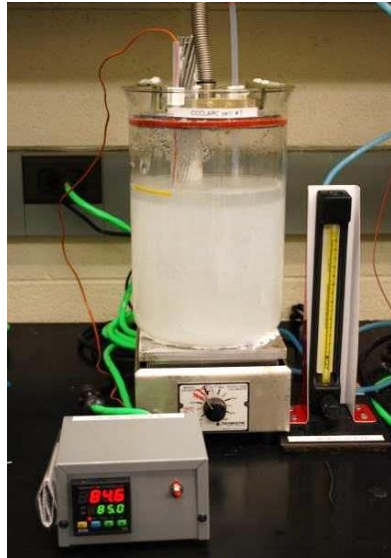


Figure 18: The C3LARC testing cell as used for test A.

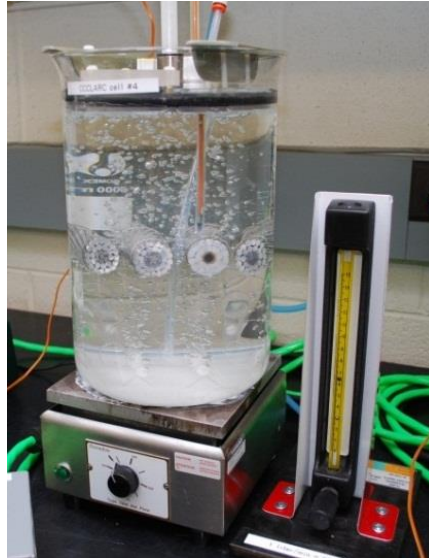
The core part of the setup is a standard 5000 ml borosilicate beaker on a hotplate. A PID controller controls the temperature of the electrolyte and a custom made lid of

acrylic holds samples, reflux condenser, air tube, thermocouple etc. The glass beaker allows for visual inspection of the samples during test. An entire “testing cell” of the C³LARC instrument can be built for about \$300 or less (excluding the hotplate and the flow meter).

Test A: Partially submerged



Test B: Fully submerged



Initial testing of galvanic corrosion

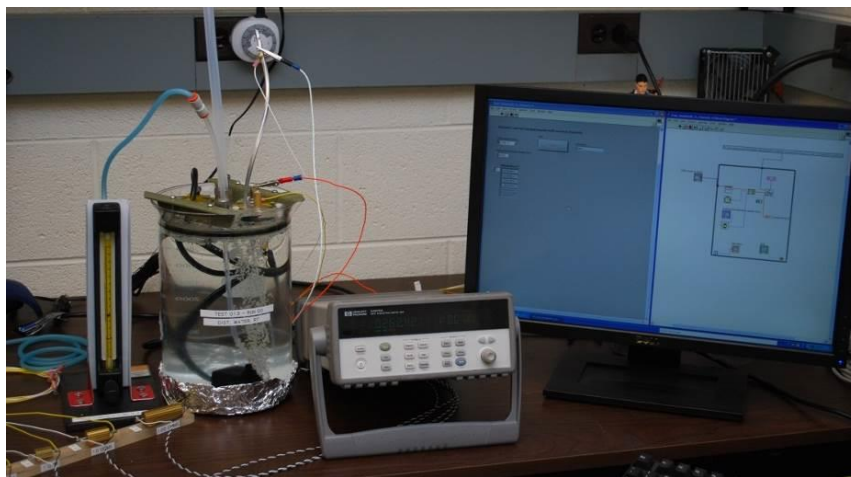


Figure 19: The C³LARC instrument.

The C³LARC instrument setup for partially submerged corrosion testing (Test A), fully submerged corrosion testing (Test B) and galvanic corrosion testing (initial testing).



Figure 20: Manufacturing of the C³LARC testing cell.
 The C³LARC instrument can be built with simple manufacturing methods.
 Drawings are found in Appendix A.



Figure 21: C³LARC sample holders.
 The sample holders are based on the KF-40 vacuum flange system which provides a standardized system for the easily modifiable sample holders.

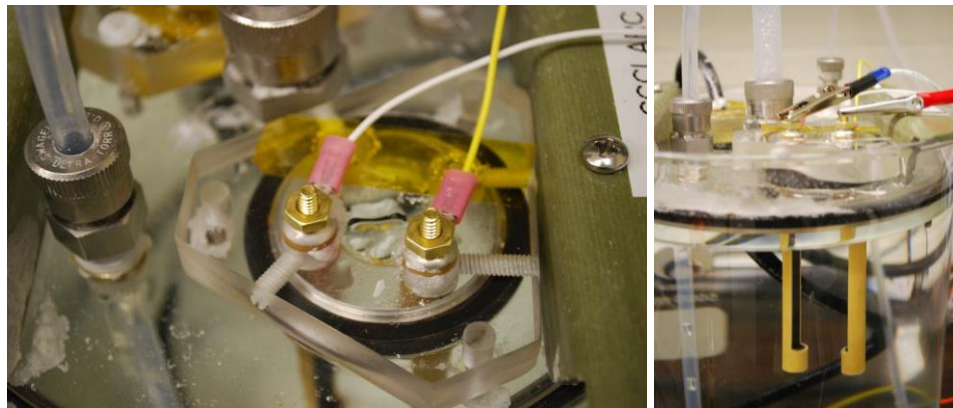


Figure 22: Electrical connections.
 The electrical connections to the samples are made outside the testing cell, making careful insulation of the connections unnecessary.

2.3 Performed corrosion tests

Table 6: Summary of the performed tests below summarizes the performed tests.

The following sections will describe the test setup and procedures in detail.

Table 6: Summary of the performed tests			
Test	Description	Based on standard	Main deviations from standard
A	Partially submerged, whole conductor Partial submersion of whole conductor samples (300 mm, of which 165 mm immersed). 85°C. Duration: 104 days. Evaluation method: Mass loss and corrosion pattern.	No.	---
B	Fully submerged, whole conductor Full submersion of 90 mm whole conductor samples. 85°C. Duration: 62 days. Evaluation method: Mass loss.	No.	---
C	Fully submerged, single strand Full submersion of 50 mm samples of single aluminum strands and a composite strand from ACCR. Duration: 62 days. Evaluation method: Mass loss and corrosion pattern.	No.	---
D	Open circuit potential, whole conductor Open circuit potential between Al strands and core material was measured during min. 30 days in partially submerged, 300 mm samples of whole conductors where core and Al strands were separated with fabric and re-assembled. (ACCC had part of the galvanic barrier removed to generate the same effect). 85°C and RT. Evaluation method: open circuit potential.	No.	---
E	Galvanic corrosion current, whole conductor The Al strands and core in each of the samples from Test D were electrically connected through an external measurement circuit and the galvanic corrosion current was measured. 85°C and RT. Evaluation method: Galvanic corrosion current density. Duration: minimum 20 hrs.	Yes. ASTM G71 - 81(2009) (ASTM 4. , 2009)	Current measured over 1 Ω shunt resistor. Samples were partially submerged.
F	Corrosion potential, conductor components The open circuit corrosion potential of aluminum strands and core material measured with reference to an Ag-AgCl reference electrode. 85°C and RT. All measurements made on “As received” material. Test duration: 1 hr	Yes. ASTM G69-12 (ASTM 3. , 2012)	85°C. Simple seasalt solution. Samples tested “As received”. 10 ⁶ Ω input impedance voltmeter.

2.3.1 Setup and procedure for mass loss tests (Test A-C)

Partially submerged (Test A):

300 mm (12 inch) samples of whole conductors were placed vertically and approximately 165 mm (6.5 inches) were submerged for 104 days. The evaluation was mass loss measurement and inspection of corrosion pattern.

Sample type and size	300 mm pieces of the whole conductors.
Sample preparation	Samples were used “as received”.
Electrolyte	3500-4000 ml 3 wt. % Morton™ Brand Natural Sea Salt aqueous solution (prepared with distilled water)
Temperature	85°C (±1°C)
Scale	Ohaus Voyager V12140 Digital Balance scale, resolution 0.0001 g
Air flow meter	Porter Instrument Co. B-125-50 Rotameter
Mixing/agitation	Aeration, approx. 0.5 liter/minute.
Test duration	104 days
Evaluation method	Mass loss, Inspection of corrosion patterns

Procedure:

1. Samples of the whole conductors were cut to approximately 300 mm length.
2. The mass of the aluminum strands and the core of each sample was carefully measured using a digital balance scale and the masses were recorded.
3. The samples were re-assembled and held together with stainless steel wire.
4. The ends of the steel cores and the polymer composite core were sealed with RTV.
5. The samples were mounted in on a plastic holder and partially submerged into the testing cell containing 3500-4000 ml of 3 wt. % seasalt aqueous solution.
6. The samples were left partially submerged for 104 days.

7. The samples are taken out, rinsed in water and dried.
8. The visual inspection revealed a relatively thick layer of corrosion products on all four samples. The brittle corrosion products were removed by a gentle cleaning with ScotchBrite sponge, which allows for mass loss measurement, without removing any of the aluminum material.
9. The samples were weighed and inspected.

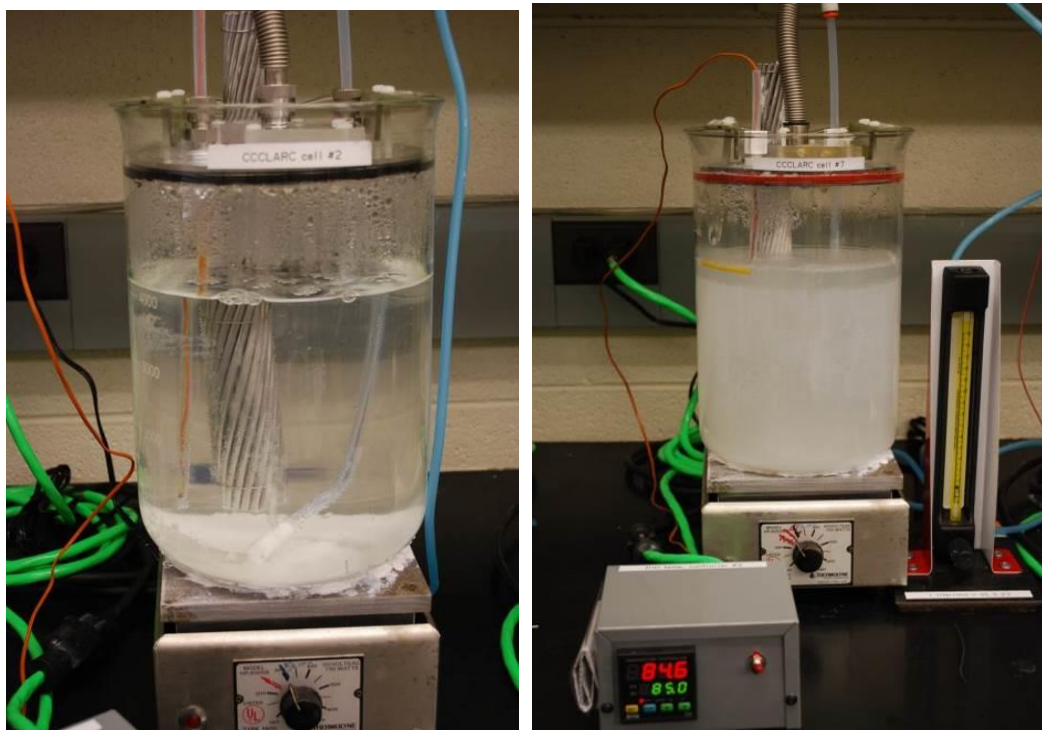


Figure 23: The C³LARC testing cell used for Test A.
Left: Start of the test. Right: About halfway through the test.
(Note: the two pictures are from two different tests).



Figure 24: Sample of ACCC mounted in the plastic sample holder.

Fully submerged (Test B):

The partially submerged test (Test A) caused severe localized corrosion at the liquid level, which made it difficult to evaluate the mass loss. A fully submerged test (Test B) was performed with the goal of obtaining more easily evaluated corrosion behavior.

90 mm (3.5 inch) samples of whole conductors were placed horizontally on a plastic holder and fully submerged for 62 days. The ends were covered with silicone RTV to simulate a continuous length of conductor. The main evaluation method was mass loss measurement.

Sample type and size	Approx. 90 mm (3.5 inch) pieces of the whole conductors.
Sample preparation	Samples were used “as received”. Ends were sealed with RTV to simulate a continuous piece of conductor.
Electrolyte	5000 ml 3 wt. % Morton™ Brand Natural Sea Salt aqueous solution (prepared with distilled water)
Temperature	85°C ($\pm 1^{\circ}\text{C}$)
Scale	Ohaus Voyager V12140 Digital Balance scale, resolution 0.0001 g
Air flow meter	Porter Instrument Co. B-125-50 Rotameter
Mixing/agitation	Aeration, approx. 0.5 liter/minute.
Test duration	62 days
Evaluation method	Mass loss, Inspection of corrosion pattern

Procedure:

1. Samples of the whole conductors were cut to approximately 90 mm length.
2. The mass of the aluminum strands and the core of each sample was carefully measured using a digital balance scale and the masses were recorded.
3. The samples were re-assembled and held together with stainless steel wire.
4. The ends were sealed with RTV to simulate a continuous length of conductor.

5. The samples were placed on the plastic holder in the testing cell.
6. 5000 ml of 3 wt. % seasalt aqueous solution was added to the cell.
7. Heating and aeration were turned on.
8. The samples were left submerged for 62 days.
9. The samples are taken out, rinsed in water and dried.
10. The visual inspection revealed a relatively thick layer of corrosion products on all four samples. The brittle corrosion products were removed by a gentle cleaning with ScotchBrite sponge, which allows for mass loss measurement, without removing any of the aluminum material.
11. The samples were weighed and inspected.

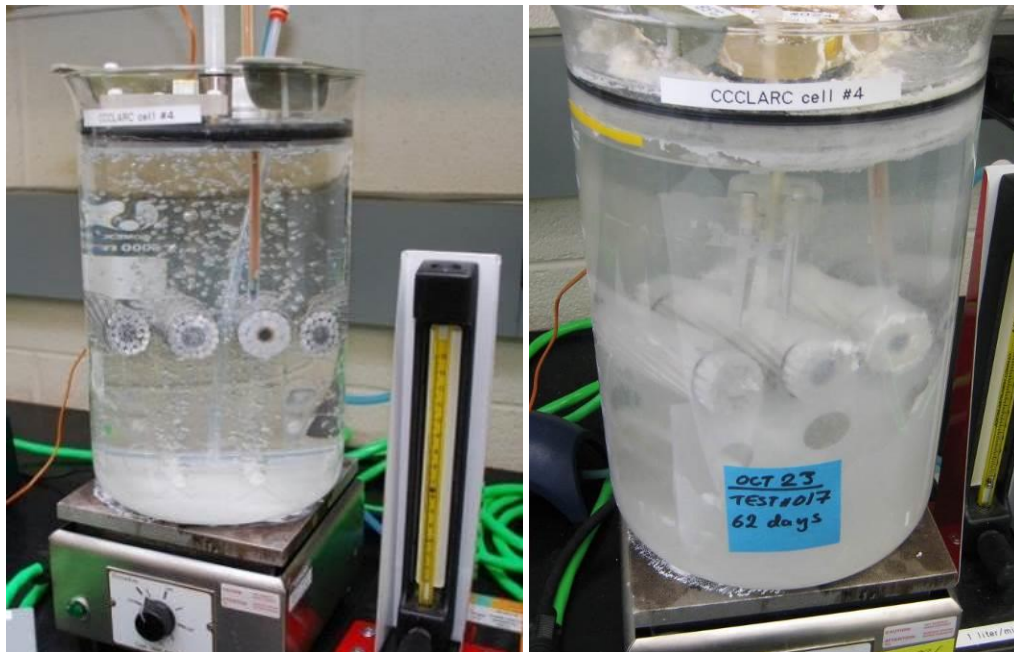


Figure 25: Test B – fully submerged.
Left: Start of test. Right: End of test (after 62 days).

Single strand, fully submerged (Test C):

50 mm (2 inch) samples of the aluminum strands from all four conductors (and a composite core strand from ACCR) were fully immersed for 62 days. The samples were hanging vertically from plastic holders. Corrosion pattern and mass loss was evaluated.

Sample type and size	Approx. 50 mm (2 inch) pieces of the current carrying aluminum strands and the metal matrix composite in ACCR.
Sample preparation	Cleaning with isopropyl alcohol
Electrolyte	5000 ml 3 wt. % Morton™ Brand Natural Sea Salt aqueous solution (prepared with distilled water)
Temperature	85°C (±1°C)
Scale	Ohaus Voyager V12140 Digital Balance scale, resolution 0.0001 g
Air flow meter	Porter Instrument Co. B-125-50 Rotameter
Mixing/agitation	Aeration, approx. 0.5 liter/minute.
Test duration	62 days
Evaluation method	Mass loss, Inspection of corrosion patterns

Procedure:

1. Samples of approximately 50 mm length were cut from the current carrying strands of all four conductors and from the aluminum composite core of ACCR.
2. The mass of each sample was carefully measured using a digital balance scale and the masses were recorded.
3. The samples were mounted in a plastic holder (see Figure 26).
4. The samples were submerged in the aerated, 85°C 3 wt. % seasalt aqueous solution.
5. The samples were left submerged for 62 days.
6. The samples are taken out, rinsed in water and dried.

7. The visual inspection revealed a relatively thick layer of corrosion products on all four aluminum strand samples. The brittle corrosion products were removed by a gentle cleaning with ScotchBrite sponge, which allows for mass loss measurement, without removing any of the aluminum material. The aluminum composite sample was covered in corrosion products and disengaged fibers. The corrosion products and the loose fibers were removed with a plastic brush.
8. The samples were weighed and inspected visually.

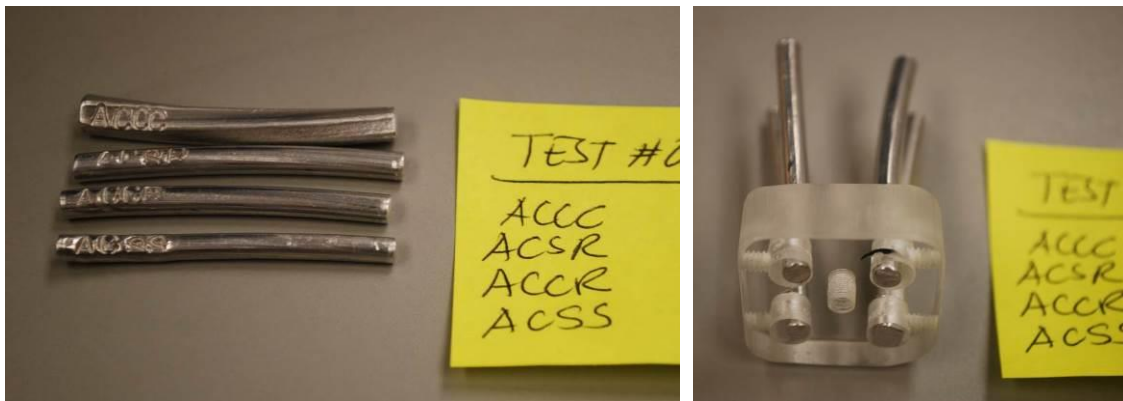


Figure 26: Samples for Test C.

The single strand aluminum samples (left) and the samples mounted in the holder (right). (ACCR composite strand sample not in picture)

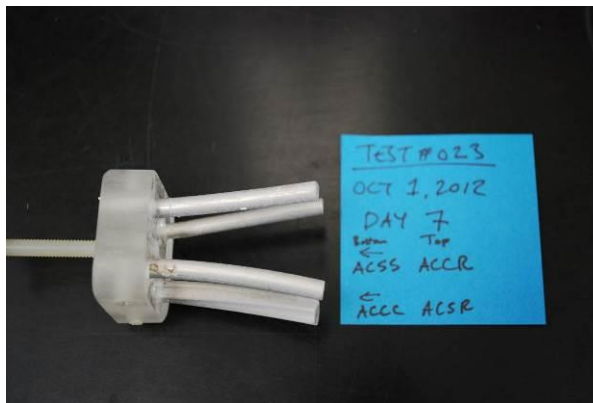


Figure 27: The aluminum strands after submersion for 7 days.

Evaluation of mass loss corrosion tests

The samples from test Tests A, B and C were mechanically cleaned from corrosion products (the whole conductor samples were taken apart before cleaning). Several cleaning methods including ultrasonic cleaning and immersion in phosphoric acid were attempted, but only gentle mechanical cleaning with ScotchBrite pad and a plastic or stainless steel brush managed to remove the corrosion products without removing significant amounts of aluminum. The mass loss was measured and the corrosion patterns were evaluated by visual inspection and microscopy.



Figure 28: Samples from Test B.
Samples just taken out from Test B (left), and typical sample before cleaning (right).

2.3.2 Setup and procedure for electrochemical tests (Test D-F)

Open Circuit Potential (Test D):

If the two metals (or the metal and graphite) are submerged in an electrolyte but not electrically connected to each other, they will reach an equilibrium potential called the Open Circuit Potential, (E_{OC} .) The measurement of E_{OC} is the first step in most electrochemical experiments. Note that the terms E_{OC} and E_{corr} (Corrosion Potential) often are used interchangeable (Gamry Instruments, 2011), but in this study E_{OC} will be used for the potential between the two materials in Test D and E_{corr} will be used for the potential with reference to the Ag-AgCl reference electrode in Test F.

Open circuit potentials were measured using the whole conductor samples where core and aluminum strands were separated by fabric as described in section 2.2.6. The sample was partially submerged and the open circuit potential between the core and the strands was measured daily with a digital voltmeter. The tests were performed both at 85°C and at room temperature (approximately 24°C). The duration of the test was minimum 30 days.

Table 10: Test setup, open circuit potential (Test D)	
Sample type and size	Approx. 300 mm pieces of the whole conductors with polyester fabric insulation between core and aluminum strands.
Sample preparation	Samples used “As Received”.
Electrolyte	5000 ml 3 wt. % Morton™ Brand Natural Sea Salt aqueous solution (prepared with distilled water)
Temperature	Room temperature (approx. 24°C) 85°C ($\pm 1^{\circ}\text{C}$)
Volt meter	VIOT M7 Digital Multimeter, calibrated against Metex M4640-A
Air flow meter	Porter Instrument Co. B-125-50 Rotameter
Mixing/agitation	Aeration, approx. 0.5 liter/minute
Test duration	Minimum 30 days
Evaluation method	Measurement of open circuit potential.

Procedure:

1. The samples were prepared as described in section 2.2.6.
2. The samples were partially submerged into the aerated 85°C, 3 wt. % seasalt aqueous solution, with the ends protruding allowing for electrical connection.
3. The potential with reference to the core material was measured daily (or almost daily) for a minimum of 30 days. The meter was only connected during the actual measurement to avoid leakage currents through the meter from interfering with the test. The positive test lead was always connected to the current carrying aluminum strands.

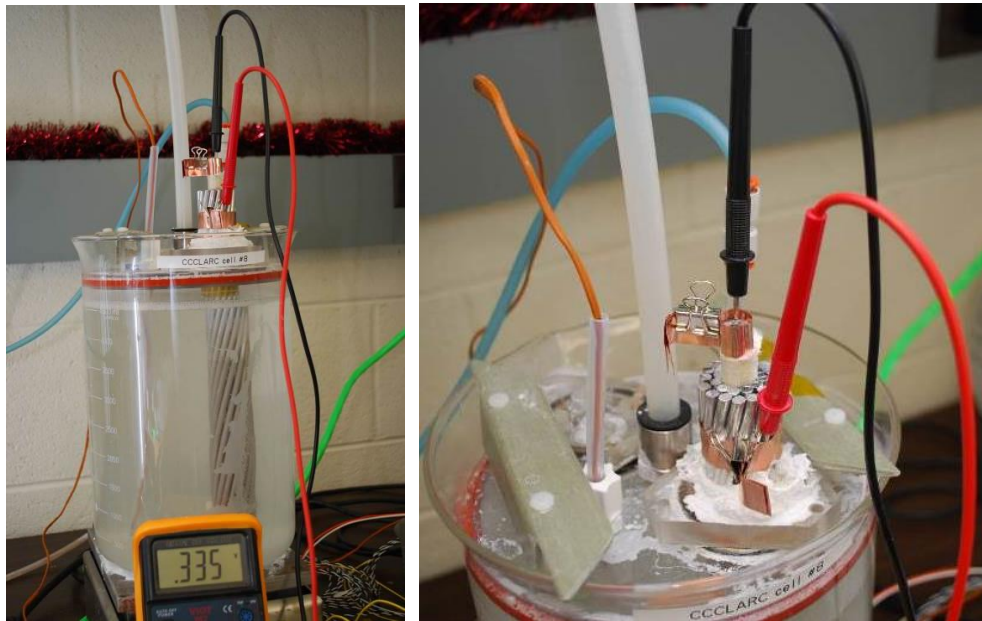


Figure 29: Open circuit potential measurement.
Measurement of the open circuit potential of the ACCC sample at 85°C during Test D.

Galvanic Corrosion Current (Test E):

Galvanic corrosion tests according to ASTM G71 - 81(2009) Standard Guide for Conducting and Evaluating Galvanic Corrosion Tests in Electrolytes were performed at both room temperature and 85°C. The main discrepancy from the standard was that the galvanic current was measured with a 1.0 Ω precision shunt resistor instead of a zero-resistance ammeter, and that the samples were partially submerged instead of fully submerged. The partially submerged samples had two main advantages: 1) It is the same test condition as in Test A, 2) There was no risk of galvanic corrosion at the electrical connection since the connections were made outside the testing cell.

The tests were performed on the samples from Test D after the samples had shown a stable open circuit potential for at least 10 days. The inner and the outer strands were electrically connected through the precision shunt resistor, and the current was measured with a four-wire measurement and automatically logged every minute (more often during the first hour). The test duration varied depending on how quickly the current reached a plateau, but was typically performed for at least 20 hours. The current density was calculated using the area of the corroding material that was exposed the electrolyte. The positive test lead was always connected to the current carrying aluminum strands.

Due to the strong effect of agitation observed in initial galvanic corrosion tests between aluminum and carbon described in section 2.2.2, the aeration was turned on and off in 30 minute intervals during the entire test to determine if the corrosion reactions were diffusion limited (with the exception of the last 85°C test with ACCR - more about this in Chapter four).

Table 11: Test setup, galvanic corrosion current density (Test E)	
Sample type and size	Approx. 300 mm pieces of the whole conductors with polyester fabric insulation between core and aluminum strands. (Same samples as previously used in Test D)
Sample preparation	Samples used “As Received”
Electrolyte	5000 ml 3 wt. % Morton™ Brand Natural Sea Salt aqueous solution (prepared with distilled water)
Temperature	Room temperature (approx. 24 ⁰ C) 85 ⁰ C (±1 ⁰ C)
Precision shunt resistor	Dale RH-50, 50 W, 1.0 Ω 1 % precision shunt resistor (exact resistance measured to 0.99 ohms)
Air flow meter	Porter Instrument Co. B-125-50 Rotameter
Data logging	HP 34970A DASU and LabView, sampling rate once a minute (once every second for first few minutes of test)
Mixing/agitation	Aeration, approx. 0.5 liter/minute, turned on and off in 30 minute intervals
Test duration	At least 20 hour
Evaluation method	Measurement of galvanic current

Procedure:

1. The sampling was started in LabView.
2. One sample from Test D was connected to the external measurement circuit with the 1.0 Ω precision resistor.
3. The galvanic current was measured every second for the first few minutes of the test, and then every minute.
4. The test was run for a minimum of 20 hours. The aeration was turned on and off in 30 minute intervals.
5. The procedure was repeated with the other seven samples from Test D.
6. The corrosion current density was calculated using the surface area of the corroding material that was exposed to the electrolyte.

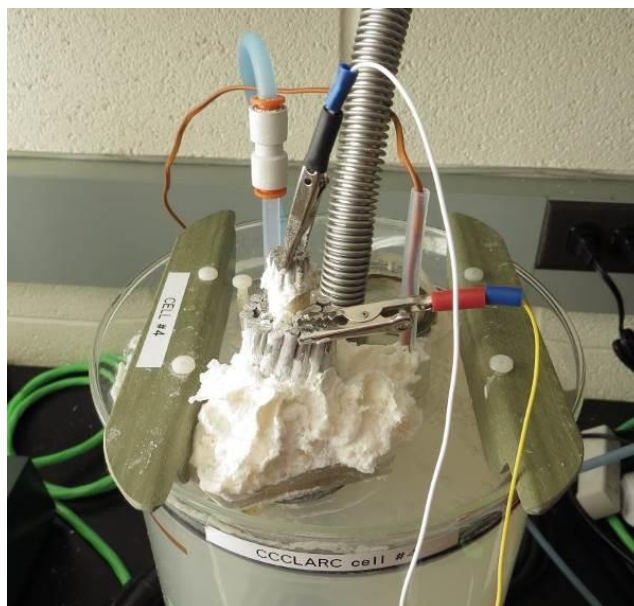


Figure 30: The ACCR sample at room temperature during Test E. Salt and corrosion products had crept up between the strands and crystallized on top of the sample holder.

Calibration

To ensure that the recorded galvanic current really was galvanic current and not background noise, a zero calibration test was performed. Two identical samples of carbon composite (see Figure 31) were connected to the measurement circuit and partially submerged into the electrolyte. The identical samples should give no measurable galvanic corrosion current. The zero test showed zero current. One of the samples was then replaced with an aluminum sample, and a galvanic corrosion current could instantly be measured. The test was repeated with the same results and it was concluded that the measured current was really galvanic current and not electrical noise.

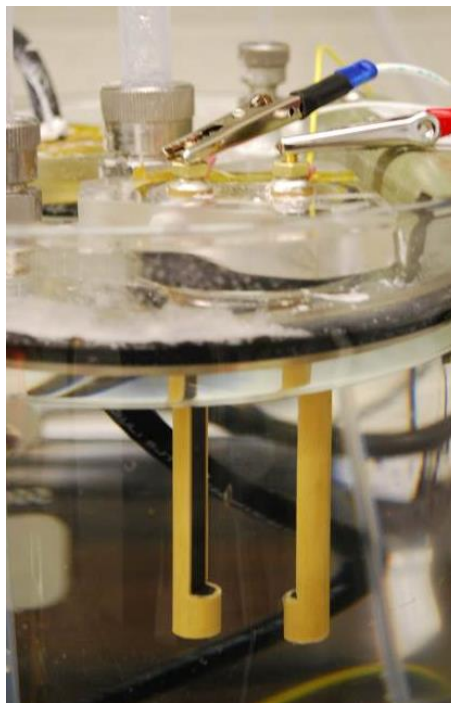


Figure 31: Zero calibration of the galvanic current measurement circuit.

Removal of noise

The calibration procedure described above was performed at room temperature. At the high temperature some of the measurements of Test E (galvanic corrosion current) and Test F (open circuit potential with reference electrode) did suffer from some noise. The noise was in the form of slight oscillations of the current in Test E and potential spikes in Test F. The noise issue was finally tracked down to the solid state relay in the PID controllers in test E. In Test F, the spikes were caused by the hotplate turning on and off. The noise was removed in the data analysis by using a moving average for Test E and by ignoring the very obvious spikes in Test F.

Corrosion (open circuit) Potential E_{corr} (Test F):

To further investigate the susceptibility to galvanic corrosion, measurements of corrosion potentials of the conductor components were performed according to *ASTM G69-12 Standard Method for Measurement of Corrosion Potentials of Aluminum Alloys* (ASTM 3. , 2012). The main discrepancies from the standard method are the non-standard electrolyte, the use of “as received” samples instead of cleaned samples, the use of an Ag-AgCl reference electrode instead of a Calomel electrode and the use of a multimeter with only $10^6 \Omega$ input impedance.

Sample type and size	Conductor components with 100 mm^2 exposed surface area
Sample preparation	Samples used “As Received”
Electrolyte	140 ml 3 wt. % Morton™ Brand Natural Sea Salt aqueous solution (prepared with distilled water)
Temperature	Room temperature (approx. 24°C) $85^\circ\text{C} (\pm 1^\circ\text{C})$
Air flow meter	Porter Instrument Co. B-125-50 Rotameter
Data logging	Fluke 192 Scopemeter with $10^6 \Omega$ input impedance and FlukeView software
Mixing/agitation	Aeration, approx. 0.05 liter/minute.
Test duration	60 minutes
Evaluation method	Measurement of corrosion potential

Procedure

1. Samples with an exposed area of approximately 100 mm^2 were prepared from individual conductor strands by masking with RTV (room temperature curing silicone rubber). The only surface treatment was degreasing with isopropyl alcohol, with the expectation samples of the steel core strands from ACSR and ACSS that had the coatings removed to allow measurements of E_{corr} for the steel. (See Figure 34: Samples for Test F. for sample design)

2. The sampling was started with the Fluke 192 ScopeMeter.
3. The assembly with the sample, salt bridge and reference electrode was placed on top of the two glass beakers submerging the sample area, the reference electrode and the ends of the salt bridge.
4. The potential was measured for 60 minutes.
5. The data was downloaded from the Scopemeter to the computer with FlukeView.
6. The corrosion potential was evaluated at 50, 55 and 60 minutes. If the two or more values were the same, this was used as the result. None of the samples had three different values.



Figure 32: Test F performed at 85°C.

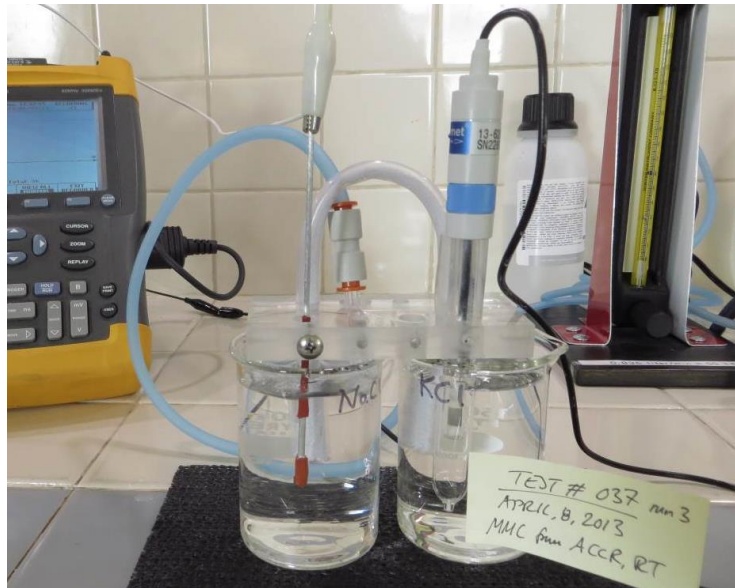


Figure 33: Test F performed at room temperature.



Figure 34: Samples for Test F.

The samples for Test F were masked with RTV (silicone rubber) to give an exposed area of approximately 100 mm^2 for all samples. The only surface preparation was degreasing with alcohol.

CHAPTER THREE: RESULTS

This chapter presents the results from the six performed tests and selected pictures of the samples after testing.

3.1 Results from mass loss tests

3.1.1 Test A: Partially submerged

Test A was the first test to be performed. Due to the pioneer nature of this study, the outcome of Test A determined the design of the following tests.

The table and plots below show the mass loss of the current carrying aluminum strands and the core material after 104 days in aerated 85°C, 3 wt. % seasalt aqueous solution.

Sample	Mass loss Al in gauge section ^A (%)	Mass loss of inner Al strands (gauge section) (%) ^A	Mass loss of outer Al strands (gauge section) (%) ^A	Mass loss of core (%)
ACSR	2.4 %	4.7 %	0.92 %	2.8 % ^A
ACSS	7.7 %	8.0 %	7.5 %	0.40 % ^A
ACCC	0.84 %	2.0 %	0.2 %	-0.28% ^B
ACCR	0.38 %	0.45 %	0.34 %	100 % ^C

^A Since a part of the sample was sticking outside the cell, the mass loss in percent is based on the section that was subject to corrosion. For the ACCC conductor, this was the part of the sample inside the testing cell. For the other three samples with round strands, the electrolyte had crept up between the strands and some corrosion also occurred outside the cell (see Figure 35 for salt creeping up between the strands). The part subjected to corrosion is here called “gauge section”.

^B The ACCC core gained mass due to absorption of water

^C Percent mass loss of matrix material in the submerged section.

Figure 35: Salt and corrosion products creeping up between the strands.



Highly localized corrosion of aluminum strands

The corrosion of the current-carrying aluminum strands was highly localized at the end of the sample and at the liquid surface level. This made it a bit difficult to accurately evaluate the mass loss. This method gave, however, very interesting information regarding corrosion patterns. To eliminate the liquid level effect, Test B was performed with fully submerged samples (see next section).

ACSS had both highest mass loss (total of 7.7 %) and most severe localized corrosion. Several of the outer strands were completely corroded off (see Figure 39). ACSR came in second with a mass loss of 2.4 % and one strand completely corroded off (see Figure 37).

ACCC had only 0.84 % mass loss, and no strand was completely corroded off.

ACCR exhibited significantly less mass loss (0.38%) than any of the other three conductors.

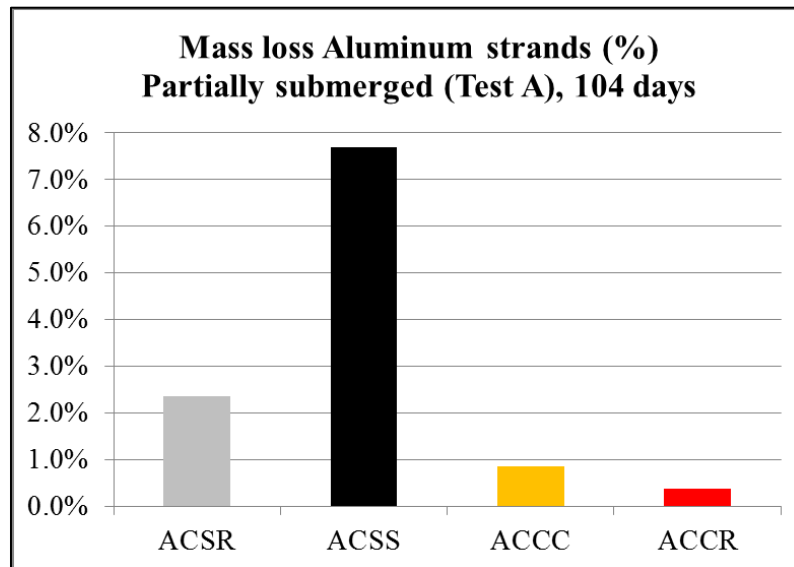


Figure 36: Mass loss aluminum strands (Test A).

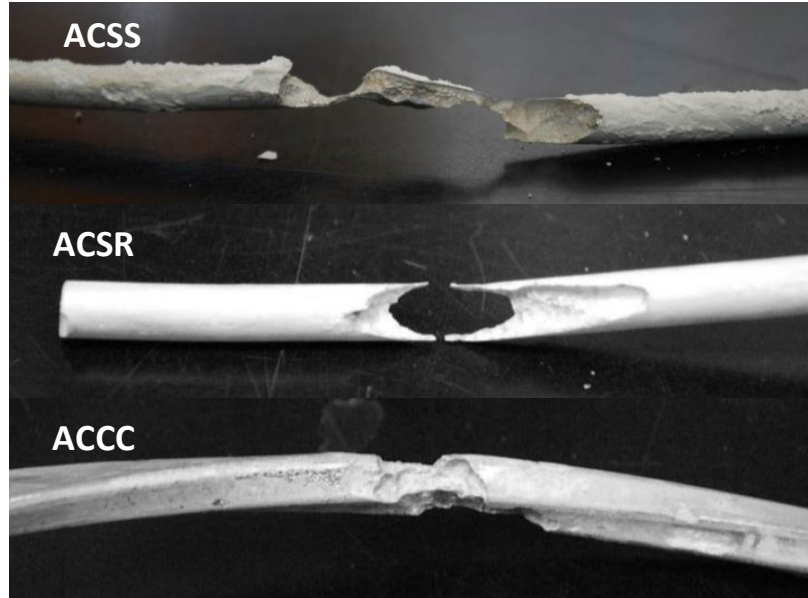


Figure 37: Localized corrosion on ACSS, ACSR and ACCC.
(Picture of ACSS taken before cleaning, ACSR and ACCC taken after cleaning).



Figure 38: ACCR and ACCC after Test A.
ACCR (top) and ACCC (bottom) had very little visual damage before cleaning.

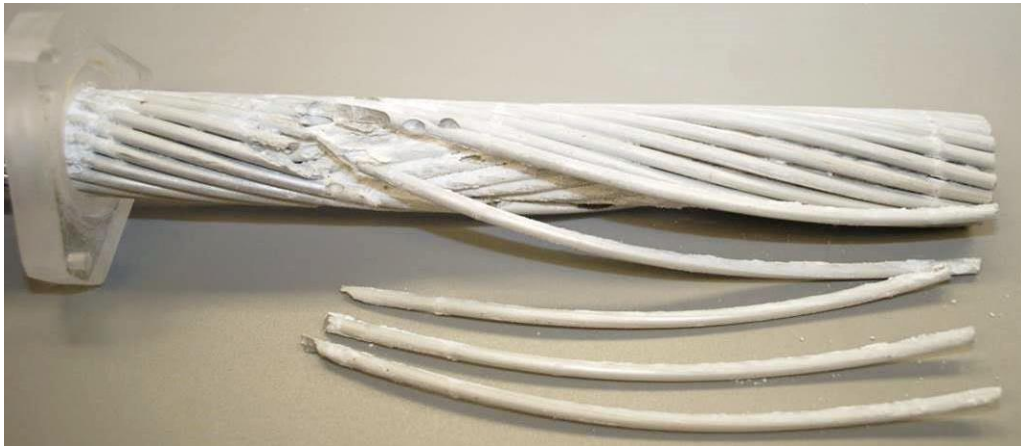


Figure 39: ACSS after Test A.

The corrosion of ACSS was so severe that several strands were completely corroded off. The conductor sample fell apart when the stainless steel wire holding it together was removed.



Figure 40: Localized corrosion at the end of the ACSS sample.

(Left: RTV seal covering the ends of the steel strands still in place, middle: RTV removed, right: some corrosion products brushed off)

Corrosion or other degradation of the load bearing cores

The corrosion damage of the cores varied much more between the conductor designs. None of the cores have yet been tested for mechanical strength. This will be done after the completion of this thesis.

Minor surface damage was observed to the fiberglass galvanic barrier. The damage is believed to be caused by a combination of the hot water and the alkaline corrosion products (aluminum hydroxide) from the corrosion of the aluminum strands. The light areas in Figure 42 are disengaged glass fibers due to degradation of the epoxy matrix. The depth of the damage cannot be fully assessed without cutting the core, which would preclude future mechanical testing of the sample. The damage was not deep enough to expose any of the carbon fiber composite to the aluminum, and thus no galvanic corrosion occurred. The ACCC core exhibited a mass gain of 0.28 % because of absorption of water and perhaps due to some embedded corrosion products in the disengaged glass fibers.

The ACSR and ACSS both exhibited minor loss of the coating above the liquid level. The ACSR core had lost 2.8 % of its mass while ACSS had only lost 0.40 %. ACSR had a very thin layer of rust in the places where the galvanization was lost (see Figure 44), while ACSS has a very light brown but still shiny appearance where the Galfan coating was lost.

The ACCR metal-matrix composite core showed severe degradation of its core material in the submerged section. All the aluminum matrix was lost and only a “broom” of the aluminum oxide fibers (Al_2O_3) was left (see Figure 48). This means that virtually all its mechanical strength was lost.

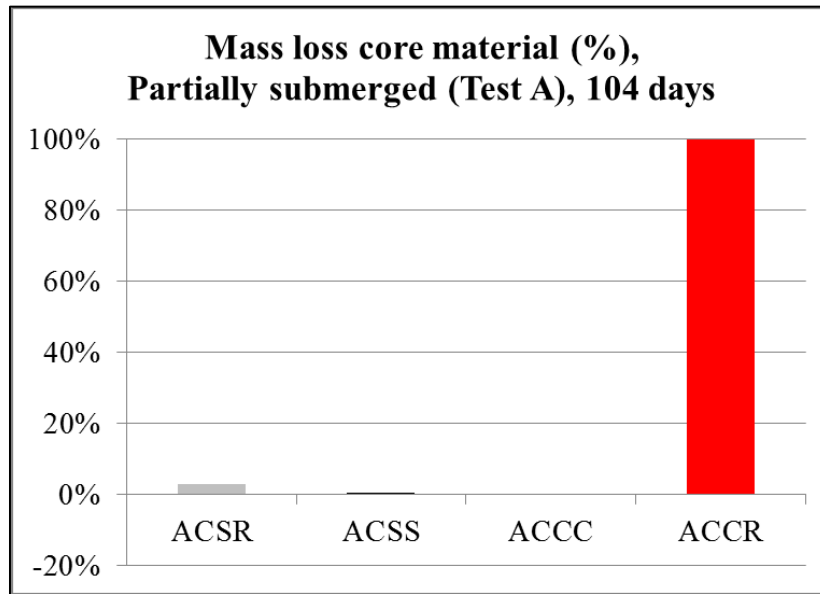


Figure 41: Mass loss core material (Test A)



Figure 42: ACCC core after Test A.

The ACCC core had minor surface damage after Test A. The light areas are disengaged glass fibers (and a little bit of corrosion products (aluminum hydroxide)).



Figure 43: The core in the ACCC before removal.

Note that there is barely any noticeable damage to the polymer composite core next to the large corrosion pit.



Figure 44: The loading bearing steel core in ACSR after being partially submerged in 85^oC, 3 wt. % seasalt for 104 days. The red arrow shows spots where the galvanization is lost.



Figure 45: Core strands of ACSS after Test A. The coating is lost in areas above the liquid level.



Figure 46: The metal-matrix composite core of ACCR after Test A, still surrounded with some of the aluminum strands.



Figure 47: Damage to the ACCR core.

The yellowish appearance of the core (left) indicated that there were an abundance of disengaged aluminum oxide fibers, but the extent of the damage was not revealed until the sample was washed to remove the corrosion products (right).

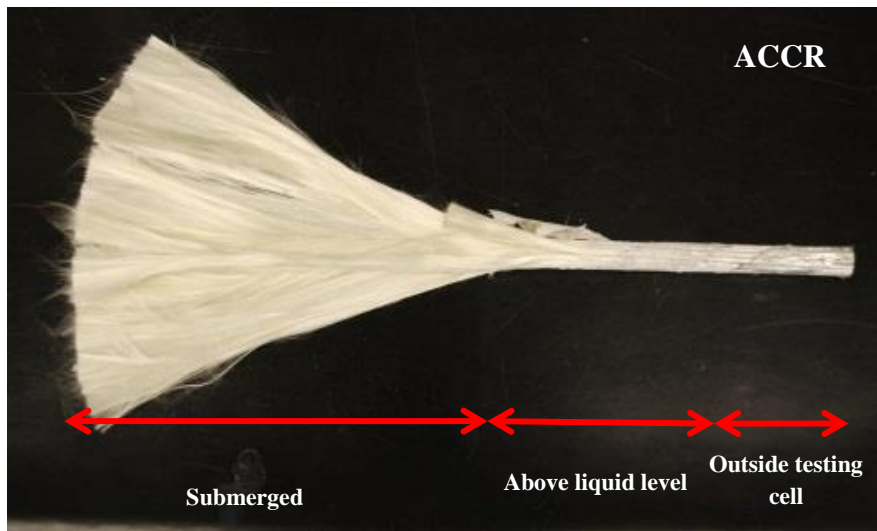


Figure 48: The metal matrix composite core of the ACCR after Test A (104 days in 85°C, 3 wt. % seasalt aqueous solution). Only the aluminum oxide fiber are left in the submerged section.

3.1.2 Test B: Fully submerged

After 62 days in 85°C, 3 wt. % seasalt aqueous solution, the 3.5 inch samples had lost the following percentages of the current carrying aluminum strands and the core material:

Table 14: Results from Test B – fully submerged, 62 days, 85°C				
	Mass loss, Al total (%)	Mass loss of inner Al strands (%)	Mass loss of outer Al strands (%)	Mass loss, core (%)
ACSR	2.3%	5.5 %	0.3 %	1.72%
ACSS	3.0%	4.4 %	2.2 %	0.77%
ACCC	2.7%	3.1 %	2.5 %	-0.29%
ACCR	1.4%	2.9 %	0.4 %	21%

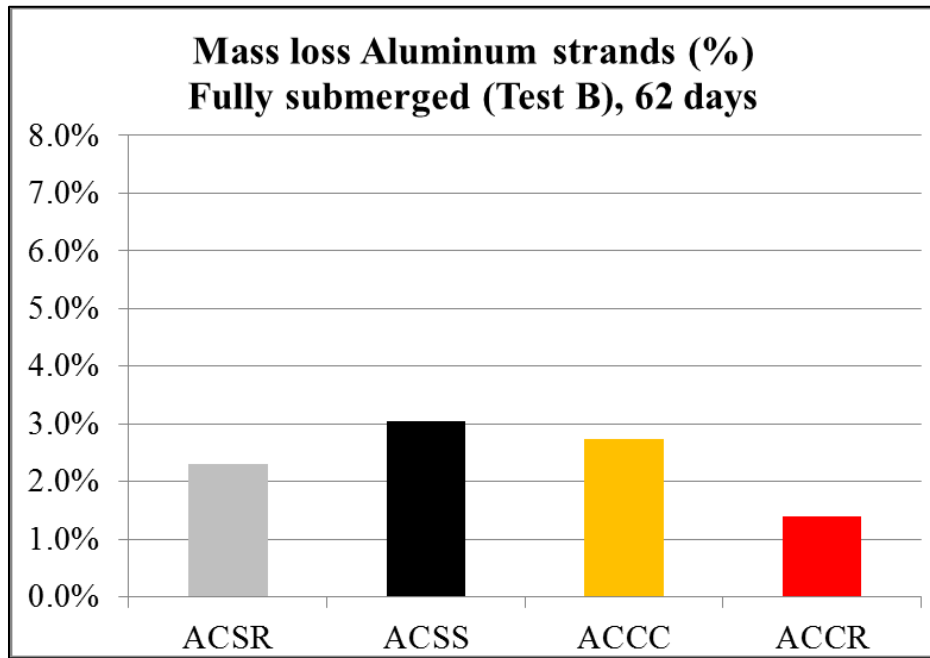


Figure 49: Mass loss aluminum strands (B)

More uniform corrosion of aluminum strands

The fully submerged samples exhibited a more uniform corrosion and a more similar corrosion rate than the partially submerged samples. However, there were still locations with highly localized corrosion, particularly on the inner strands.

The mass loss of the aluminum strands in the ACCC, ACSS and ACSR samples was between 2.3 and 3.0 %, or within 30 % of each other. ACCR had again a much lower mass loss, only 1.4 %.

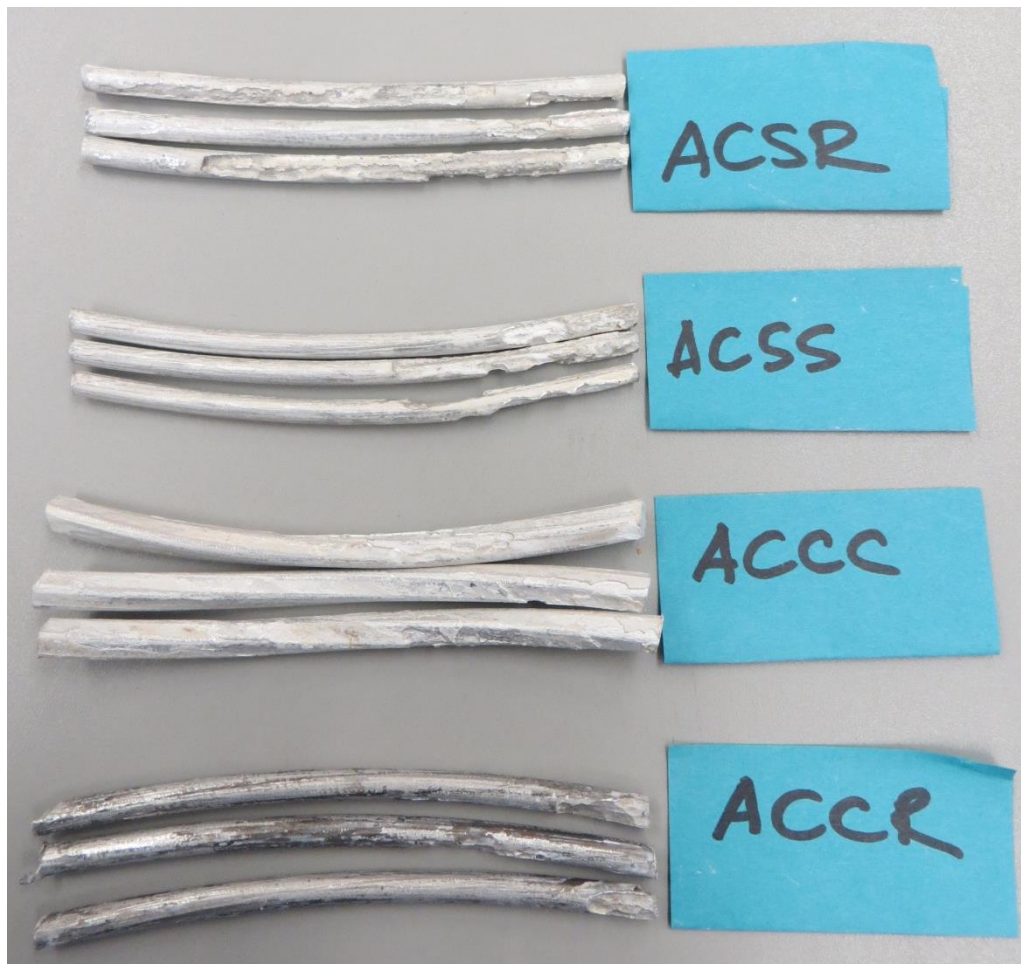


Figure 50: More uniform corrosion of aluminum strands in Test B. The three most corroded strands from each sample. No strand was fully corroded off.

Corrosion or other degradation of the load bearing cores

The ACSR steel core had lost 1.7 % of its mass. There were no signs of rust.

ACSS had lost 0.77 % and did also not show any signs of rust.

ACCC had again a mass gain, this time of 0.29 %. The polymer matrix composite core had similar kinds of minor surface damage as in Test A (see Figure 55). At least half the thickness of the fiberglass composite also appears to be unaffected.

The damage to the ACCR core was less severe than in Test A, but still 21 % of the matrix material was lost due to corrosion.

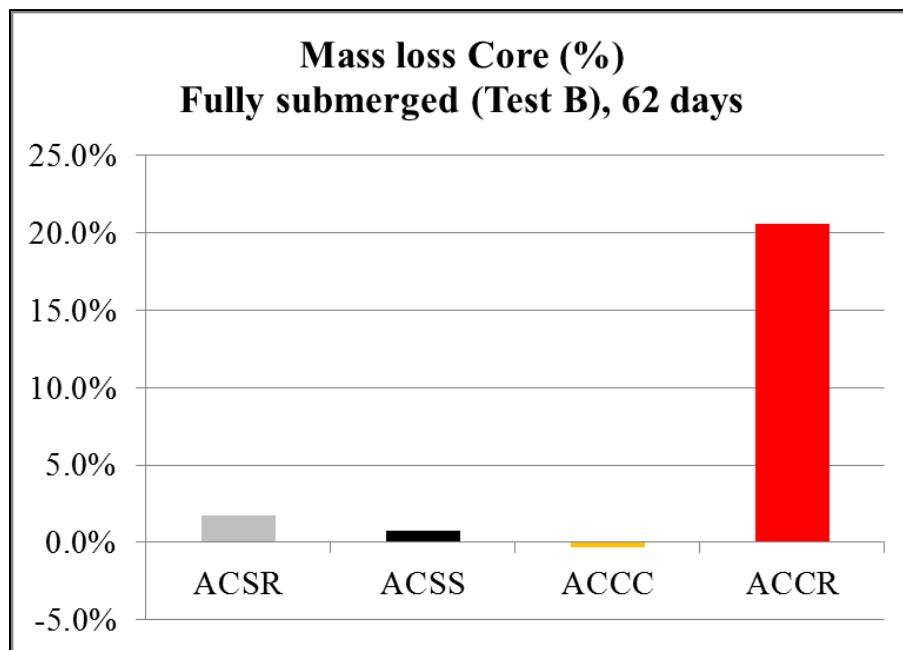


Figure 51: Mass loss core material (Test B)



Figure 52: Typical sample before cleaning (Test B).



Figure 53: No signs of rust on the ACSR core (Test B).



Figure 54: Neither the ACSS core had any signs of rust (Test B).



Figure 55: Three views of the same ACCC sample (Test B).
The minor surface damage is similar to that seen in Test A.



Figure 56: The ACCR sample before cleaning (Test B).



Figure 57: End view of the ACCR core strands (Test B).

The loss of matrix was calculated by cutting all the strands exactly in half. One set of the half strands was kept in the condition as above for reference. The other set of halves were cleaned with a plastic brush to remove all disengaged fibers and corrosion products. The matrix loss was calculated from the mass of the remaining composite compared to the original mass.

3.1.3 Test C: Single strand

Sample	Mass loss, Al strand (%)	Mass loss of matrix, core strand (%)^c
ACSR	1.60%	(test not performed)
ACSS	4.71%	(test not performed)
ACCC	1.57%	(test not performed)
ACCR	3.73%	13.5 %

^cTest only performed for ACCR.

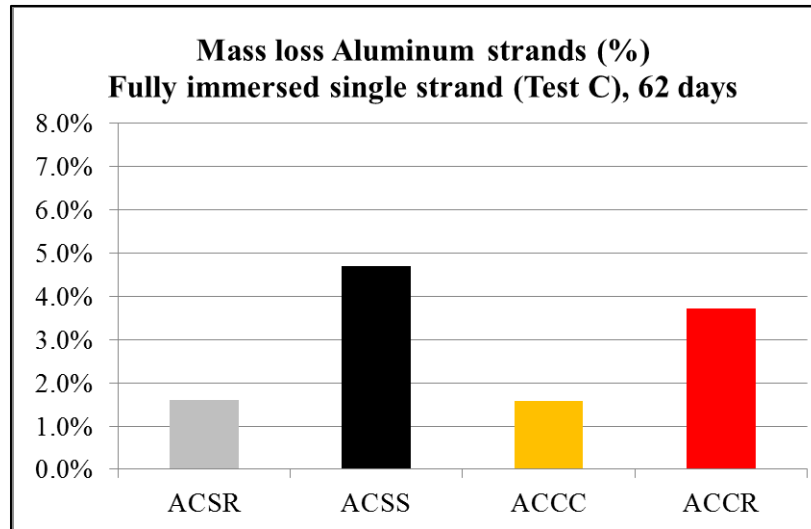


Figure 58: Mass loss aluminum strands (Test C)

The result from Test C has large uncertainty due the development of large corrosion pits under the holder for all four aluminum strands (see Figure 59). The chemical composition of the aluminum strands from ACSR, ACSS and ACCC is identical (1350 alloy). The strands from ACSS and ACCC also have the same heat treatment (fully annealed). Similar corrosion performance would therefore be expected. The large spread in mass loss from 1.57 % for ACCC to 4.71 % for ACSS should therefore be interpreted with caution.

The ACCR core strand did not develop large corrosion pits under the holder.



Figure 59: Samples after Test C.

Note the large corrosion pits to the left in the top picture. These were all created under the sample holder.

3.2 Results from electrochemical tests

3.2.1 Test D: Open circuit potential

Table 16: Results from Tests D open circuit corrosion potential (negative lead connected to core material)				
Sample	Room temperature		85°C	
	Open Circuit Potential, at RT (V)	Least noble material (will potentially corrode)	Open Circuit Potential, at 85°C (V)	Least noble material (will potentially corrode)
ACSR	+0.066 V	Galv. steel core	-0.041 V	Aluminum strands
ACSS	+0.19 V	Coated steel core	-0.17 V	Aluminum strands
ACCC	-1.13 V	Aluminum strands	-0.97 V	Aluminum strands
ACCR	+0.25 V	Composite core	+0.63 V	Composite core

Note: These values are with reference to the core material in the conductor, not to a reference electrode.

Note that the values reported in Table 16: **Results from Tests D open circuit corrosion potential** are not in relation to a standard electrode, but referenced to the core material in the conductor. If the potential is positive, the core material may corrode preferentially. If the potential is negative, the aluminum strands may corrode preferentially.

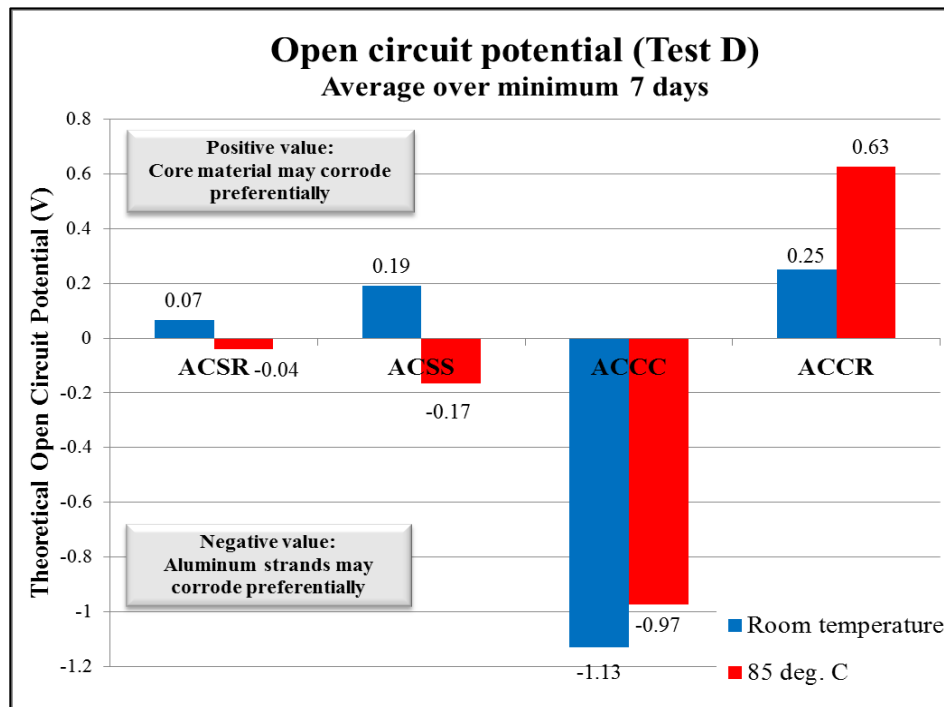


Figure 60: Open circuit potential (Test D).

It should also be noted that the open circuit potential *only* predicts the *direction* of possible galvanic corrosion. It is grossly inadequate for predicting the magnitude of galvanic corrosion since it does not take into account such factors as polarization and area ratio effects.

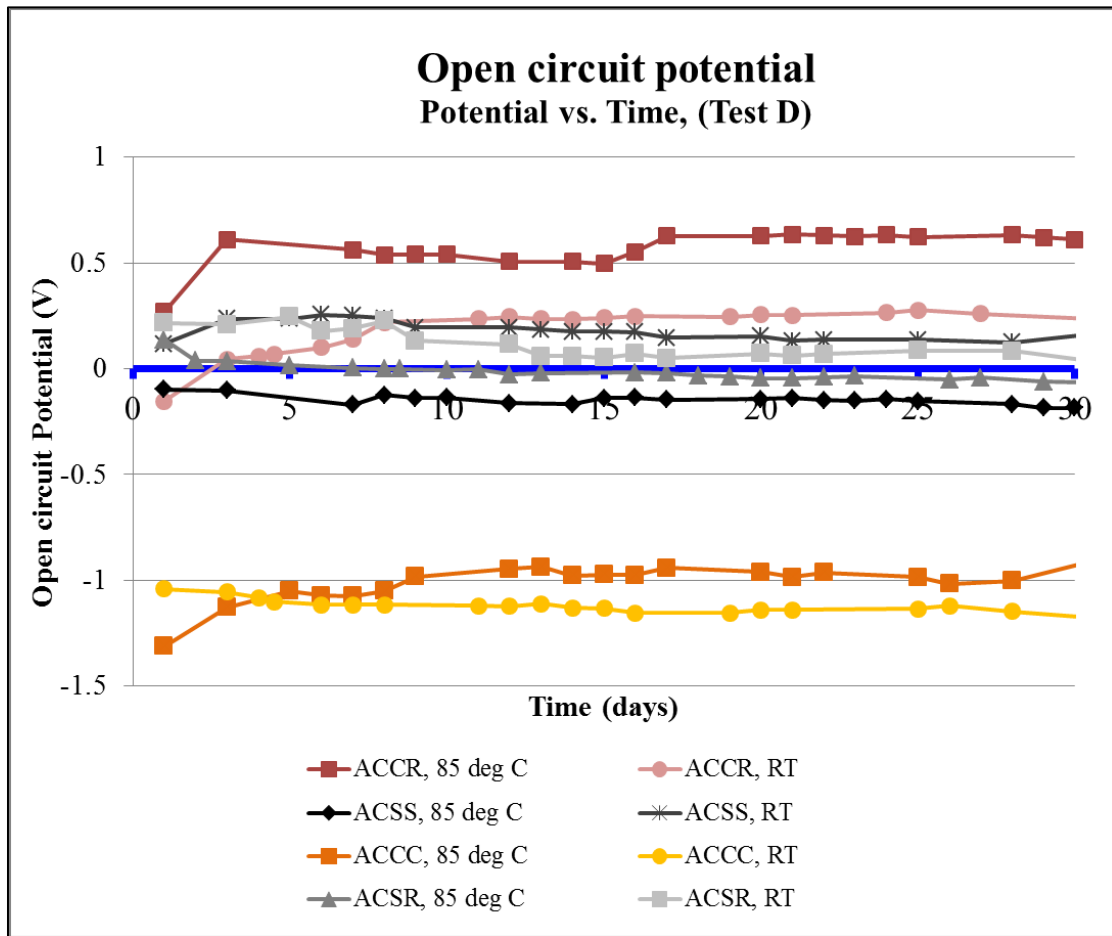


Figure 61: Open circuit potential vs. time (Test D)

The directions of the galvanic coupling for ACSR, ACSS and ACCC at room temperature were all expected and agree with the galvanic series in Figure 8. In ACSR and ACSS the coating on the steel may corrode first, which is a well-known behavior. In ACCC, the aluminum strands corrodes first due to the graphite being more noble than most metals.

The room temperature result for ACCR indicated that the aluminum matrix composite might be more susceptible to corrosion than the Al-Zr alloy current carrying strands. However, 0.25 V is a borderline case with regards to the rule of thumb stating that for a 0.10-0.25 V potential difference galvanic corrosion may start to become an issue. However, the result for 85°C at 0.63 V is well above the rule of thumb value.

The 85°C potential for ACCC was very similar to the potential at room temperature and was approximately -1 V.

The change of polarity of the potential in ACSR and ACSS between room temperature and 85°C was a major surprise. This will be discussed more in chapter four.

3.2.2 Test E: Galvanic corrosion current

The open circuit potential in the previous test only pointed out the possible direction of galvanic corrosion, while the measurement of the galvanic corrosion current in this test gives an actual measurement of the corrosion rate. The following data came from the whole conductor samples with the core and aluminum strands separated by fabric.

Table 17: Results from Test E galvanic corrosion current density (negative lead connected to core material)						
Sample	Room temperature		85°C			
	Galvanic corrosion current density at RT ($\mu\text{A}/\text{cm}^2$)	Corroding material at RT	Galvanic corrosion current density at 85°C ($\mu\text{A}/\text{cm}^2$)	Corroding material at 85°C	Theoretical mass loss in 104 days (grams)	% of actual lost mass in Test A
ACSR	+3.8 $\mu\text{A}/\text{cm}^2$	Core	-1.7 $\mu\text{A}/\text{cm}^2$	Al strands	0.93 g	14 %
ACSS	+1.24 $\mu\text{A}/\text{cm}^2$	Core	-10.0 $\mu\text{A}/\text{cm}^2$	Al strands	4.9 g	22 %
ACCC	-0.14 $\mu\text{A}/\text{cm}^2$	Al strands	-0.060 $\mu\text{A}/\text{cm}^2$	Al strands	0.035 g	1.4 %
ACCR	0.2 $\mu\text{A}/\text{cm}^2$	Core	+15.5 $\mu\text{A}/\text{cm}^2$	Core	3.0 g	21 %

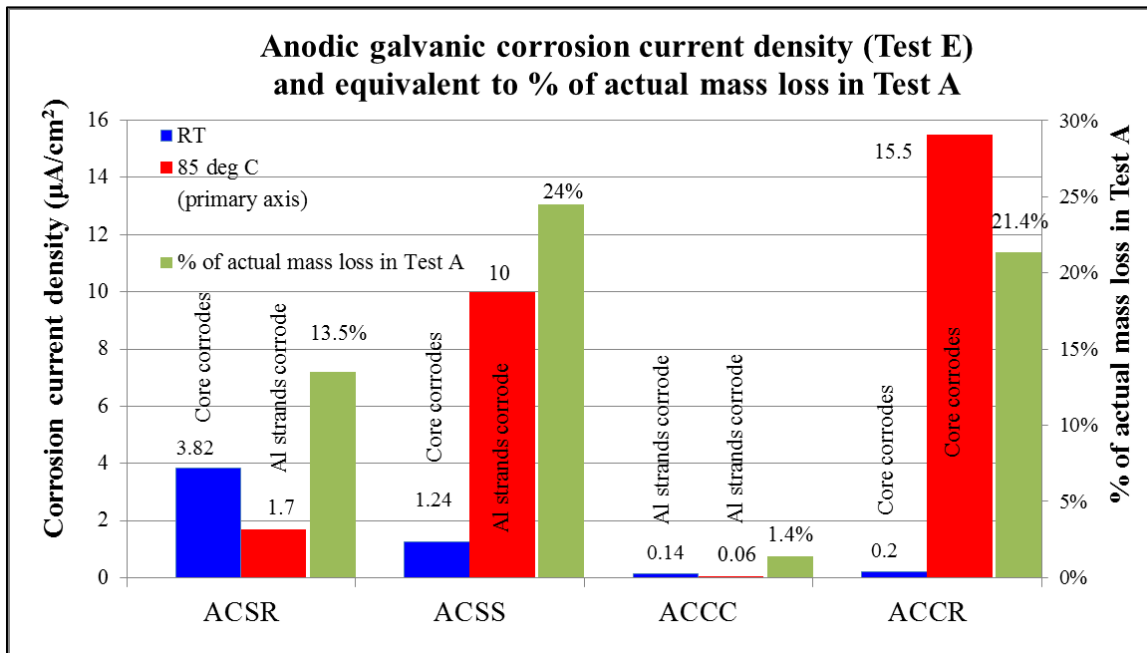


Figure 62: Anodic galvanic corrosion current density (Test E) and equivalent to % of actual mass loss in Test A

Test E confirmed the direction of galvanic corrosion indicated by Test D. It also confirms the well-known fact that the magnitude of the open circuit potential *cannot* be used to predict the corrosion rate. ACCC had the highest open circuit potential, but the lowest corrosion rate. ACSS had the second lowest open circuit potential at 85°C, but the second highest corrosion rate. ACSR at room temperature was the only sample that showed a distinct dependency on agitation of the electrolyte (see waveform in Figure 63).

The fifth column in Table 17 states the theoretical mass loss if the measured galvanic corrosion current would continue for 104 days at the same level. The last column and the green bars in Figure 62 illustrate this theoretical mass loss compared to the actual mass loss measured in Test A.

It should be noticed that the current density reported in this section and in subsequent sections is only an average over the whole anode area. The current density can be a lot higher locally where pits are operating.

The results will be discussed in detail in chapter four.

Calculation of results

All the samples showed a transient behavior (see Figure 63). The current decreased very fast within the first few minutes, and had reached plateau values within a couple of hours for all samples except ACCR (this is discussed in detail in chapter four). The current then remained steady for the remainder of the test. All tests were run for at least 20 hours, and the current reported in Table 17 is the average value of the plateau.

The test with ACCR was eventually extended to 240 hours (10 days). The results in Figure 64 are extensively discussed in chapter four.

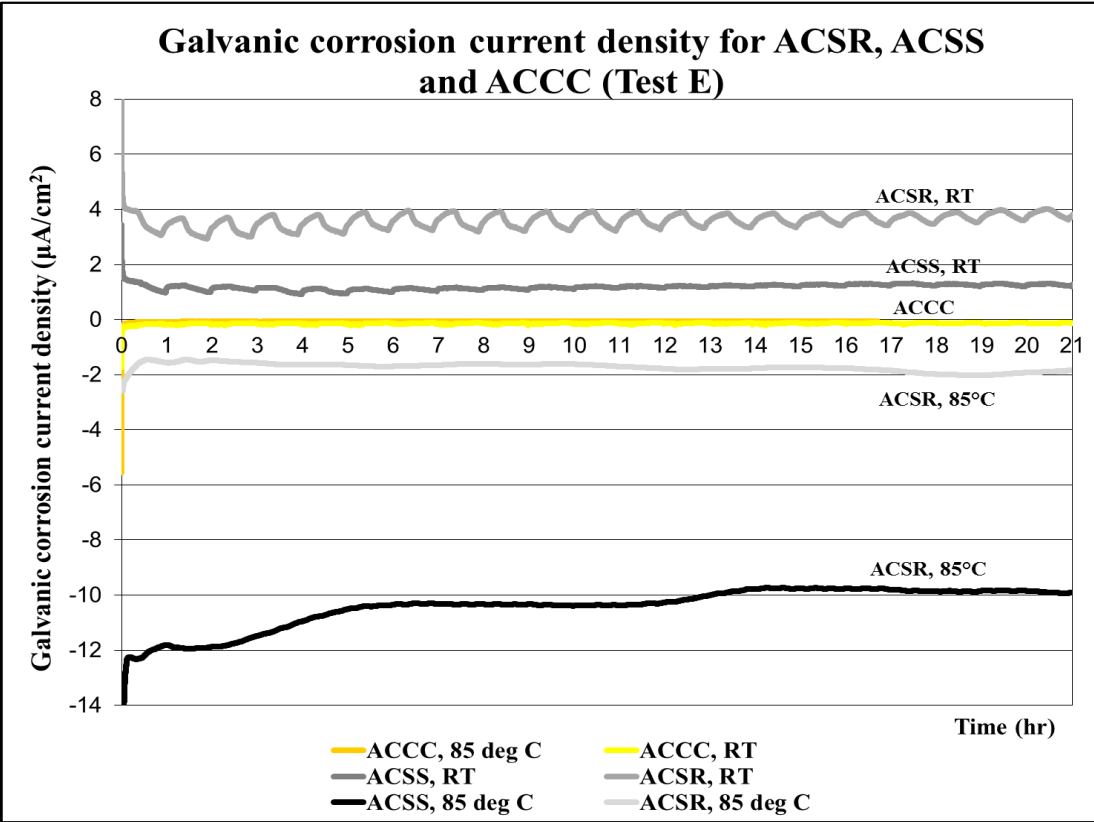


Figure 63: Galvanic corrosion current density (Test E)

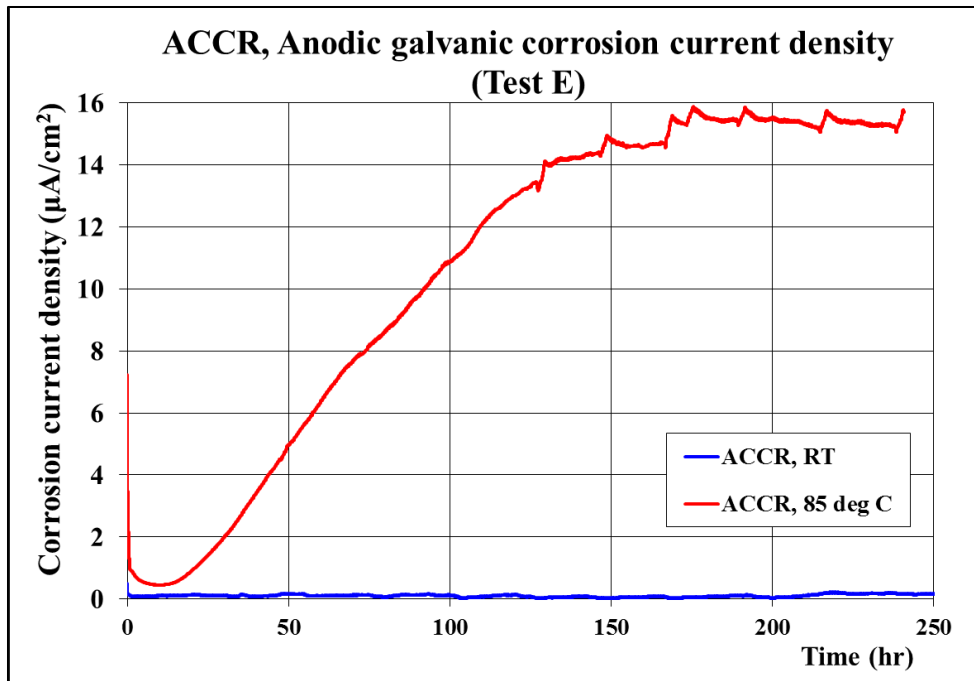


Figure 64: Galvanic corrosion current density for ACCR.
This plot is discussed extensively in chapter four.

3.2.3 Test F: Corrosion potential with reference to Ag-AgCl reference electrode

Table 18: Results from Tests F - open circuit corrosion potential (E_{corr}) (with reference to Ag-AgCl reference electrode)

Sample		E_{corr} (V) at RT	Theoretical potential relative to Al strands (V)	Corroding material (theoretical)	E_{corr} (V) at 85°C	Theoretical potential relative to Al strands (V)	Corroding material (theoretical)
ACSR	Al strands (1350-H19)	-0.70 V	--	--	-0.85 V	--	--
	Core (galvanized steel)	-0.98 V	-0.28 V	Core	-1.01 V	-0.16 V	Core
	Core (steel, galvanization removed)	-0.48 V	+0.22 V	Al str.	-0.60 V	+0.25 V	Al str.
ACSS	Al strands (1350-O)	-0.74 V	--	--	-0.84 V	--	--
	Core (Galfan coated Steel)	-0.98 V	-0.24 V	Core	-0.99 V	-0.15 V	Core
	Core (steel, coating removed)	-0.54 V	+0.20 V	Al str.	-0.62 V	+0.22 V	Al str.
ACCC	Al strands (1350-O)	-0.70 V	--	--	-0.82 V	--	--
	Core (carbon fiber composite)	+0.10 V	+0.80 V	Al str.	+0.10 V	+0.92 V	Al. str.
ACCR	Al strands (Aluminum-Zirconium alloy)	-0.72 V	--	--	-0.89 V	--	--
	Core (aluminum-matrix composite)	-0.68 V	+0.04 V	None*	-1.42 V	-0.53 V	Core
Ref.	99.999 % aluminum, polished	-0.84 V	--	--	-1.08 V	--	---

* The potential is below the 0.10-0.25 V where galvanic corrosion is expected to be a problem.

Test F, performed with an Ag-AgCl reference electrode, confirmed the direction of the galvanic corrosion measured in Test E in all but two cases. The measurements with the reference potential indicated that the core material in ACSR and ACSS at 85°C always would be the core material until the coating is gone and the more noble steel is exposed. This result is opposite to the results from Test D and E and will be discussed in detail in chapter four.

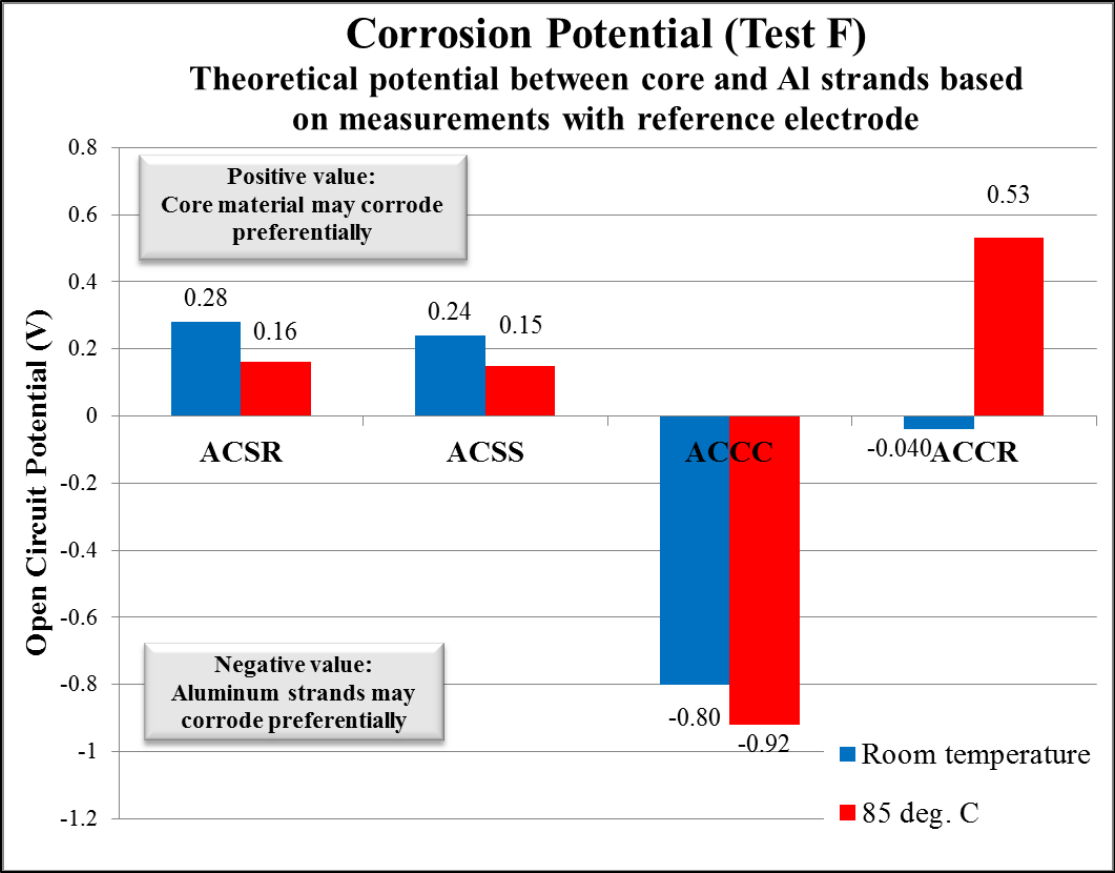


Figure 65: Theoretical open circuit potential in the conductor based on the measurements of the individual components. Note that the polarity is flipped compared to Table 18 to make the numbers comparable to the results from Test D.

3.3 Error analysis

This study is a master's project, which means that the time constraints would not permit long-term (many years) of testing. Accelerated testing was therefore absolutely necessary. The pioneer nature of this study and the limited availability of testing equipment resulted in fewer tested samples than desired. For all of the performed tests, one sample of each conductor was tested for each temperature. Some tests were repeated due to errors during the testing (such as power black-outs). Limited supply of conductor specimens also limited the number of tested samples.

Another possible source of errors is that three of the conductors (ACCC, ACSR and ACCR) were of the size "Drake 795 kcmil", while the ACSS conductor was of "Redwing 795 kcmil". ("Redwing" and "Drake" are model names referring to the specific geometry, while "795 kcmil" is the cross section area in kcmil (1 kcmil = 0.5067 mm²)).

They all have very similar outer diameters. The Redwing ACSS has thinner strands than the other three. The ACCC was also stranded with trapezoidal strands, while the others were using round strands. The trapezoidal strands are thicker, resulting in less surface area for the same cross section. Since corrosion to a large extent is a surface phenomenon, the different stranding may have affected the results.

The mass loss measurements were evaluated using a high-quality digital scale with 0.0001 g resolution. However, the mechanical cleaning method used in this study does likely add a significantly larger error. All the mass loss percentages are therefore only reported with two significant figures. The results from the electrochemical tests are also only reported with two significant figures.

CHAPTER FOUR: DISCUSSION

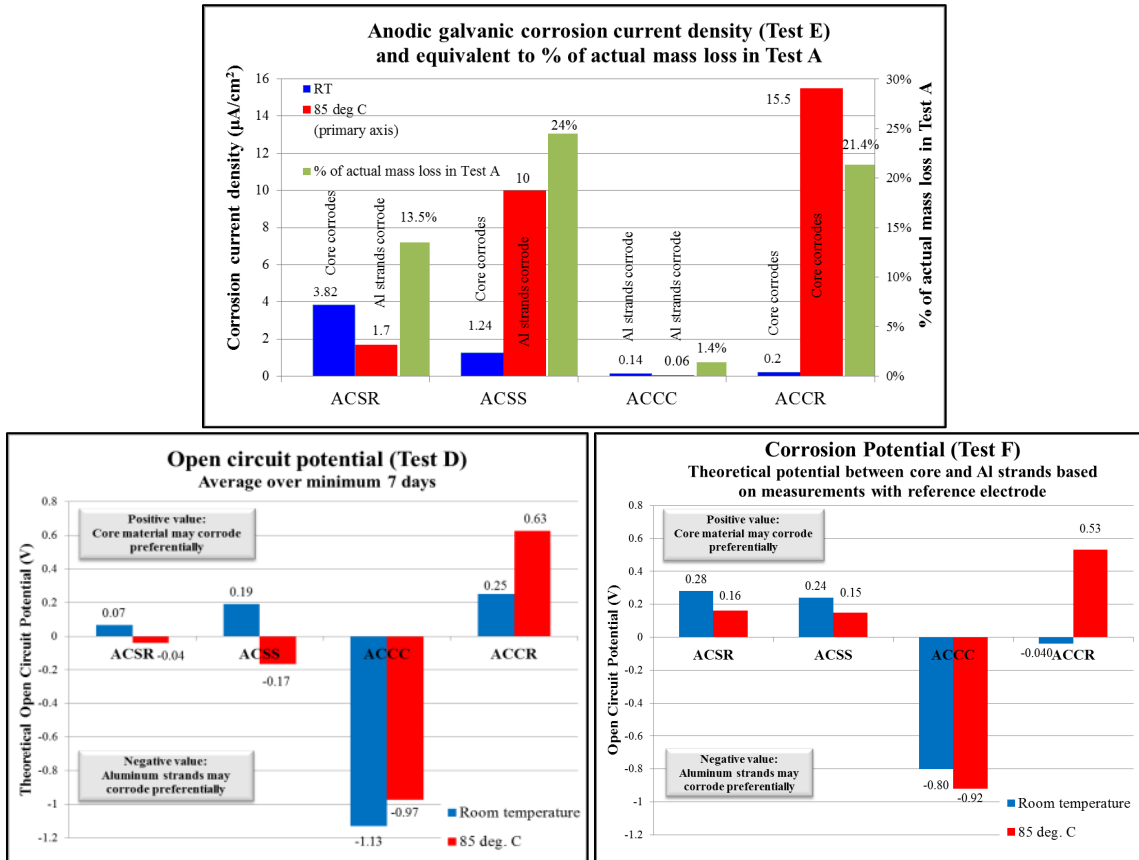
This chapter will discuss some of the more interesting results in detail. The corrosion results from the three HTLS conductors will be compared to the performance of the conventional ACSR conductor that was used as a baseline reference.

4.1 ACSR

It is well-known that ACSR can suffer from galvanic corrosion in humid environments such as coastal areas. The performed tests confirm that the aluminum strands and the galvanized steel core create a galvanic couple. According to the galvanic series in seawater at 25°C, zinc is less noble than aluminum while steel is more noble. Galvanic corrosion at this temperature will therefore first cause a loss of the zinc coating, and then corrosion of the aluminum. This relation was confirmed by all three electrochemical measurements (see Tables 16-18 and Figures 60-63 and 65). (Figures 60, 62 and 65 repeated on next page).

At 85°C, the picture was less clear. While the standard measurements with reference electrode (Test F, Table 18 and Figure 65) indicated that the situation was similar to room temperature, the measurements of the whole conductor (Test D and E, Table 16-17) gave a very different result. The open potential in the whole conductor sample indicated that the aluminum was less noble than zinc coated steel core and would

corrode preferentially. The galvanic corrosion current measurement in Test E also confirmed that (see Figures 60 and 62).



Figures 62, 60 and 65 (repeated).

It was surprising that the sign of the potential shifted between room temperature and 85°C in ACSR. The aluminum strands went from being the more noble material to being the less noble in the whole conductor samples. The literature (Roberge, 2008) reports that zinc and steel can switch polarity at about 60°C, making zinc the more noble and steel the less noble metal above 60°C. Nothing has been found in the literature regarding zinc and aluminum, but it appears that the negativity of zinc in tests D and E decreased to such an extent that it became more noble than aluminum. Another possible solution is that the zinc disappeared quickly at 85°C leaving the steel exposed. Figure

61 shows that the aluminum is the less noble at the very beginning of the 85°C test. It is, however, possible that the RTV seal of the ends of the core material did not sufficiently cover the steel cross-section that became exposed while cutting the sample. The exposed steel may have dominated the open circuit potential as well as during the galvanic corrosion testing

The discrepancy between the potential measured in the whole conductor sample and the potential measured with a reference electrode points out the need for testing whole conductors in their actual geometry, and not only the individual components.

The mass loss of the aluminum strands and the core material were of the same order of magnitude in the immersion tests A and B (2.4 and 2.3 % for Al strands and 2.8 and 1.7 % for core material, table 3). Since no material appears to have corroded preferentially, the galvanic corrosion rate at 85°C appears to have been low in this particular environment. The green bar for ACSR in Figure 62 confirms a relatively low galvanic corrosion rate. If the measured galvanic corrosion current were to be extrapolated for 104 days, the galvanic corrosion would only account for 13.5 % of the mass loss of aluminum. Both the galvanic corrosion rate and the fraction of aluminum loss that can be related to the galvanic corrosion are much lower than for ACSS, which is discussed in detail in the next section.

It is, however, important to emphasize that different environments might give very different corrosion rates. This study only points out the *possibility* of galvanic corrosion but that the galvanic corrosion appears to be relatively low in the tested environment; it does not aim to quantify the corrosion rate in an actual service environment.

Corrosion pattern

While the corrosion of the aluminum strands in ACSR was highly localized in the form of pitting corrosion (see Figure 37), the corrosion of the core appeared to be much more uniform. The corrosion of the core was also much less severe. The steel strands had started to rust in some locations. The rust was, surprisingly enough, located above the liquid level at the seal of the testing chamber. In some of the places, the galvanization was completely lost (see Figure 44). No mechanical tests were performed on the core, but the core material appears to have performed well in this very aggressive testing environment.

4.2 ACSS

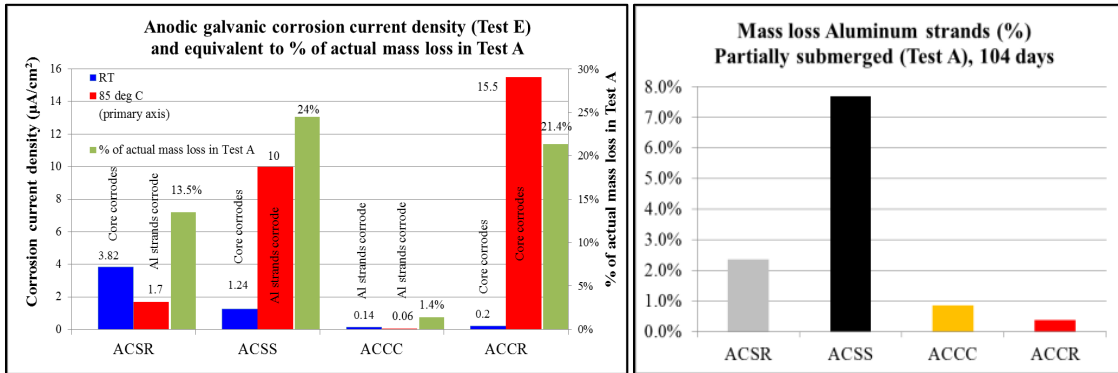
ACSS has a design very similar to ACSR. The main difference is the use of a higher strength steel and the Galfan-coating instead of traditional galvanization.

Just as with ACSR, the measurements with reference electrode of the ACSS components indicated that the coated core always was less noble than the aluminum strands, while the measurements of whole samples showed the same switch of polarity between room temperature and 85⁰C (see Tables 16-18 and Figures 60-63).

The mass loss in the immersion tests indicates that ACSS might be more susceptible to galvanic corrosion than ACSR. ACSS had the highest mass loss of aluminum in the strands in both the partially submerged and fully submerged tests; 7.7 % and 3.0 % respectively (3.2 and 1.3 times the mass loss in ACSR, Tables 13-14 and Figures 83 and 49). This high mass loss combined with a low mass loss of the core material (0.77 % in test A and 0.40 % in Test B) points in the direction of a possible galvanic corrosion situation where the aluminum works as a sacrificial anode.

This fact was confirmed by the corrosion current density at 85⁰C in test E where the aluminum was the corroding material and the current density for ACSS was almost 6 times larger than for ACSR. Figures 62 and 36 (repeated below) show a direct correlation between the galvanic corrosion current density and the mass loss of aluminum strands in Test A. Of the conductors that preferentially corroded the aluminum strands at 85⁰C (all except ACCR), ACSS has the highest corrosion current density and also the highest mass loss of the strands. ACSR exhibited a lower current density and lower mass loss of aluminum. ACCC had no galvanic corrosion present in Test A and has an aluminum mass loss lower than both ACSR and ACSS. (ACCR represents an extreme case where

the core preferentially corrodes and in doing so provides anodic protection to the aluminum strands. ACCR exhibited the lowest mass loss of aluminum strands. The results for ACCR will be extensively discussed in section 4.4.)



Figures 62 and 36 (repeated).

Test B

The results from Test B (Figure 49, repeated below) do not fully agree with the observations in Test A and E described above. While ACSS still has the highest mass loss of aluminum and ACCR has the lowest, ACSR and ACCC have switched places. It appears that the galvanic corrosion rate was much lower in this test.

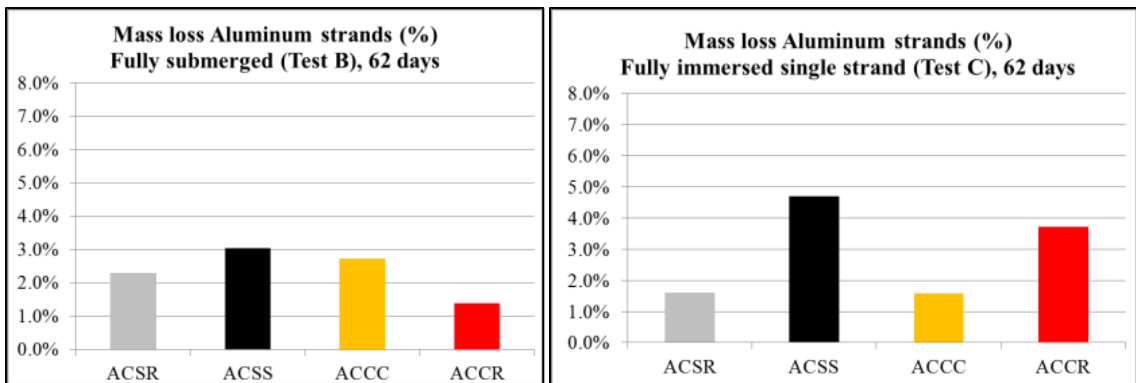


Figure 49 and 58 (repeated).

A possible hypothesis is that the results from Test B are influenced by the very short samples (only 90 mm). First, let us repeat here the necessary conditions for galvanic

corrosion to take place. Three conditions have to be fulfilled simultaneously for galvanic corrosion to occur: 1) There must be two materials present with different corrosion potentials. 2) There must be an electrolyte present. 3) The two materials must be in direct electrical contact with each other. If one or more of these conditions are not satisfied, galvanic corrosion will not occur. All samples except ACCC fulfill requirement 1) (two different metals). All samples fulfill requirement 2) (electrolyte present). However, requirement 3) might not have been fulfilled during the entire test duration of Test B. Let us examine the differences in sample design in Test A and Test B.

The samples in Test A were about 300 mm long and were sticking out of the testing cell. The very top of the sample was not subject to corrosion, and there was always a low-resistance electrical connection between the aluminum strands and the core material. The samples in Test B were only 90 mm long and the entire sample was submerged. It is conceivable that the passive film on the aluminum or the build-up of corrosion products could result in an electrically insulating layer between the core material and aluminum strands. An electrically insulating layer would prevent galvanic corrosion from occurring.

The aluminum strands in ACSS have the identical chemical composition as in ACSR and ACCC and the identical heat treatment as ACCC. The exact chemical composition of the aluminum strands in ACCR is not known. If an insulating layer was formed preventing galvanic corrosion, a similar mass loss would be expected for at least three of the samples, which also was the case in Test B (see Figure 49). The generally higher mass loss per unit time in Test B compared to Test A could be explained by differences in the testing environment such as more efficient agitation due to a different

sample holder design. The mass loss in Test B is also within the range of the results of Test C of single aluminum strands (Test C should be interpreted with caution due to large corrosion pits under the sample holder). In the real service environment, a direct electrical connection is likely always present. The core and the aluminum strands are electrically connected in dead ends and splices (ACCC may or may not be an exception). The motion of the conductor may also remove an insulating layer consisting of oxide, dirt and/or corrosion products.

Another possible explanation for the higher mass loss in ACSS compared to ACSR are the thinner strands in ACSS give a larger exposed surface area. However, calculations show that this would still not explain the large difference and the severe corrosion that can be seen in Figure 66 below. At this point, the most likely explanation is that the corrosion in ACSS is accelerated by the galvanic coupling to the core material. It is currently unclear why the Galfan coating appears to give a stronger galvanic corrosion than a conventional zinc coating. Further testing would also be required to determine if this can be a potential problem in the real service environment.



Figure 66: Severe localized corrosion on the ACSS sample after Test A.

4.3 ACCC

ACCC is based on a design aimed to mitigate the expected problem of galvanic corrosion between the aluminum strands and the carbon fiber composite core. When the fiberglass galvanic barrier is intact, no galvanic corrosion can occur. The absence of galvanic corrosion is a possible explanation for the low mass loss of aluminum strands in the partially submerged test (Test A). The mass loss was 0.84 %, which is 1/3 of the mass loss in ACSR. However, the mass loss in the fully submerged test (Test B) was comparable to ACSR. A possible explanation for this was given in the previous section.

The long-term immersion tests A and B caused some minor surface damage to the fiberglass galvanic barrier (see Figures 42 and 55). The damage is believed to be caused by a combination of the hot solution and the alkaline corrosion products (aluminum hydroxide) from the corrosion of the aluminum strands, since reference samples placed in the precipitated alkaline corrosion products at the bottom of the testing cell caused similar surface damage. Other reference samples placed in hot saltwater alone did not exhibit this kind of surface damage (see figure 67).



Figure 67: Three samples of ACCC core exposed to 85°C for approx. 100 days.
Top: Sample exposed to same electrolyte as used in this study, but without presence of aluminum hydroxide. Middle: sample placed in the “slurry” of aluminum hydroxide at the bottom of the testing cell during Test A. Bottom: Sample from Test A.

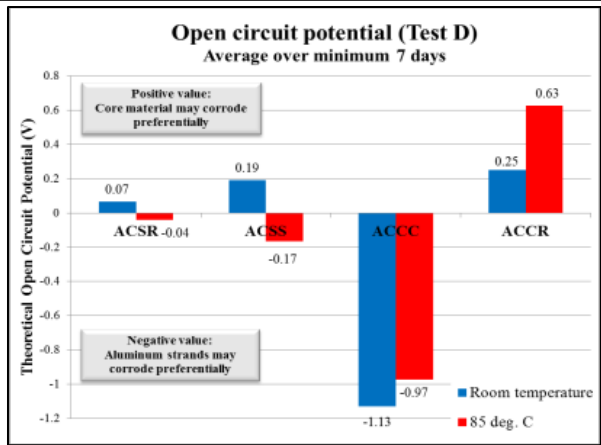
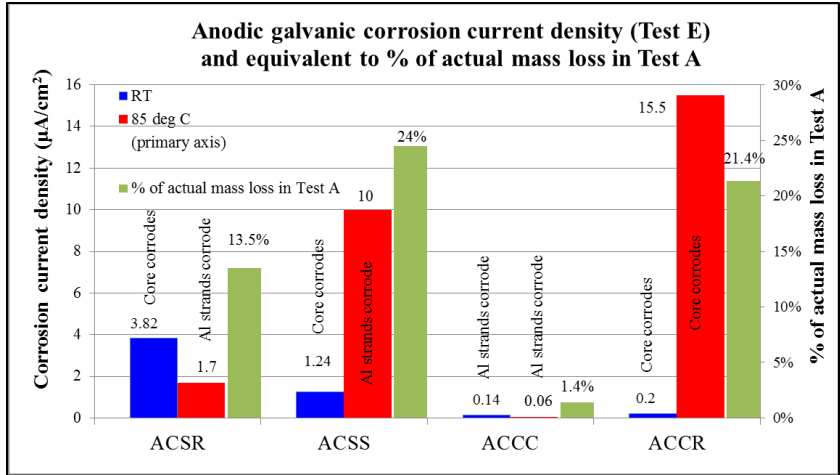
The damage to the fiberglass was not deep enough to expose any of the carbon fiber composite to the aluminum, and since there was no exposed carbon fiber composite

and no direct electrical contact between the carbon and the aluminum, no galvanic corrosion occurred.

Test D, performed with intentional damage to the fiberglass barrier (see Figure 17C), showed a strong galvanic coupling between carbon and aluminum with an open circuit potential of 1.13 V at room temperature and 0.97 V at 85⁰C (the carbon fiber composite is the more noble material, see Figure 60). The relation was confirmed by the measurements with a reference electrode in Test F (Table 18 and Figure 65).

Despite the fact that ACCC does not suffer from galvanic corrosion in its undamaged condition, it was of interest to evaluate potential problems with galvanic corrosion if the fiberglass is damaged, for example, by atmospheric aging, over-bending, or contains manufacturing defects.

Initial tests on single strands of aluminum coupled to longitudinally sectioned composite cores of the same exposed area showed a high galvanic corrosion rate at 85⁰C with current densities of over 160 $\mu\text{A}/\text{cm}^2$ (these tests are not reported in the tables or figures). This corrosion rate would be completely unacceptable in service. However, Test E (with the whole conductor sample with a section of the core cut down to the carbon fiber composite) gave a very different result. The corrosion current density plateaued at about 0.060 $\mu\text{A}/\text{cm}^2$ at 85⁰C and 0.14 $\mu\text{A}/\text{cm}^2$ at RT (see Figures 62 and 63), which were the lowest corrosion rates measured of all samples. The very large area ratio of 1:53 between the exposed carbon fiber composite and the aluminum strands was the reason for the low corrosion rate. The much larger anodic area compared to the cathodic area is favorable from a corrosion resistance point of view.



Figures 62 and 60 (repeated).

The large area ratio does not, however, fully explain the difference between the initial test of the small samples and the whole conductor. There appear to be additional corrosion mechanisms that limit the galvanic corrosion in the actual geometry of the conductor. These mechanisms were not further investigated, but a possible explanation could be that the likely cathodic reaction (occurring at the carbon fiber composite) consumes oxygen and the corrosion rate would be limited by the diffusion of oxygen into the conductor.

Despite the very low measured galvanic corrosion rate, and a favorable cathode to anode area ratio in ACCC, damage to the fiberglass barrier should be avoided to prevent

galvanic corrosion. Different environments may cause much larger corrosion rates, and it is also unclear if the corrosion products may deteriorate the mechanical properties of the composite core. As long as the fiberglass barrier is intact, galvanic corrosion cannot occur.

In spite of these favorable results from a galvanic corrosion point of view, the service life of ACCC is still discussed due to concerns of chemical and physical degradation of the polymer matrix composite. This aspect is outside the scope of this study but is being studied by other researchers at the University of Denver.

4.4 ACCR

ACCR contains an aluminum based composite core material surrounded by strands of aluminum alloy, and it would be acceptable to assume that it would not suffer from galvanic corrosion. It was therefore a major surprise to us that the matrix in the core material had selectively corroded in both long-term immersion tests (Test A and B).

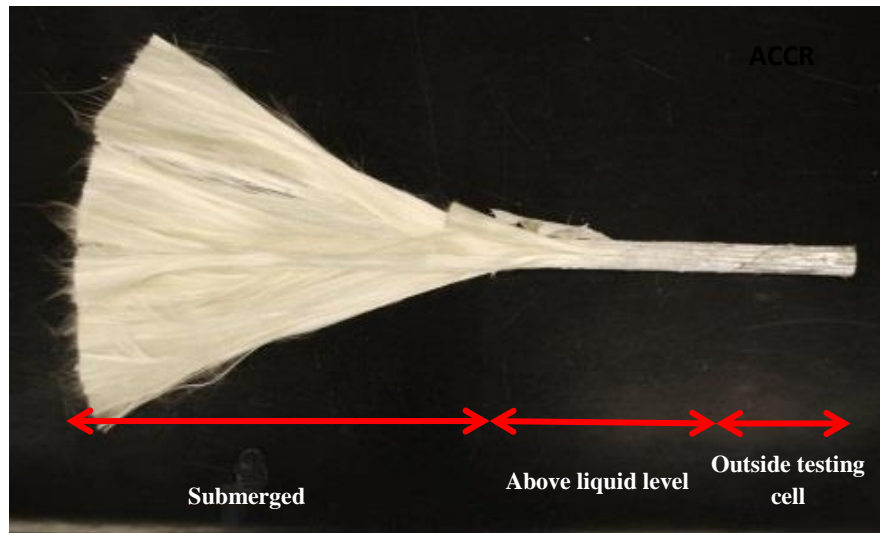


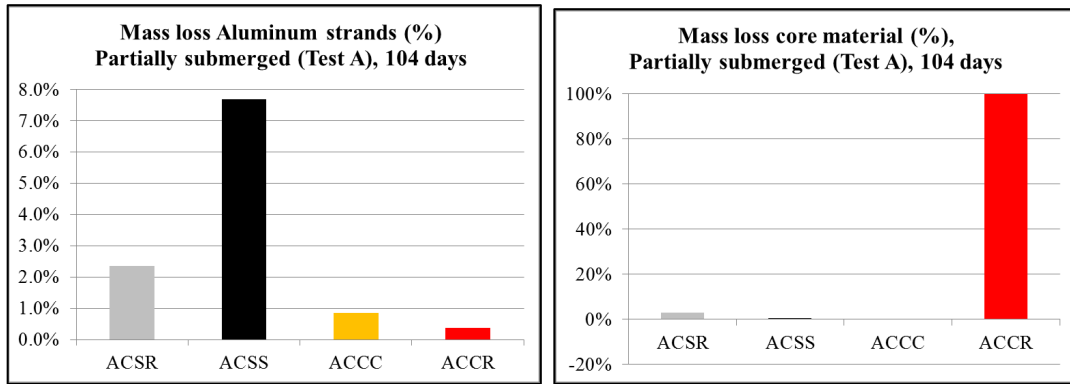
Figure 48 (repeated): The metal matrix composite core of the ACCR after Test A (104 days in 85°C, 3 wt. % seasalt aqueous solution). Only the aluminum oxide layers are left in the submerged section.



Figure 68: Build-up of corrosion products at the end of the ACCR core. Picture taken on day 7 of 104 in Test A.

In the partially submerged test (A), all the aluminum matrix was gone in the submerged part of the sample after 104 days (see Figure 41). Only the Al_2O_3 fibers were left (see Figure 48). In the fully submerged test (B), approximately 21 % of the matrix

material was lost in 62 days (see figure 57). At the same time, the mass loss of the current carrying Al-Zr strands was only 0.38 % and 1.4 % respectively (see Figures 36 and 49).



Figures 36 and 41 (repeated)

The selective corrosion of the core material pointed to a possible galvanic corrosion situation, despite both materials being aluminum-based.

The electrochemical tests D and F confirmed that the two materials can create a galvanic coupling, particularly at 85°C. Test D, performed on a whole conductor sample with the core and the Al-Zr strands separated with fabric, gave an open circuit potential of 0.63 V (Al-Zr being the more noble material). The standardized Test F gave a difference in E_{corr} of 0.53 V. This is well over the rule of thumb of 100-250 mV where galvanic corrosion often is found to be a problem.

Room temperature – low corrosion rate

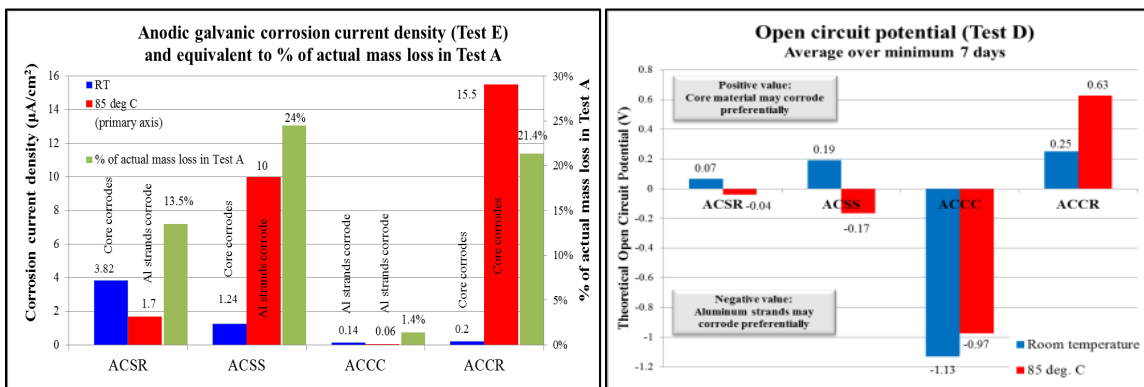
At room temperature, the results are inconclusive. Test D of the whole conductor sample showed an open circuit potential of 0.25 V between the two materials (Al-Zr as the more noble), while the corrosion potentials (E_{corr}) were measured to be within 0.040 V in the standardized Test F (with the core material as the more noble material).

The corrosion potentials appeared to be stable within minutes when measured with the reference electrode, while the potential of the whole samples (Test D) took seven

days to build up to 0.22 V in Test D, and the potential continued to increase during the remaining 14 days of the test. The reason for this is currently unclear. It is possible that Test F (with reference electrode) at RT would show a similar result to Test D (whole conductor) if given enough time. The test was stopped after 1 hour since that was specified by ASTM G69-12.

The galvanic corrosion current measurement at RT was also inconclusive. The first run of Test E, performed directly after Test D using the same samples, gave a steady-state corrosion current density of $1.0 \mu\text{A}/\text{cm}^2$. This is of the same order of magnitude as the corrosion current density in ACSR. The sample was thereafter left in the saltwater for several weeks. The open circuit potential stayed between 0.19 V and 0.38 V during this time. However, when the external corrosion current circuit was connected and the test repeated, corrosion current density was less than $0.2 \mu\text{A}/\text{cm}^2$ and stayed at that level even when the test was extended to 250 hours. The core material appears to have formed a passive oxide layer that did not break down during the galvanic corrosion test at RT.

Based on these results, ACCR seems to have very low susceptibility to galvanic corrosion in saltwater at room temperature (see Figure 62).



Figures 62 and 60 (repeated).

85°C – galvanic corrosion potential problem

At 85°C, the resistance of ACCR to galvanic corrosion appears to be very different. The possibility of galvanic corrosion in the particular environment used in this study (3 wt. % seasalt aqueous solution) was confirmed by Test E. Test E also revealed a possible synergistic effect between different corrosion mechanisms, working together in an unfavorable way.

All four conductors exhibited a transient behavior when they were initially connected to the external measurement circuit. The current density for all of them, with the exception of ACCR, stabilized within minutes or a few hours and stayed the same for the remaining 20 hours of the test. The tests were repeated with very similar results. The ACCR, on the other hand, remained unstable. The test was repeated several times with different results. The test was finally extended to 10 days for the ACCR sample at 85°C, and it revealed an interesting corrosion behavior (see figure 64).

After the initial transient decay, the corrosion current density started to increase again. After about 15 hours, the increase was approximately linear for the next 110 hours. The current density plateaued at about 150 hours and remained relatively stable for the remainder of the test. When the current density had not changed significantly for more than 4 days (100 hours), the test was stopped. The final corrosion current density was $15.5 \mu\text{A}/\text{cm}^2$. If this current density was sustained, it would in 104 days (the duration of Test A) cause a loss of 21 % of the aluminum matrix in the core (see Figure 62).

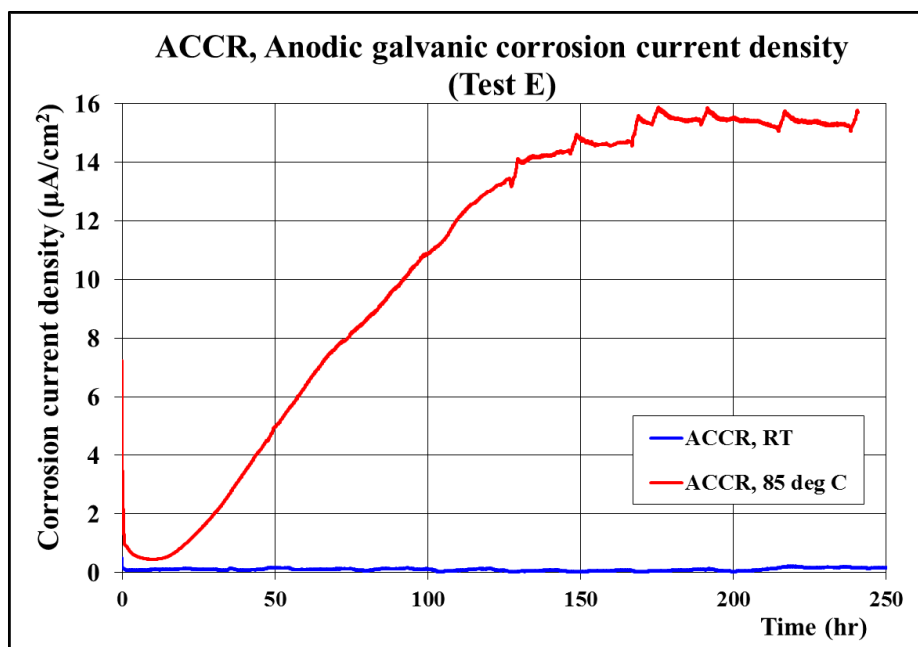


Figure 64 (repeated). The sharp peaks are caused by refilling of water in the testing cell.

The increase in corrosion rate over several days indicates that this is not a typical galvanic corrosion situation. It is known that aluminum-matrix composites are susceptible to pitting corrosion and breakdown of the passive film due to the physical and chemical heterogeneities caused by the reinforcing fibers (see sections 1.3.4 and 1.3.5). Figure 69 shows the fiber-matrix interface in the ACCC core damaged by corrosion.. The image came from a lightly corroded ACCR composite strand that was submerged in the 85°C electrolyte for a few days. Figure 70 show that the surface on the composite can be relatively uneven and provide many initiation sites for corrosion. It has not been determined if it is the fibers or something else in the composite that causes the material to lose its passivity, but the standardized Test D did confirm that the composite material is very active at 85°C. The open circuit corrosion potential (E_{corr}) was measured at -1.42 V for the composite compared to -0.89 V for the Al-Zr strands (table 5).

The electromotive force resulting from the difference in corrosion potentials is likely causing the initial galvanic corrosion current to drop while a passive film forms. However the galvanic coupling appears to accelerate the naturally occurring pitting corrosion caused by the aggressive electrolyte. Pitting corrosion is autocatalytic in its nature. Once the passive film is broken and the pit starts to grow, the local environment is altered in such a way that further pit growth is promoted. The fact that the corroding composite is surrounded by the more passive Al-Zr strands with an unfavorably large cathode/anode area ratio may also cause a simultaneous increase of Al^{3+} ions and decrease of oxygen in the core area of the conductor, both of which would promote the corrosion.

Based on the results from the tests performed in this study, it appears that the two materials in the ACCR conductor under some circumstances can act as an active-passive cell. At room temperature, both materials passivate and exhibit good corrosion resistance. At 85°C, the composite cannot keep its passivity with galvanic corrosion as a result.

The presence of the galvanic corrosion explains the low mass loss of the current-carrying Al-Zr strands in the long-term immersion tests (A and B). The less noble core matrix worked as a sacrificial anode and protected the more noble Al-Zr strands.

Even if the observed corrosion may appear dramatic, one should keep in mind that these are all highly accelerated tests. Different environments may cause much less corrosion, as the tests at room temperature clearly showed. In the actual service environment, the corrosion takes place in a thin layer of moisture and the corrosion rate will certainly be much lower and may never accelerate in the way it did in this study.

However, one should also keep in mind that HTLS conductors are designed to operate at high temperatures. The observed problems in this study might diminish at operating temperatures over 100°C since no aqueous solution will be present on the conductor much above 100°C.

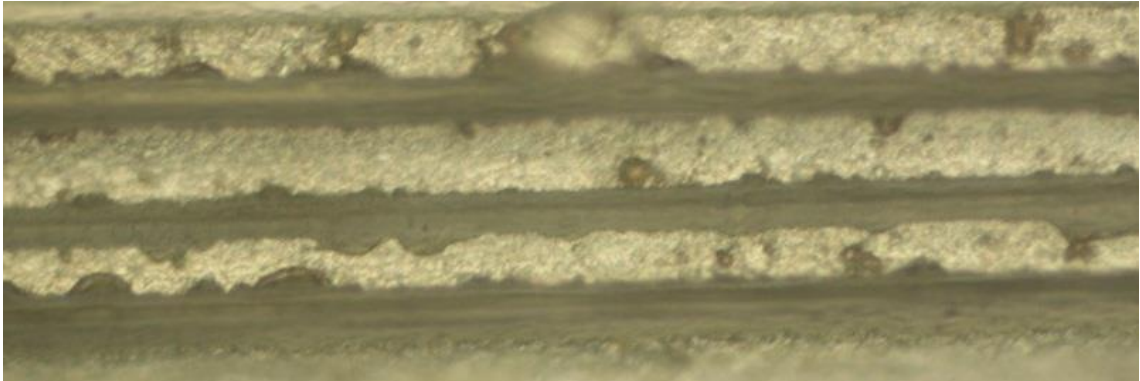


Figure 69: Initiation of corrosion pits along the fiber-matrix interface in the ACCR composite core. The light fields are the aluminum matrix, the dark stripes are the fibers. Optical microscopy, 500x magnification

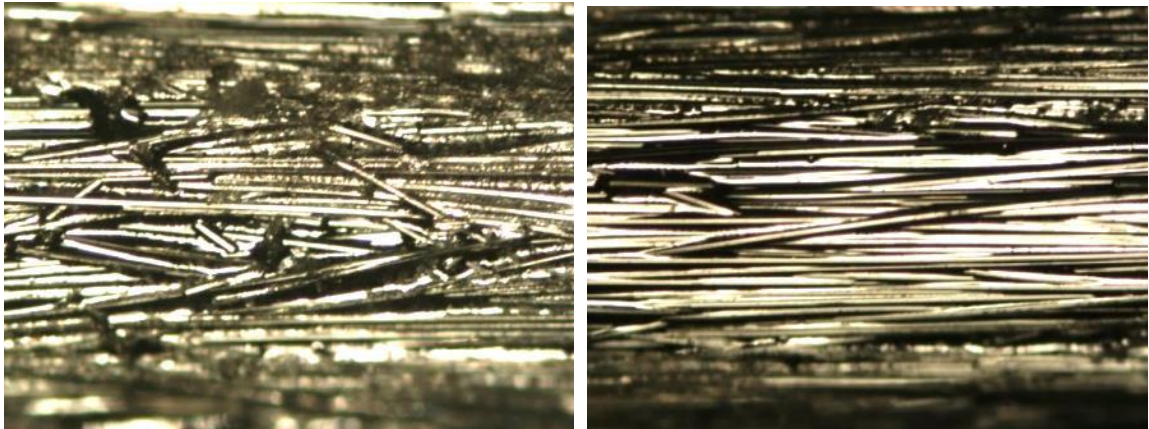


Figure 70: The surface of un-corroded ACCR. Optical microscopy, 100x magnification

4.5 General discussion

The galvanic corrosion behavior of traditional ACSR conductors is relatively well-known. The power utilities avoid potential corrosion problems in high corrosiveness areas by careful selection of conductor types and by the use of corrosion resistant grease, claddings and other preventive methods. In contrast, the experience with HTLS conductors is very limited.

The simple tests performed in this study quickly identified potential problems in all three HTLS designs: high galvanic corrosion rate in ACSS, possible galvanic corrosion in ACCC if the fiberglass galvanic barrier is damaged, and potentially severe galvanic corrosion in ACCR at high temperatures. The critical question is if these will actually become a problem in service. More multiscale testing in other environments is required to answer that question. The environment used in this study is quite severe for aluminum-based materials, and is likely much more severe than the actual service environment. The results here are therefore *not* sufficient to make service life predictions of any of the tested HTLS conductors.

The unexpected corrosion of the ACCR really highlights the fact that corrosion is a complex phenomenon that is sometimes difficult to explain. It also highlights the fact that galvanic corrosion is very hard to predict, particularly when aluminum is involved. The peculiar corrosion behavior of aluminum has been obvious in this study. Large swings in corrosion rate of orders of magnitude is typical for passivated alloys and most high performance advanced structural materials rely on passivation for their corrosion resistance. (Ricker R. , 2013). High voltage conductors are no exception. To ensure that highly engineered aluminum based material such as aluminum matrix composite will

remain passive and thus corrosion resistant in the actual environment, all new designs need to be thoroughly tested.

The very low galvanic corrosion rate in ACCC with the galvanic barrier intentionally damaged also showed the difficulty to reliably predict galvanic corrosion. Contact between aluminum and carbon fiber composite can often result in severe galvanic corrosion, but the geometry with the more noble material (the carbon fiber composite) surrounded by the corroding material (the aluminum strands) appeared to work in a favorable way to limit the corrosion rate. The cathodic reaction occurring at the carbon fiber composite appears to be limited by diffusion of oxygen into the conductor, limiting the total reaction rate. The opposite was the case in the ACCR that exhibited an accelerating corrosion rate, likely caused by a concentration gradient working in an unfavorable direction.

HTLS conductors will be a viable alternative for large-scale installations if they can gain the power utilities' confidence from a corrosion point of view. It has historically taken at least 20 years for a new conductor to go from the inception to the acceptance stage. With the rapid increase in electricity demand, we cannot afford to wait 20 years for HTLS conductors.

Accelerated corrosion tests are necessary to evaluate new products, but the main problem with accelerated laboratory testing for prediction of corrosion behavior is that different tests often give different results. In the same way as there are standards and codes for mechanical and electrical properties, a corrosion code is needed for high voltage conductors. Power companies, conductor manufacturers and standardization bodies such as NACE, ASTM and IEEE need to cooperate to develop a corrosion code

for new conductor designs with accelerated tests that accurately simulate the actual service environment.

CHAPTER FIVE: CONCLUSIONS

1. This study has shown that all three of the studied HTLS conductors (ACSS, ACCC and ACCR) can, under certain circumstances, develop galvanic corrosion. However, ACCC can only develop galvanic corrosion if the fiberglass galvanic corrosion barrier is compromised.
2. In the tested environment of aerated 3 wt. % seasalt aqueous solution at room temperature and 85°C, the main findings were:
 - The galvanic corrosion rates were low at *room temperature* for all the tested conductors. The corrosion rates of all three HTLS conductors were lower than for the conventional ACSR that was used as a baseline comparison.
 - The galvanic corrosion rates for ACSS and ACCR at 85°C were significantly higher than for the conventional ACSR (6 and 9 times higher, respectively). The preferentially corroding material in ACSS is the current carrying aluminum strands, while the aluminum matrix in the core material corrodes preferentially in ACCR.
 - ACCC does not suffer from galvanic corrosion unless the fiberglass galvanic corrosion barrier is compromised. Even if the barrier is compromised, the galvanic corrosion rate for ACCC was still significantly lower than for the conventional ACSR (the

corrosion rate was approximately 1/28th of ACSR both at room temperature and 85°C). The aluminum strands was the corroding material.

- The galvanic corrosion of ACSR and ACSS caused corrosion of the galvanization on the steel core at room temperature, while the aluminum was the corroding material at 85°C. The reason for the difference between room temperature and 85°C is not confirmed.

3. In the tested environment of 3 wt. % seasalt aqueous solution, ACCC appears to have the best corrosion performance of all the tested conductors. This can be explained by the absence of galvanic corrosion. Even if the galvanic barrier is compromised in such a way that galvanic corrosion occurs in ACCC, the geometry with the more noble material (the carbon fiber composite) surrounded by the corroding material (the aluminum) appears to work in a favorable way to limit the galvanic corrosion rate. The cathodic reaction occurring at the carbon fiber composite appears to be limited by diffusion of oxygen into the conductor, limiting the total reaction rate. This phenomenon is likely a function of the samples being submerged and may not occur in the real service environment.
4. In the tested environment of 85°C aerated 3 wt. % seasalt aqueous solution, ACCR exhibited a concerning galvanic corrosion behavior. The

aluminum matrix composite core material corroded preferentially. The corrosion rate was very high at 85°C. The geometry with the corroding material surrounded by the more noble material appeared to cause one or more concentration gradients that accelerated the galvanic corrosion rate. This phenomenon is likely a function of the samples being submerged and will likely not occur in the real service environment.

5. The study has clearly demonstrated that galvanic corrosion is very difficult to predict reliably, particularly when aluminum-based materials are involved in the corrosion mechanism.
6. The results from the galvanic corrosion testing of whole conductor samples have also shown that geometry may influence corrosion mechanisms and corrosion rates. New conductor designs therefore need to be tested in their actual geometry.
7. To be a viable alternative for large-scale installations, all new HTLS designs need to be thoroughly tested by direct measurements of galvanic corrosion in the environment of interest.
8. A corrosion code, with a selection of suitable accelerated tests, is needed for high voltage conductors. Power companies, conductor manufacturers and standardization bodies such as NACE, ASTM and IEEE need to cooperate to develop a corrosion code for new conductor designs with accelerated tests that accurately simulate the actual service environment.

SUGGESTIONS FOR FURTHER RESEARCH

1. Multiscale modeling of HTLS conductors subjected to corrosion.
2. Perform corrosion testing in other environments than salt (nitric acid, sulfuric acid, ammonia, combinations, etc.)
3. More extensive testing of ACCR to determine if the observed galvanic corrosion is a potential problem in the real service environment.
4. Continued testing of ACCC to determine if the degradation of the galvanic barrier can cause galvanic corrosion in the real service environment.
5. Continued testing of ACSR and ACSS to determine the cause of the observed polarity switch and to determine if it may cause potential problems in the real service environment.
6. Mechanical testing of conductor components at different stages of corrosion damage.
7. Development of more accurate simulations of the service environment such as simulated rain instead of submersion.

BIBLIOGRAPHY

- 3M. (2012). *Aluminum Conductor Composite Reinforced (ACCR) – Technical Summary for Common Constructions and Sizes (Metric Units)*. 3M.
- 3M Composite Conductor Program. (publication date unknown). *3M's comments on the electricity commission's draft decision on Transpower's Auckland 400 kV grid investment proposal*. 3M Composite Conductor Program, 3M New Zealand Ltd.
- 3M News. (2005, July 14). 3M joins National Electric Energy Testing Research and Applications Center. *Press release*. 3M.
- 3M News, 2. (2004, August 16). 3M reports initial sale of composite conductor for boosting power line capacity. *Press release*. 3M.
- 3M, 2. (2005). *Composite Conductor Field Trial Summary Report: Hawaiian Electric Company, Inc-Hawaii*. 3M.
- 3M, 3. (2003). *Aluminum Conductor Composite Reinforced, Technical Notebook (477 kcmil family), Conductor and Accessory Testing v.1.1*. 3M.
- ASTM. (2008). ASTM D1141 - 98(2008) Standard Practice for the Preparation of Substitute Ocean Water. ASTM.
- ASTM, 2. (2010). ASTM B941 – 10 Standard Specification for Heat Resistant Aluminum-Zirconium Alloy Wire for Electrical Purposes. ASTM.
- ASTM, 3. (2012). ASTM G69-12 Standard Test Method for Measurement of Corrosion Potentials of Aluminum Alloys. ASTM.
- ASTM, 4. (2009). ASTM G71 - 81(2009) Standard Guide for Conducting and Evaluating Galvanic Corrosion Tests in Electrolytes. ASTM.
- Bates, R. M. (1978). Standard potential of the silver-silver chloride electrode. *International Union of pure and applied chemistry, Pure & Appl. Chem.*, Vol 50, pp. 1701-1706.
- Brennan, G. (2004). Refurbishment of Existing Overhead Transmission Lines. *Integral Energy Australia, CIGRE Session 2004, B2-203*.
- Builes, G. E. (2008). Salt Contamination impact on Transmission Line Insulation performance and Corrosion. Some Possible Handling Measures. *IEEE*.
- Clairmont, B. (2008). High-Temperature Low-Sag Conductors. *Transmission Research Program Colloquium, Sacramento, CA, September 11 2008*. EPRI.
- Colbert, M. (2005). *Kinetrics North America Inc. Test Report for 3M to compare the salt spray corrosion performance of 795-kcmil 3M brand composite conductor to 795 ACSR conductor*, Kinetrics North America Inc., Report No.: K-422113-RC-0001-R01, November 4, 2005. Kinetrics.
- CTC-Global. (2012). *ACCC – The World's Most Efficient High Capacity Transmission Conductor*. CTC Global.
- Davis, J. (1999). *Corrosion of Aluminum and Aluminum Alloys*. ASM International.
- Delmonte, J. (1981). *Technology of carbon fiber and graphite fibers composites*. Van Nostrand Reinhold – Litton Educational Publishing Inc.
- Deve, H. (2013, February 7). ACCR - Presentation at University of Denver. Denver, CO: 3M.

- Electricity today. (2007, March). Upgrading your distribution without disrupting the neighborhood. *Electricity today*.
- EPRI. (2002). *High-Temperature, Low-Sag Transmission Conductors, 1001811*. Palo Alto, CA: EPRI.
- EPRI, 2. (2000). *Inspection & assessment of overhead line conductors: A state-of-the-science report, 1000258*. Palo Alto, CA: EPRI.
- Ergon Energy. (2013). *Network Lines Standard Guidelines for Overhead Line Design, Reference P56M032R09 Ver 1*. Retrieved January 2013, from Ergon Energy: http://www.ergon.com.au/__data/assets/pdf_file/0015/6612/P56M02R09-Ver-1-Guidelines-for-Overhead-Line-Design.pdf
- Frankel G.S., O. S. (2003). Pitting Corrosion. In J. e. S. D. Cramer and B. S. Covino, *Metals handbook Vol 13A*. ASM International.
- Frankel, P. L. (2002). A Study of Corrosion and Pitting Initiation of AA2024-T3 Using Atomic Force Microscopy. *Journal of The Electrochemical Society*, 149 (6) B239-B247(2002).
- GalvInfo Center. (2011). *GalvInfo Note 1.9: Zinc-5% Aluminum Allo-Coated Steel Sheet, Rev 1.1*. GalvInfo Center.
- Gamry Instruments. (2011). *Getting started with electrochemical corrosion measurement, Application note Rev 1.1*. Gamry Instruments.
- Geary, R. C. (2012). Introduction of high temperature low sag conductors to the Irish transmission grid. *CIGRE B2-104*.
- Goch, W. P. (2013). *Corrosion and Splices*. Retrieved January 2013, from Classic Connectors Inc.: <http://classicconnectors.com/2012/05/30/corrosion-and-splices/>
- Groysman, A. (2010). *Corrosion for everybody*. Springer.
- Harvard, D. B.-G. (1991). Aged ACSR Conductors, Part I – Testing Procedures for Conductors and Line Items. *IEEE*.
- Isozaki, M. A. (2008). Study of Corrosion Resistance Improvements by Metallic Coating for Overhead Transmission Line Conductor. *Electrical Engineering in Japan*, Vol. 163, No. 1.
- Johnson, D. A. (2010). A new generation of high performance conductors. *IEEE*.
- Jones, W. D. (2006, June). More Heat, Less Sag. *IEEE Spectrum*.
- Karabay, S. Ö. (2004). An approach for analysis in refurbishment of existing conventional HV-ACSR transmission lines with AAAC. *Electric Power Systems Research*, 72 (2004) 179-185.
- Kupke, S. (2012). Pilot project – high temperature low sag conductors. *E-ON Netz, Conference presentation, Stockholm, May 21 2012*. E-ON Netz.
- Lancaster, M. (2011). High Temperature Low Sag Conductor, Director of Transmission Engineering at Southwire. *Conference proceeding, November 29 2011*. Southwire.
- Linares, L. T. (2006). Failures Analysis by Corrosion in Power Conductors of Aluminum Alloys in Coastal-Lacustrine Environments. *2006 IEEE PES Transmission and Distribution Conference and Exposition Latin America, Venezuela*.

- Mandel, L. K. (2012). Electrochemical corrosion studies and pitting corrosion sensitivity of a self-pierce rivet joint of carbon fibre reinforced polymer (CFRP) – laminate and EN AW-6060-T6. *DOI*, 10.1002/mawe.201200945.
- Matweb. (2013). *Aluminum 1350-O*. Retrieved 2013, from Matweb.com:
<http://matweb.com/search/DataSheet.aspx?MatGUID=6ff3f965352a40d3bb4361bc509d57fe>
- Matweb, 2. (2013). *Aluminum 1350-H19*. Retrieved 2013, from Matweb.com:
<http://matweb.com/search/DataSheet.aspx?MatGUID=adb451e1fc0a41ca90ff4ee41f8896a6>
- Matweb, 3. (2013). *Galfan An-5Al-MM Zinc Alloy Ingot (UNS Z38510)*. Retrieved 2013, from Matweb.com:
<http://matweb.com/search/DataSheet.aspx?MatGUID=538a0086e3724a798a7db3b561d5219e>
- Mayer, P. (1998). *Corrosion Evaluation Methods for Power Transmission lines*. Ontario Hydro Technologies.
- McCullough, C. (. (2006). *Composite Conductor, Al-Zr Alloy Wire: Thermal Aging Behavior and Lifetime Modeling for Aluminum-Zirconium Alloy used in ACCR*. 3M.
- McCullough, C. G. (2005). *Uses and Test Results on High Temperature Low Sag ACCR Conductors*. PowerPoint presentation from 3M.
- Moreira, P. L. (2008). Internal Corrosion in Conductor Cables of Power Transmission Lines: Characterization of the Atmosphere and Techniques for Faults Detection. NACE. (2002). *Corrosion costs and preventive strategies in the United States*. NACE.
- NACE/ASTM. (2012). NACE/ASTM G193-12d Standard terminology and acronyms relating to corrosion. NACE/ASTM.
- National Energy Technology Laboratory. (2007). *A compendium of Modern Grid Technology*. National Energy Technology Laboratory.
- Power Systems Engineering Research Center. (2009). *Characterization of Composite Cores for High Temperature-Low Sag (HTLS) Conductors, Final Project Report*. PSERC Publication 09-05.
- Predecki, P. (2013). Professor Emeritus in Materials Science at University of Denver. (E. Hakansson, Interviewer)
- Rhaiem, E. B. (2012). Corrosion evolution of the aluminum alloys used in overhead transmission lines,. *IOP Conference Series: Materials Science and Engineering* 28.
- Ricker, R. (2013). Program Director, NIST Gaithersburg. (E. Hakansson, Interviewer)
- Ricker, R. E. (2012). *Estimating galvanic corrosion rates*.
- Riggs Larsen, K. (2011). Supporting the Nation’s Power Grid through Coatings Management. *NACE International*, Vol. 50, No. 12.
- Roberge, P. R. (2008). *Corrosion Engineering – Principles and Practice*. McGraw-Hill.
- Schumacher, M. (1979). *Seawater corrosion handbook*. William Andrew Publishing/Noyes.
- Southwire. (2007). *New steel turns Southwire ACSS into high-temperature, low-sag conductor*. Retrieved January 15, 2013, from SNL Financial: www.southwire.com

- Southwire, 2. (2012). *Bare Aluminium Conductor, List Price Sheet, BA45*.
- Sutton, J. (2010, April 26). How do electricity transmission lines withstand a lifetime of exposure to the elements? *MIT Engineering*.
- Svenningsen, G. (2003). *Corrosion of Aluminum Alloys*. Department of Materials Technology, 7491 Trondheim, Norway.
- Syed, S. A. (2006). Atmospheric corrosion of materials. *Saudi Arabia, Emirates Journal for Engineering Research*, 11 (1), 1-24 (2006).
- Taihan Electric Wire Co Ltd. (2013). *Overhead Electric Aluminum Conductors, product brochure*. Taihan Electric Wire Co. Ltd.
- Taniguchi, T. W. (1991). Electrolytic corrosion of metal hardware of HVDC line and station insulators. *IEEE Transactions on Power Delivery, Vol. 6, No. 3, July 1991*.
- Thrash, F. R. (2013). *Transmission conductors – A review of the design and selection criteria*. Retrieved January 9, 2013, from Southwire:
<http://www.southwire.com/support/TransmissionConductoraReviewOfTheDesignandSelectionCriteria.htm>
- U.S. Energy Information Administration. (2012, April 27). *Energy in Brief - Questions and answers about the power grid*. Retrieved from U.S. Energy Information Administration: www.eia.gov
- Vargel, C. (2004). *Corrosion of Aluminum*. Elsevier.
- Wald, M. L. (2004, March 4). WHAT'S NEXT; To Avert Blackouts, a Sag-Free Cable. *New York Times*.
- Wolf, G. (2007, June 1). Is there a solution for more wire in the air? *Transmission & Distribution World*.

APPENDIX A: DRAWINGS FOR THE C³LARC INSTRUMENT

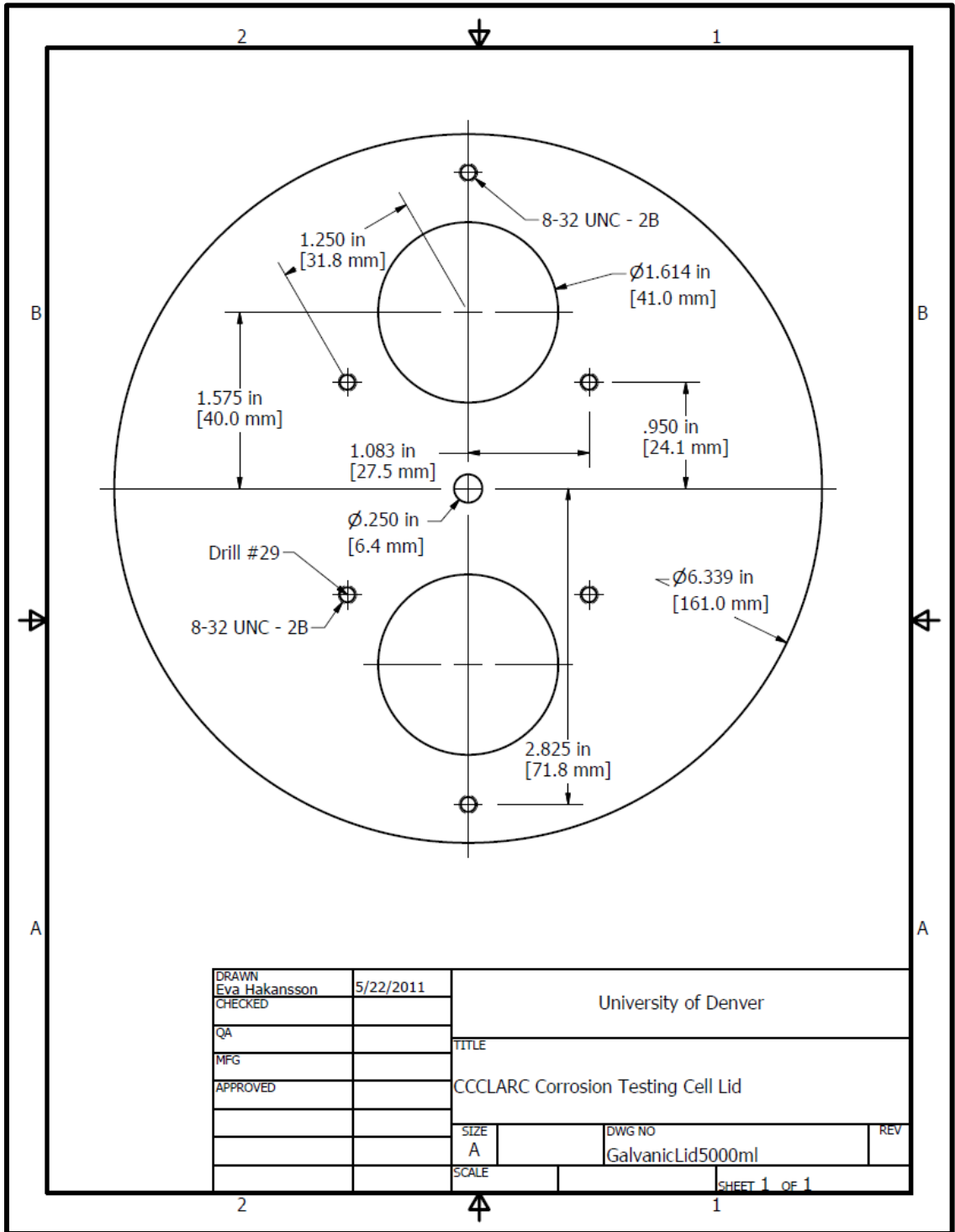


Figure 71: Drawing of lid for the C3LARC testing cell.

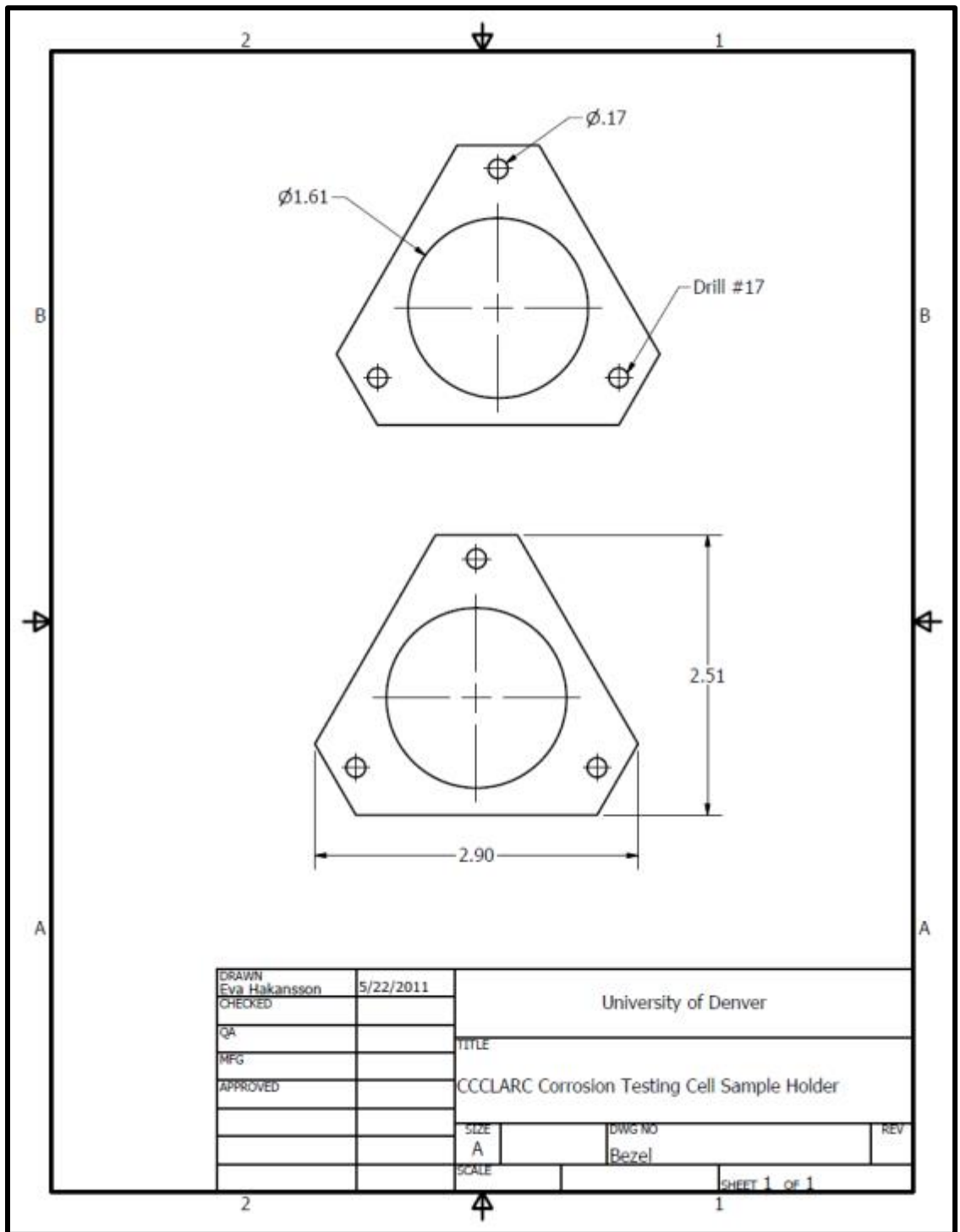


Figure 72: Drawing of sample holder for the C³LARC testing cell.

APPENDIX B: ACRONYMS, TERMINOLOGY AND SYMBOLS

A	Ampere
AAAC	All Aluminum Alloy Conductor
AAC	All Aluminum Conductor
ACCC	Aluminum Conductor Composite Core
ACCR	Aluminum Conductor Composite Reinforced
ACIR	Aluminum Conductor Invar Reinforced
ACSR	Aluminum Conductor Steel Reinforced
ACSS	Aluminum Conductor Steel Supported
ASTM	<i>American Society for Testing and Materials</i> , an international standards organization that develops and publishes technical standards
Ag	Silver
Al	Aluminum
Al ³⁺	Aluminum Ion
Al ₂ O ₃	Aluminum oxide, also known as Alumina
BPA	<i>Bonneville Power Administration</i>
C ³ LARC	<i>Composite Conductor Corrosion Lifetime Accelerated Reaction Cell</i>
CCCLARC	See C ³ LARC
Cl	Chlorine
Cl ⁻	Chloride ion
ΔG	Change in Gibb's Free Energy
e ⁻	electron
E _{corr}	Corrosion potential [V]

E_{oc}	Open circuit potential (sometimes used interchangeable with E_{corr}) [V]
F	Faraday's constant (96 485 C/mol)
GOALI	<i>Grant Opportunities for Academic Liaison with Industry</i>
G(Z)TACSR	Gap-type (Super) Thermal resistant Aluminum alloy Conductor Steel Reinforced
HTLS	High Temperature Low Sag (Conductor)
HS285	Ultra-high strength steel, option for core material in ACSS
H^+	Hydrogen ion
H_2	Hydrogen gas
I	Current [A]
I_{corr}	Galvanic corrosion current [A]
KCl	Potassium Chloride
kcmil	Unit of cross section area of a conductor, 1 kcmil = 0.5067 mm ²
kV	kilo volts
Life extension	Extensive renovation or repair of an item without restoring their original design working life.
MMC	Metal Matrix Composite
NaCl	Sodium Chloride
O_2	Oxygen gas
OH^-	Hydroxyl Ion
PMC	Polymer Matrix Composite
Refurbishment	Extensive renovation or repair of an item to restore their intended design working life. (Brennan, 2004)
ROW	Right-of-way
RTV	Room Temperature Vulcanizing silicone rubber

SO ₂	Sulfur Dioxide
TDH	Time of wetness – the number of hours per year that the relative humidity is over 80 % and the temperature is ≥0°C.
Tri-State	<i>Tri-State Generation and Transmission Association Inc.</i>
TW	Conductor stranded with trapezoidal wire (for example “ACSS/TW”)
Upgrading	Increase the original mechanical strength of an item due to, for example, a requirement for: higher meteorological actions. (Brennan, 2004)
Uprating	Increasing the electrical characteristics of a line due to, for example, a requirement for higher electrical capacity of larger electrical clearances. (Brennan, 2004)
WAPA	<i>Western Area Power Administration</i>
Zr	Zirconium